Modulating Chemokine Receptor Expression in Neural Stem Cell Transplants to Promote Migration after Traumatic Brain Injury

by

Caroline Addington

A Dissertation Presented in Partial Fulfillment
of the Requirements for the Degree
Doctor of Philosophy

Approved November 2015 by the
Graduate Supervisory Committee:

Sarah Stabenfeldt, Chair
Michael Caplan
Jonathan Lifshitz
Jeffrey Kleim
Stephen Massia

ARIZONA STATE UNIVERSITY

December 2015

ABSTRACT

Traumatic brain injury (TBI) is a significant public health concern in the U.S., where approximately 1.7 million Americans sustain a TBI annually, an estimated 52,000 of which lead to death. Almost half (43%) of all TBI patients report experiencing long-term cognitive and/or motor dysfunction. These long-term deficits are largely due to the expansive biochemical injury that underlies the mechanical injury traditionally associated with TBI. Despite this, there are currently no clinically available therapies that directly address these underlying pathologies. Preclinical studies have looked at stem cell transplantation as a means to mitigate the effects of the biochemical injury with moderate success; however, transplants suffer very low retention and engraftment rates (2-4%). Therefore, transplants need better tools to dynamically respond to the injury microenvironment.

One approach to develop new tools for stem cell transplants may be to look towards the endogenous repair response for inspiration. Specifically, activated cell types surrounding the injury secrete the chemokine stromal cell-derived factor-1α (SDF-1α), which has been shown to play a critical role in recruiting endogenous neural progenitor/stem cells (NPSCs) to the site of injury. Therefore, it was hypothesized that improving NPSC response to SDF-1α may be a viable mechanism for improving NPSC transplant retention and migration into the surrounding host tissue. To this end, work presented here has 1. identified critical extracellular signals that mediate the NPSC response to SDF-1α, 2. incorporated these findings into the development of a transplantation platform that increases NPSC responsiveness to SDF-1α and 3. observed increased NPSC responsiveness to local exogenous SDF-1α signaling following transplantation within our novel system. Future work will include studies investigating NSPC response to endogenous, injury-induced SDF-1α and the application of this work

to understanding differences between stem cell sources and their implications in cell therapies.

DEDICATION

First and foremost I would like to thank my wonderful family. I cannot imagine having the fortitude to undertake a challenge as large as a Ph.D. without the unwavering love and support that I have been so lucky to receive from my parents, Laura and Joe, and my sister, Lizzie. All three of you are wise beyond your years and have given me unique sets of advice and support that have worked together to create a robust framework of motivation. You have provided a loving and supportive haven for me as needed that is free of any expectation other than that I not neglect my sense of self and my happiness. In this way, you have helped me to find and define a space for my own happiness in the context of my work. I wholly credit the encouragement of my family with having found the optimistic side of failure in my work and for reminding me to enjoy the ride regardless of where it goes.

Second, I would like to thank the incredible patience, love and support of my partner-in-crime, John. Thank you for always having my best interest in your heart and for always acting from a place of love and support. Your belief in my capabilities never fails to amaze and inspire me and it serves as an incredible source of strength in all of my endeavors. My health and happiness are greatly indebted to your open ears, arms, mind and heart.

Lastly, I would like to acknowledge the loving support I have been lucky to receive from my climbing buddies and wonderful friends Laura, Chris and Sergio. I am very thankful to have found great friends who do not hold it against me when I have to disappear into the lab for weeks at a time. Friends like these are few and far between and their understanding has been a saving grace for me.

I love all of you tremendously!

ACKNOWLEDGMENTS

I would like to thank the guidance of my advisor, Dr. Sarah Stabenfeldt. Under Sarah's mentorship, I have been given the opportunity to develop my skills in all areas of my academic career. She has provided an excellent example of how to conduct sound science, how to effectively communicate scientific work through multiple mediums, and how to navigate a career in academia. Her door is always open to her students; a trait I have become more appreciative of in recent years as my own obligations have increased and the urge to close my door arisen. Lastly, she has always been supportive of her students' needs to lead whole and healthy lives outside of the lab. Were it not for her understanding of my need to take long weekends for trips to the desert to climb and attend music festivals in preservation of sanity, I certainly would not have finished my project in as timely a manner as I did!

I would also like to thank the guidance and support of my committee members, Drs. Jeff Kleim, Jonny Lifshitz, Michael Caplan and Steve Massia. I am fortunate to have had a very engaged and constructive committee to help guide my work, shape my knowledge base, and expand my scientific perspective.

This work was also greatly enhanced by the vibrant research community at Arizona State University, affording me the use of state-of-the-art facilities. Specifically, I would like to thank Dr. Jeff Kleim and Nagheme Thomas for allowing me extensive use of their surgical suite and for their training and guidance in all matters of animal work; Debra Baluch and the William M. Keck Imaging Lab for assistance with confocal imaging and her patience with my experimental (albeit unsuccessful) attempts at live cell imaging; David Lowry and the College of Liberal Arts and Science Bioimaging Facility for assistance with electron microscopy and appropriate sample preparation; John

Heffernan for assistance with NMR spectroscopy; and Dipankar Dutta for assistance with scanning electron microscopy.

Moreover, our collaborators outside of Arizona State University have been integral to the success of this work through their contribution of knowledge, time and resources. Specifically, I would like to thank Dr. Rachael Sirianni of the Brain Tumor Research Center at Barrow Neurological Institute for her support of this work as she provided consistent and thoughtful feedback on many of the studies performed serving to enhance the work through her relevant material-centric perspective. I would also like to thank Dr. Sirianni's students, John Heffernan and Sanjay Srinivasan for assistance with material development and characterization.

I would also like to acknowledge the support of the Stabenfeldt lab members. Specifically, Dipankar Dutta, Vimala Bharadwaj, William Marsh, and Dr. Christine Pauken for contributing to a happy, healthy lab environment and for their willingness to help troubleshoot experiments, feed cells, and manage the workings of the lab. I would also like to acknowledge the many undergraduates I have worked with over the course of this project for their contributions to this body of work and/or to my repertoire of mentoring skills. Specifically, Shruti Dharmaraj, Emma Goddery, Catherine Millar-Haskell, Sabrina Freeman, Emerson Tucker and Rupika Kapur.

This work was generously supported by the National Institutes of Health, National Science Foundation, Mayo Clinic Center for Regenerative Medicine, Acheivement Reward for College Scientists Foundation, Arizona State University Start-Up Funding, the Ira A. Fulton Schools of Engineering, and Barrow Neurological Institute. Moreover, presentation of this work at several conferences was supported in part by the School of Biological and Health Systems Engineering and the Graduate and

Professional Student Association at Arizona State University. I am thankful to these institutions and funding agencies for their faith in Dr. Stabenfeldt's young lab and for their continued support as the lab moves forward at the cutting edge of regenerative medicine research.

TABLE OF CONTENTS

Page

LIST OF TABLES

Table Page

LIST OF FIGURES

Figure Page

Figure Page

PREFACE

The work represented in this dissertation document has been previously published in the form of a review article (Chapter 1, *Biomarker Insights*, *2015*[1]) and two original research articles (Chapters 2, 3, *Biomaterials, 2014 & 2015*[2,3]). These published works have been expanded upon and adapted for use in this dissertation document.

CHAPTER 1

INTRODUCTION

1.1. Epidemiology of Traumatic Brain Injury (TBI)

Within the U.S., approximately 5.3 million individuals are affected by traumatic brain injury (TBI) annually, 53,000 of which result in patient death[4-6] . Of the TBI patients who survive, 43% report having sustained disabilities one year after injury [7]. The incidence of TBI has been on the rise in recent years with wars in Iraq and Afghanistan significantly contributing to increased numbers of TBI [4,8]. In total, TBI accounts for an estimated $76.5 billion strain on U.S. healthcare and economy each year with lifetime cost estimated for TBI exceeding $400 billion[9]. Given the societal and financial expense of TBI coupled with its increase in incidence, TBI represents a substantial public heath concern that has garnered public attention in recent years.

1.2. Pathophysiology of Traumatic Brain Injury

1.2.1. Types of TBI

While each incident of TBI has its unique parameters, most are either focal or diffuse in nature. Focal injuries are characterized by substantial force loading in a small area and typically involve skull fracture although fracture does not necessarily translate to dural compromise[10]. Injuries that incorporate dural compromise are termed open head injuries and these are often accompanied by object penetration within the neural tissue[10]. Diffuse injuries are sustained by force loading over a larger area and often involve a combination of rotational, translational or shearing forces[10,11]. Diffuse injury can be either direct or indirect in nature, meaning that injuries can be sustained after head contact with an object (direct) or brain contact with the skull plate without the presence of a secondary object (indirect)[8,10]. While diffuse injuries typically stand

alone, focal injuries can often incorporate diffuse-type injuries in regions surrounding the focal injury lesion further complicating the injury parameters.

1.2.2. Injury Progression

Injury parameters (i.e. focal, diffuse, severity) dictate the injury progression and as such there is variability among injuries; however the pathological progression of all injuries typically encompasses both a primary injury associated with the initial mechanical insult and a secondary injury, which is a result of the primary injury and propagates at cellular and subcellular levels (Figure 1.1).

The primary injury, namely in focal injuries, is characterized by immediate contusion, laceration and intracranial hemorrhaging at the tissue level. At the cellular level, there is immediate neuronal death (by necrosis) and axonal dysfunction within the lesion area. Immediate widespread necrosis is also observed in diffuse injuries as well as brain swelling and diffuse axonal injury (DAI), in which shear forces disrupt and eventually disintegrate axons.[8,12]

The hemorrhaging and swelling induced during the primary injury contribute to increases in intracranial pressure, which limits cerebral blood flow to the affected areas. Cerebral blood flow is also affected by the disregulation of vasoconstriction and vasodilation and, in many cases, widespread vasospasms[13,14]. Taken together, these sequelae lead to an ischemic injury microenvironment. While ischemia has negative effects on all neural cell types, neurons are particularly sensitive to ischemia to the extent that ischemia has been identified as a strong prognostic indicator after injury [8,13].

Alongside the ischemic injury there is a significant cellular influx of Ca^{2+}, Na^{+} and K^{+} ions, which leads to metabolic and ion pump dysfunction [13,15]. While other

pathologies also contribute to astrocyte activation, Ca^{2+} influx is thought to be primarily responsible for reactive astrocytes[16]. Under normal physiological conditions, astrocytes serve to maintain healthy extracellular concentrations of excitatory neurotransmitters and reactive oxygen species (ROS) that may negatively affect the surrounding neurons if allowed to accumulate in the extracellular space[17,18]. However upon activation, astrocyte efficiency in depleting extracellular glutamate and ROS is significantly reduced and accumulation of these molecules leads to neuron excitotoxicity and peroxidation of cellular structures, respectively[13,15,17,18].

Increased extracellular ROS is, by itself, quite destructive to cell structure and DNA, however it also serves to propagate the inflammatory response, further exacerbating the secondary insult[19]. Inflammation following TBI is mediated by both the activated resident microglial cells as well as leukocytes and macrophages that infiltrate from the breakdown of the blood brain barrier[20-22].

All of these underlying pathologies ultimately result in the formation of the glial scar: a dense, fibrous scar tissue laid down by reactive astrocytes that creates a blockade to neural growth and development [23,24]. The glial scar is formed between 7 and 14 days after the injury is sustained, after which time the potential for therapeutic intervention is greatly decreased. Therefore, the “golden window” for cell therapy is considered to be the time between the initial wave of necrosis and the formation of the glial scar (ranging between 2-7 days after injury)[25].

During this time, the injury microenvironment is complex and dynamic and there are many active cell types that influence injury progression. Of particular interest to the

work presented here are neural progenitor/stem cells for their role in mediating endogenous repair after injury.

1.3. Endogenous Repair Response to Neural Injury and its Mediating Factors

The capacity for endogenous repair within the adult central nervous system has only recently been realized through discoveries of neurogenesis concentrated within regions identified as neural niches – the subgranular zone (SGZ), which lines the dentate gyrus within the hippocampus, and the subventricular zone (SVZ), which lines the lateral ventricle[26-30]. While alteration in both the SGZ and SVZ progenitor populations have been reported after TBI, our focus is largely on the SVZ neural niche as its resident neural progenitor/stem cells (NPSCs) have been observed to migrate longer distances and are therefore more likely to be recruited to the injury penumbra after TBI[31].

1.3.1. The Subventricular Zone (SVZ)

The SVZ is closely approximated with vasculature[32-34] where a single cell (type B cells) spans its width, extending processes to contact vasculature on one side and the lateral ventricle on the other[34,35]. Type B cells thus have access to both ventricular and vascular signaling, which is critical to niche maintenance[30,35]. Neural stem cell phenotype is thought to be more effectively maintained in close proximity to endothelial cells and proliferation within the SVZ arises within 10-15 microns away from blood vessels[33,36]. Proliferation within the SVZ is typically observed in type C cells, the highly proliferative transit-amplifying cells that arise from type B cells and in turn will give rise to type A cells[37,38]. Type A cells are GFAP+ neuroblasts or neural progenitor/stem cells (NPSCs) that exit the niche by migrating along the nearby vasculature. Under normal physiological conditions migration occurs along the rostral

migratory stream to the olfactory bulb where they become interneurons[39]. However, following injury the fate of cells derived from the SVZ is altered.

1.3.2. NPSC Response to Neural Injury

1.3.2.1. Injury-Induced Changes Within the Niche

Evidence suggests that the cells of the SVZ undergo proliferative and phenotypic changes following a neural injury as the SVZ niche has been shown to increase in size, total number of cells, and number of proliferative cells[40-43]. It is thought that the type C cells are largely responsible for increased proliferation within the niche after injury[42,44]. However, Thomsen et al. have recently proposed a non-proliferative mechanism by which the SVZ increases in size and total cell number in which injury-induced phenotypic subsets of SVZ cells dedifferentiate[42]. While findings of increased cell number and SVZ thickness after injury have been robust across the field, these injury-induced changes within the niche are complex and there is still much about niche dynamics after injury that has yet to be understood.

1.3.2.2. NPSC Recruitment to Site of Injury

Neural injury not only affects NPSCs within the niche but also those leaving the niche. Following injury, NPSCs stray from their normal physiological migratory route and home to the site of injury in a vasophilic manner[40,43,45-48]. While the signals driving this behavioral change are still being investigated, it is thought to be driven by chemokines and inflammatory factors secreted by activated cell types in the injury microenvironment.

1.3.3. Injury-induced Factors that Mediate the Endogenous Repair Response

The active cell types of neural injury create a complex microenvironment through the secretion of a myriad of signaling factors that can facilitate and/or mitigate the injury progression (Figure 1). These factors range from pro-inflammatory to neurotrophic in nature, and it is important to note that there is much interplay between signaling molecules that further complicates their respective roles within the injury sequelae. The cell source and temporal and spatial expression patterns (Figures 2 and 3) help to inform the nature of each signaling molecules' roles, specifically in mediating the behavior of endogenous neural progenitor/stem cells (NPSCs) after injury (see Table 1 for breakdown of specific molecules and their effect on NPSCs). For the purpose of this review, several extracellular factors and cytokines that have been found to affect NPSCs were selected for discussion; however, numerous factors not discussed here, including critical transcription factors, can directly or indirectly affect NPSC behavior and it is important to acknowledge their effect on endogenous behaviors as well. For a more thorough review of signaling factors not described here, interested readers are encouraged to refer to recommended reviews[49-51].

1.3.3.1. Stromal Cell-Derived Factor 1α (SDF-1α)

Increased expression of the chemokine SDF-1α has been observed within the injury penumbra within 24 hours after neural injury and persists out to 3 days before decreasing[52,53]. Both *in vitro* and *in vivo* data indicate that local increases in SDF-1α after neural injury are generated by reactive astrocytes within the surrounding tissue[54-56]. Unpublished data from our lab also indicate that SDF-1α protein levels peak within the injury penumbra following the controlled cortical impact (CCI) model for TBI at 1 and 3 days with a decrease at 7 days and a return to baseline at 14 days.

There is compelling evidence that the chemokine SDF-1α plays a critical role in recruiting endogenous NPSCs to the site of injury in that the local SDF-1α source within the injury microenvironment is thought to be chemottractive to NPSCs leaving the niche[53,55]. NPSC chemotactic response to SDF-1α has been well characterized *in vitro*[2,57,58] and has been shown to work synergistically with vascular basement membrane protein laminin to increase NPSC migration[2], implicating its relevance to vasophilic mechanisms of endogenous NPSC recruitment after injury. Moreover, blocking activity of the SDF-1α receptor CXCR4 attenuated the migration of NPSCs to the injury environment following stroke[59].

SDF-1α may also play a role in increased NPSC proliferation observed within the SVZ niche after injury as *in vitro* studies have shown that SDF-1α promotes NPSC proliferation[2,58]. However, this relationship has yet to be fully elucidated within the context of TBI.

1.3.3.2. Vascular Endothelial Growth Factor (VEGF)

Increased expression of VEGF has been observed in several models of TBI. Much like SDF-1α, VEGF secretion is associated with reactive astrocytes and endothelial cells within the injury penumbra; however, infiltrating inflammatory cell types also contribute significantly to early elevated VEGF levels[60-64]. Neutrophil-derived VEGF is elevated within 4 hours after injury and persists out to 2 days[60,61]. At approximately 1 day after injury, endothelial cells begin contributing significantly to elevated VEGF levels within the injury penumbra and their contribution persists out to 5 days after injury[60]. Between 3-7 days after injury, reactive astrocytes appear to secrete VEGF within the penumbra[60,62-64] coinciding with macrophage VEGF secretion, which peaks from 4-6 days after injury[60,62].

VEGF may be chemottractive to NPSCs after injury through both direct and indirect mechanisms. *In vitro,* VEGF has been shown to increase NPSC migration after direct stimulation[65] and to promote NPSC migration indirectly through endothelial cells and/or other growth factors[66,67]. The concept of indirect VEGF NPSC stimulation further underlines the importance of the niche's close proximity to vasculature. Moreover, VEGF-overexpression in transgenic mice has shown to increase NPSC recruitment to ischemic areas after stroke[68].

Much like SDF-1α, VEGF may also contribute to NPSC proliferation within the SVZ after injury. *In vitro,* both direct and indirect evidence of VEGF-mediated NPSC proliferation have been observed [69,70], and Wang et al. found SVZ proliferation after stroke to increase in VEGF-overexpressing transgenic mice[68]. VEGF may not only promote proliferation, but may also reduce apoptosis in NPSCs, thus contributing to increased SVZ size and survival after neural injury as reduced NPSC apoptosis following stroke within neurogenic regions (i.e. SVZ, dentate gyrus, rostral migratory stream, olfactory bulb) was observed by Schänzer et al. after VEGF intraventricular perfusions[70].

1.3.3.3. Epidermal Growth Factor (EGF)

Increases in EGF after neural injury are relatively short-lived, peaking within the first 24 hrs in the injury penumbra, CA3 and dentate gyrus regions and returning to baseline levels by 3 days [52,71]. A more sustained EGF increase is observed in the hippocampus (CA1 region), increasing from 24 hrs to 3 days and returning to basal levels by 7 days[71]. Early increases in EGF have been attributed to neuronal upregulation, while the sustained response in the CA1 past 24 hrs has been attributed to glial cells[71].

It is important to point out that given the proliferative response to injury within the SVZ and the known mitogenic effects of EGF on NPSCs[72,73], one might anticipate increases in EGF expression to spatially coincide with this proliferative zone. However, it has been proposed that rather than an increased level of EGF, TBI induces increased sensitivity of endogenous cell types to EGF signaling by upregulating its receptor, EGFR[44,74]. These data paint a complex picture when taken together with those of Thomsen et al. that describe a new lineage of EGFR+ neural stem cells that appear to arise from de-differentiating neuroblasts after TBI[59]. Regardless of the mechanism by which NPSCs respond to EGF after injury, studies in EGF knock-out mice have illustrated that EGF plays a critical role in promoting proliferation within the SVZ and in mitigating apoptosis within the SVZ and injury penumbra[75].

1.3.3.4. Fibroblast Growth Factor (FGF)

Increases in FGF have been shown to occur as early as 4 hrs after injury and persist for 14 days following TBI in several models; however, increased FGF expression remains spatially restricted to the injury region [76-80]. Early upregulation of FGF is due to macrophages and microglia (4 hrs – 3 days), while late FGF upregulation originates from reactive astrocytes (7 days – 14 days), alluding to its potential to play multiple critical roles during the endogenous repair response [77,80].

Much like EGF, FGF is a well characterized mitogen *in vitro* where EGF and FGF are often used in combination to maintain NPSCs in culture[73,81]. Increased FGF following ischemic insult has been observed to increase hippocampal NPSC proliferation *in vitro* and this effect was attenuated in FGF knock-out mice *in vivo*[82]. Moreover, NPSC proliferation following injury was reduced to basal levels upon inhibition of FGF indicating that even in the presence of other injury-relevant signaling molecules, FGF

appears to play a critical role in regulating injury-induced NPSC proliferation[83]. In the same study, injury conditioned media increased NPSC neuronal differentiation; however, FGF inhibition was not observed to significantly reduce neuronal differentiation[83] suggesting that there are other factors that contribute to neuronal differentiation following injury. Nonetheless, FGF is not completely inactive in mediating neuronal differentiation as studies have demonstrated its role in neurogenesis[13,28].

1.3.3.5. Brain-Derived Neurotrophic Factor (BDNF)

While there is evidence in ischemic injury models of BDNF upregulation within the injury penumbra, increased BDNF within the injury region have not yet been observed in TBI models [52,84,85]. Following stroke, BDNF in the hypoxic core increased by 2 hrs and remained elevated out to 3 days[84,86]. However, following a fluid percussion model of TBI, BDNF showed no significant increase within acute timepoints after injury [85]. The most robust increases in BDNF after TBI have instead been observed in the dentate gyrus and the CA3 regions of the hippocampus[22,87,88]. Hicks et al. observed an ipsilateral increase in BDNF within the hippocampus 3-6 hrs following mild fluid percussion injury model (FPI) and found this trend to extend bilaterally after severe FPI in which BDNF increased at 1 hr and was sustained out to 72 hrs[87]. While studies have been in agreement regarding hippocampal BDNF expression, increases within the injury penumbra appear to be largely dependent on the injury model where more severe models are more likely to elicit a cortical BDNF response[85,89]. Regardless of location, BDNF appears to originate from granule cells and activated microglia[85,88,89].

BDNF plays a critical role in mediating both the differentiation and survival of new neurons. Several studies *in vitro* have demonstrated that BDNF both suppresses the proliferation of undifferentiated NPSCs and promotes the neuronal differentiation of NPSCs[90-93]. Moreover, BDNF has been shown to promote the survival of new neurons[94-96], a critical characteristic in the context of TBI in which endogenous NPSCs face a complex injury microenvironment upon recruitment to the lesion. Gao et al. convincingly elucidated this critical role for BDNF after TBI using BDNF conditional knockout mice in which the death of new neurons within the dentate gyrus was significantly increased compared to wild type mice after injury[95].

1.4. Stem Cell Transplantation after TBI

One approach many have taken to enhance the endogenous repair response after injury is the introduction of exogenous stem cells. There are still many questions surrounding the mechanisms by which stem cell transplants may function to mitigate the secondary injury of TBI as well as the fate of these cells (i.e. viability, phenotypic fate) after transplantation. In part, these questions arise from the modulation of many different transplant parameters and metrics of success in the literature. One of the parameters often modulated is stem cell type as both NPSCs and mesenchymal stem cells (MSCs) have been observed to differentiate into cells of a neural lineage under the appropriate conditions[25,97-101]. For this reason, there have been numerous studies investigating the efficacy of NPSC and/or MSC transplantation following neural injury and several approaches to transplanting both NPSCs and MSCs will be discussed for the purpose of this review.

1.4.1. Bolus Stem Cell Transplantation

Several critical parameters have been observed to influence the survival, phenotype and functional benefits of bolus stem cell transplantation following TBI including cell type, injury model and severity, and transplant timing and location, among others. Studies in MSCs have indicated that they are capable of expressing neuronal lineage markers after transplantation into animals that have sustained a TBI[97,100,101]and that MSC transplantation may facilitate motor function recovery out to 1 month after injury[97,100]. However, concerns have arisen regarding the safety of transplanting MSCs into the brain as MSCs have been observed to form masses that elicit a significant inflammatory response, where NPSCs transplanted in the same conditions did not form such masses[98,99]. Therefore, NPSC transplantation is appealing for both its perceived relative safety and the innate neuronal differentiation capacity of NPSCs.

Several studies have been performed using NPSCs to determine the effect of timing and location on transplant fate. Shear et al. found NPSC transplant survival after TBI was significantly higher at more acute time points after injury compared to the later time points, presumably due to glial scarring[102,103]. With respect to transplant location, transplant survival and migration into the surrounding tissue were significantly greater in the ipsilateral compared to contralateral hemisphere, in some cases accompanied by greater motor and cognitive function recovery[25,104]. Taken together, these data illustrate some of the many factors that can modulate the therapeutic benefit of stem cell transplantation after TBI.

One common thread among the many bolus transplant studies is that very few transplants differentiate into new neurons (< 5%)[25,102,104-106]. Most studies have observed differentiation into GFAP+ astrocytes to a greater extent than neuronal

differentiation (~5-10%); however, many transplanted cells sustain undifferentiated/unidentified phenotypes[100,105,106]. These findings have lead researchers to hypothesize that the benefit of stem cell therapy may lie in the trophic support that they provide to local degenerating neurons[107-109]. As such, a line of research has emerged in which stem cell transplants are designed to capitalize on their capacity to provide trophic support to cells within the injury microenvironment.

1.4.2. Modified Stem Cell Transplants Following Neural Injury

In recent years, several groups have looked at either pre-conditioning or genetically modifying cell transplants to prepare them for the cytotoxic injury microenvironment and/or increase their capacity for trophic support. This is an appealing option as cell transplants can theoretically be used to deliver neuroprotective factors while simultaneously providing the benefits of stem cell therapy. This approach has shown some promise as BDNF-expressing NSPCs have been observed to enhance neuronal differentiation, synaptic plasticity, and the number of transplants retained in the lesion site after TBI out to 8 weeks compared to normal NPSCs[110]. These findings were accompanied by an improvement in motor function recovery at 7 days compared to normal NPSCs, however this increase was insignificant by 4 weeks[110]. BDNF-expressing MSCs have also been shown to significantly improve neurological function compared to normal MSCs out to 90 days after a moderate TBI[111].

Another approach has been to increase transplant sensitivity to the injury-relevant factors that have been shown to promote survival, proliferation, migration and/or differentiation through overexpression of the appropriate receptor. For example, Wang et al. observed attenuation of the inflammatory response after transplanting MSCs over-expressing CXCR4, the receptor for SDF-1α, into a lesion area after moderate TBI,

and interestingly, also observed local increases in VEGF and BDNF expression[112]. Similar work in stroke models has shown CXCR4-expressing MSCs result in increased neuronal differentiation, migration into the host tissue, and improved neurological function[113].

The method of "priming" transplants to encourage neuronal differentiation upon transplantation is yet another modification that may improve transplant efficacy. Gao et al. primed NPSCs by exposing them to laminin, heparin and FGF for several days prior to transplantation and observed a post-transplant population that was ~96% positive for early neuronal markers, a marked increase over previous work[114]. However, the functional integration and neurological benefit have yet to be determined for methods such as this.

Soluble signaling such as neurotrophic factors and chemokines is critically important as evidenced by the promise demonstrated in these stem cell modification techniques; however, it is also critically important to consider the mechanical and integrin-centric signaling that transplants are exposed to. Therefore, another route taken for transplant improvement has been the development of scaffolds and novel neurotransplantation systems.

1.4.3. Scaffolds for Stem Cell Transplantation Following Neural Injury

Given the importance of both mechanical and integrin signaling in regulating cell behavior, many efforts have been made to mimic native neural tissue in the construction of transplant scaffolds. While there have been some purely synthetic polymeric scaffolds, such as the woven poly(glycolic acid) scaffold used for NPSC transplantation by Park et al[115], there has been significant attention given to incorporation of extracellular matrix (ECM) components within scaffolds to provide integrin signaling to transplants.

Moreover, these scaffolds are frequently hydrogels as they can be easily tuned to mimic the mechanical properties of native brain[116,117]. Chopp et al. have extensively investigated the use of collagen I gels as transplant scaffolds for MSCs and have found the scaffolds to increase transplant retention within the lesion site and migration into the host tissue, decrease the lesion volume, promote synaptic plasticity within the surrounding tissue, and promote cognitive function recovery when compared to bolus transplantation[118-121]. Guan et al. have also found MSC's within collagen I gels to display increased viability and neurite outgrowth following transplantation into the injury microenvironment[122].

While these data are promising, collagen I is not native to neural tissue and as such, other groups have looked to incorporating ECM components or binding motifs that are less foreign to NPSCs such as laminin. Given the vascular nature of the SVZ, it is logical that NPSCs respond favorably to laminin substrates and, as mentioned previously, laminin has the capacity to promote neuronal differentiation of NPSCs[2,114]. Indeed, increased neuronal differentiation was observed in NPSCs transplanted in a self-assembling peptide gel modified with the laminin binding motif IKVAV[123]. Moreover, Tate et al. found that NPSC transplants migrated further into the host tissue and displayed increased long-term survival when transplanted in collagen I gels modified with laminin compared to both collagen I only gels and collagen I gels modified with fibronectin[124].

Another relevant ECM component that has begun to garner attention within the neural tissue engineering field is the glycosaminoglycan hyaluronic acid (HA). Regions associated with endogenous NPSC maintenance and migration (i.e. SVZ niche and rostral migratory stream, respectively) are HA-rich compared to the rest of the adult

brain, making it especially relevant to NSPC transplantation[125,126]. HA transplant scaffolds have been used to encapsulate NPSCs in intact brains[127] and in the injured spinal cord[128] and to encapsulate mature neurons in an injured brain model[129]. In these studies, HA was combined with gelatin, methylcellulose and poly-D-lysine, respectively, to promote cell adhesion as HA alone does not do so effectively[130]. While HA provides niche-mimetic ECM cues to its encapsulated transplants, these included adhesion motifs are not native to the neural niche[34,126]. Therefore, there is room for improvement in this arena through thoughtfully designed niche mimetic and/or injury relevant adhesion motifs.

As illustrated, there are many parameters that govern the efficacy of stem cell transplantation in mediating repair (i.e. cell type, injury, transplant location and timing, cellular modifications, scaffolding, etc.). Therefore, it is critically important to use the knowledge available regarding temporal and spatial signaling patterns after injury to inform future work in developing stem cell therapies for neural injury so as to have a better command of the driving forces behind their outcomes.

1.5. Objective and Specific Aims

Current preclinical cell transplantation therapies for TBI suffer from very low rates of transplant survival and engraftment within the host tissue. In looking towards improving transplant efficacy, it is useful to allow the local signaling that drives endogenous repair to inform an intentional design. A therapy that works in concert with the local injury signaling, rather than works against or remains indifferent towards these critical signals may serve to enhance transplant survival and engraftment after injury. Therefore, it was the aim of this project to engineer a transplantation platform that provides cell transplants with tools to dynamically respond to injury-related signals.

Specifically, inflammatory cell types and activated glia release chemokines, such as SDF-1α, that recruit endogenous neural stem cells to the injury penumbra. Therefore, overexpression of receptors that respond to injury-induced chemotactic gradients may be an effective tool for enhancing transplant cell engraftment and diminishing secondary injury effects. Transplant viability and retention within the host tissue have also been shown to benefit from the structural stability afforded by scaffolding, even when made of materials not native to neural tissue. As such, we have worked to consolidate the benefits of both modified transplants and scaffolding into one transplantation platform, where the *primary objective* of this work is to develop a smart material that 1. enhances NPSC sensitivity to local injury signaling and 2. provides the appropriate infrastructure to promote migration into the host tissue. There is a great need for more effective therapies to mitigate the long-term dysfunctions associated with TBI and our work lays the groundwork for developing effective cellular therapies that target the secondary injury of TBI through the three following specific aims:

1.5.1. Specific Aim 1

Determine the critical ECM migratory cues that mediate NPSC response to injury-relevant chemokine gradients.

1.5.2. Specific Aim 2

Develop a neurotransplantation system that promotes NPSC response to critical chemotactic signals.

1.5.3. Specific Aim 3

Determine the efficacy of transplanting CXCR4 overexpressing NPSCs for enhancing NPSC migration in response to injury-relevant chemotactic signaling.

1.6. Figures

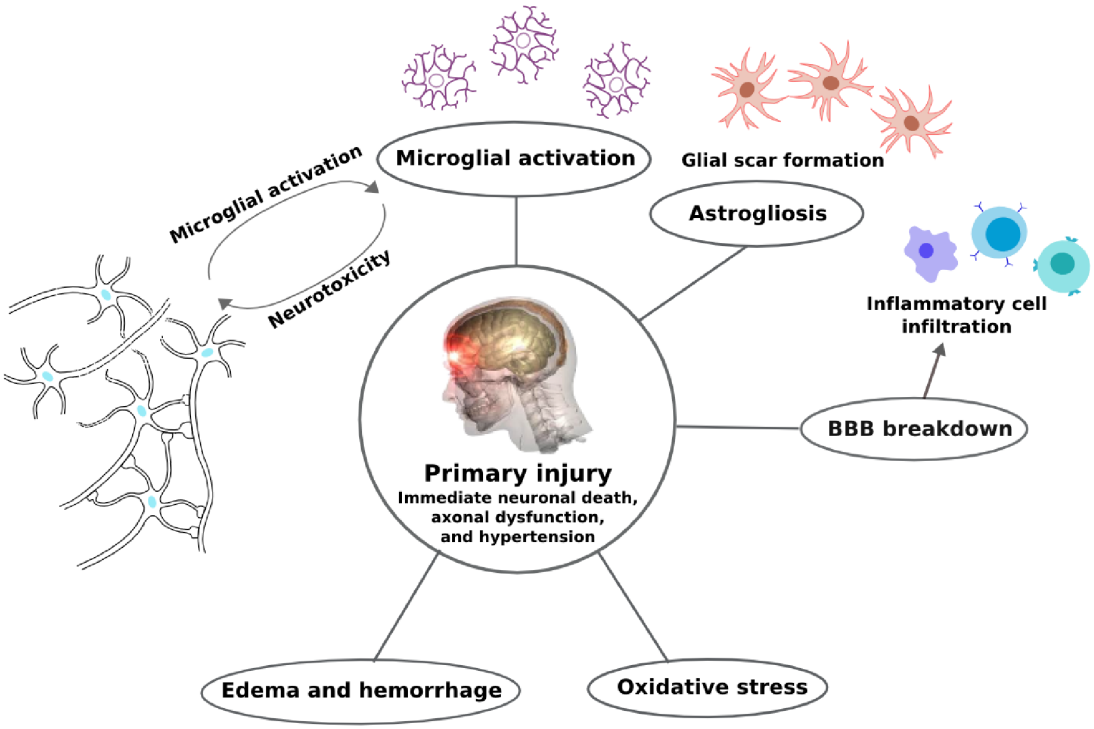

Figure 1.1: Schematic of primary and secondary injury progression. The primary injury results in numerous cellular and subcellular events, collectively termed the secondary injury. The secondary injury is largely responsible for long-term neurotoxicity and neurodegeneration.

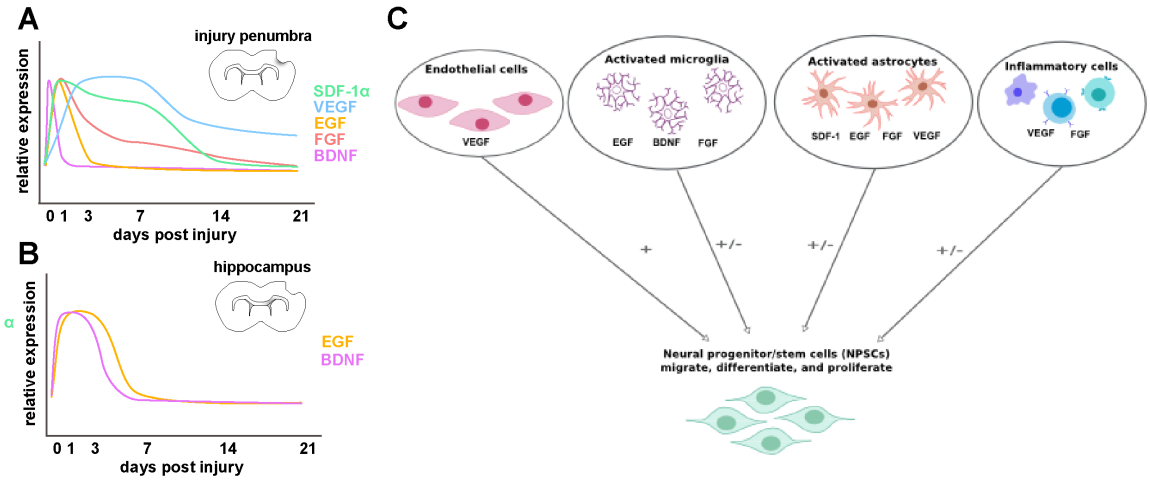

Figure 1.2: Endogenous repair signaling after traumatic brain injury. During the secondary injury, growth factors and chemokines are acutely upregulated within the injury penumbra (A) and the hippocampal niche (B) by local endothelial cells, activated glia and by infiltrating systemic inflammatory cell types (C).

Table 1.1: Current preclinical cell therapies for traumatic brain injury. MSC = mesenchymal stem cell; CCI = controlled cortical impact; NPSC = neural progenitor/stem cell; BDNF = brain derived neurotrophic factor; FPI = fluid percussion injury; EGFR = epidermal growth factor receptor; Fn = fibronectin; Lm = laminin. *Other studies from the same group (Michael Chopp) have been published reiterating these findings with variations in transplant timing and behavioral test timing, the cited studies have been chosen as representatives for this body of work. **This study did not compare against non-modified transplants.

Bolus Stem Cell Transplantation		
Transplant	**Injury Model**	**Primary Findings**
MSC	CCI	Improved motor function; Early neuronal marker (6%) and astrocyte marker (12%) expression [100,101]*
		Improved motor and cognitive function[97]
NPSC	CCI	Improved motor function irrelevant of transplant location;Mature neuronal marker and astrocyte marker expression varied as function of transplant location;No oligodendrocyte marker (CNPase) expression[104]
		Improved motor and cognitive function long-term (14 months);Oligodendrocyte marker expression after 14 months, but not neuronal or astryocyte phenotypic marker expression[102]
		Improved motor function; <2% transplant survival[106]
		Timing and location of transplants affects functional efficacy;2-7 days after injury is the optimal transplant range[25]
	Weight drop	Neuronal and astrocyte marker expression as a function of transplant location;No oligodendrocyte marker expression[105]
Modified Stem Cell Transplantation		
Transplant	**Injury Model**	**Primary Findings**
BDNF-overexpressing MSC	FPI	Improved neurological severity score[111]
BDNF-overexpressing NSPC	CCI	Enhanced survival and neuronal marker expression ;Increased local synaptic density[110]
Neuronal primed-NPSC	FPI	Improved cognitive function; Transplants primarily expressed neuronal phenotype marker[114]**
Scaffold Stem Cell Transplants		
Transplant	**Injury Model**	**Primary Findings**
MSC in collagen scaffold	CCI	Improved cognitive function; Reduced lesion volume; Increased transplant retention; Increased VEGF expression by local host cells[118,120]
		Increased synaptic density, may reduce glial scarring[121]
		Improved transplant retention; Improved neurological severity score and cognitive function; Increased local metabolic activity[122]
		Increased transplant retention and neurite outgrowth; Improved neurological severity score and cognitive function; Increased local vessel density[119]
NSC in collagen and Fn/Lm scaffold	CCI	Increased transplant survival (Lm>Fn); Improved cognitive function (Lm only)[124]

CHAPTER 2

THE ROLE OF SDF-1α-ECM CROSSTALK IN DETERMINING NEURAL STEM CELL FATE

2.1. Introduction

Central nervous system (CNS) injury, be it neurodegenerative, mechanical, and/or ischemic in nature, has permanent and disabling consequences[131]. In recent years, the endogenous regenerative capacity of neural tissue has been realized[4] and has prompted many groups to investigate potential therapies that interact with the endogenous repair response[132]. Specifically in the brain, endogenous neural progenitor/stem cells (NPSCs) maintained within the subventricular zone (SVZ) and hippocampal niche of the adult brain undergo a change in their migratory behavior following neural injury[48,55]. The SVZ residing NPSCs which typically migrate to the olfactory bulb and replenish GABAergic granule neurons instead home to regions of neural injury during repair[48,133]. The mechanisms behind this behavior are still unclear although it is thought that chemotactic signaling of several cytokines initiated by surrounding activated microglia play a critical role[134].

From a regenerative standpoint, it is apparent that the inherent repair response falls short of facilitating neural regeneration. However, providing cues to encourage cellular migration, neuronal differentiation and proliferation may prove beneficial in advancing the efficacy of NPSC recruitment following neural injury. Given the complexity of the pathophysiological environment, it is important to consider the potential for interactions between multiple signaling inputs to NPSCs when investigating appropriate cues. The cytokine stromal derived factor-1α (SDF-1α) has been shown to play a vital role in NPSC migratory behavior following neural injury[55,59]. Under normal physiological conditions, NPSCs migrate from the SVZ to the olfactory bulb in

close approximation with blood vessels; similar vasophilic NPSC migration is observed in response to exogenously induced SDF-1α gradients[48,55]. This association suggests that NPSC behavior particularly following neural injury may be acted upon by a critical crosstalk between SDF-1α and vascular basement membrane extracellular matrix (ECM).

It is well known that ECM proteins provide integrin-centric signals to cells altering numerous behaviors (viability, migration, differentiation, protein production etc.)[17-20]. For this reason among others, ECM proteins have been used for the development of tissue engineering scaffolds with success in several applications[21,22]. The effects of SDF-1α and ECM signaling on NPSC behavior have been investigated independently where both SDF-1α and laminin increase NPSC motility[39,55]. Aside from cell migration/motility, ECM proteins are well known to alter stem cell differentiation profiles, yet the role of SDF-1α in NPSC differentiation has not been thoroughly investigated. Peng et al. observed NPSCs differentially overexpress SDF-1α and its corresponding receptor (CXCR4) upon differentiation into astrocytes and neurons respectively[27], however, little is known regarding the influence of SDF-1α on NPSC differentiation moreover the influence of SDF-1α-ECM crosstalk.

Mechanistically, SDF-1α and ECM signaling appear to have intersections in the MAPK, Akt, JNK, and ROCK pathways with variability among ECM proteins[28,29]. The MAPK and Akt pathways are thought to play critical roles in modulating receptor, ligand, and integrin production, cell survival, and proliferation[30-32], while the ROCK pathway is thought to regulate actin cytoskeletal reorganization[33]. For this reason, inhibition of ROCK signaling would provide insight into the mechanisms regulating the actin cytoskeleton with regard to its involvement in SDF-1α-ECM signaling crosstalk.

Alterations in the cytoskeletal organization of NPSCs may most notably affect migration but could also affect other NPSC behaviors such as proliferation and differentiation.

Pro-regenerative behaviors such as migration, differentiation, and proliferation are critical to the efficacy of NPSC-facilitated regeneration and as such a clearer understanding of the driving forces behind these behaviors would allow for better control over NPSC fate following neural injury. Based on the many signaling intersections and independent behavioral effects of SDF-1α and the ECM on NPSCs, we hypothesize that SDF-1α-ECM crosstalk plays a role in directing NPSC fate following neural injury and that a better understanding of these axes will set the stage for the development of a regenerative intervention strategy for NPSC recruitment following neural injury.

2.2 Experimental Methods

2.2.1. NPSC isolation and culture

NPSCs were isolated from the medial and lateral germinal eminences of E14.5 C57BL/6 mice based on previously published protocols[135] and in accordance with approval by the Institutional Animal Care and Use Committee at Arizona State University. Briefly, mice were anesthetized at 3% isoflurane, rapidly decapitated, and fetuses were extracted from both uterine horns. Fetal tissue was rinsed in cold Leibovitz medium (Life Technologies, Carlsbad, CA) at each stage of the germinal eminence dissection. The germinal eminences were rinsed with sterile, cold Leibovitz medium before mechanical dissociation in working NPSC medium (glucose (6 ng/mL, Acros Organics, Geel, Belgium), HEPES buffer (5mM, Sigma Aldrich, St. Louis, MO), progesterone (62.9 ng/mL, Sigma Aldrich), putrescine (9.6 μg/mL, Sigma Aldrich), heparin (1.83μg/mL , Sigma Aldrich), B27 growth supplement (1X, Life Technologies), epidermal growth factor

(20 ng/mL, Sigma Aldrich), fibroblast growth factor (5 ng/mL, Sigma Aldrich), insulin (5 μg/mL, Sigma Aldrich), transferrin (5 μg/mL, Sigma Aldrich), sodium selenite (5 ng/mL, Sigma Aldrich) in Dulbecco's Modified Eagle Medium (Life Technologies))and plated at a density of 10^4 cells/mL in a humidified incubator at 37°C, 20% O_2, and 5% CO_2. NPSCs were cultured as non-adherent neurospheres in working NPSC medium, passaged by mechanical dissociation, and utilized for experiments between passages 3 through 6.

2.2.2. NPSC Migration

2.2.2.1. Radial NPSC Migration

NPSCs were plated in ECM coated 24-well plates at 25 neurospheres per cm^2 (n=4 replicates per group; poly-L-lysine(MP Biomedicals, Solon, OH), human fibronectin(BD Biosciences, San Jose, CA), mouse laminin-1(Sigma Aldrich), Matrigel(BD Biosciences), bovine gelatin(Fisher Scientific, Houston, TX), chondroitin 6 sulfate (Sigma Aldrich), bovine heparin sulfate (Sigma Aldrich), human collagen IV(Sigma Aldrich), chicken collagen II(Sigma Aldrich); 6 μg/cm2, human vitronectin; 0.5 μg/cm^2(R&D Systems)) in mitogenic growth factor-free media with or without supplementation of SDF- 1α (1μg/mL; PeproTech, Rocky Hill, NJ), the CXCR4 inhibitor AMD3100 (5μg/mL Santa Cruz Biotechnology, Santa Cruz, CA), and the ROCK inhibitor Y-27632 (25μM, Sigma Aldrich). Cultures were imaged via phase contrast microscopy at 10X once every 24 hours for 6 days allowing for the tracking of radial NPSC migration out of the neurosphere. Culture plates were imaged once every 24 hours. Phase contrast images (n=6 per sample well) were analyzed for longest sphere diameter as shown in Figure 2.2 using a custom-designed MatLab program (MathWorks, Inc., Natick, MA) and were normalized to baseline measurements taken 2 hours after plating.

2.2.2.2. Chemotactic NPSC Migration

NPSCs were allowed to migrate through 12μm pore Millicell cell culture inserts (Millipore, Temecula, CA) for 3 or 6 days. Insert membranes were coated with ECM substrates as described previously and NPSCs were plated in mitogenic growth-factor free media at a density of 40 neurospheres/cm^2 (n = 3 replicates per group). SDF-1α positive groups were exposed to an SDF-1α sink (1 μg/mL in mitogenic growth-factor free media) on the underside of the membrane. At specified end point, non-migratory cells were removed from the top of the membrane with a cotton swab and migrated cells on the underside of the membrane were visualized with nuclear stain (DAPI, Life Technologies). Thresholded blue channel images (n=3 per sample well) were analyzed for migrated cell count, determined using the particle counter in MatLab (MathWorks, Inc.).

2.2.3. NPSC Proliferation

2.2.3.1. Total Proliferation

Total proliferation was evaluated with the Quant-iT PicoGreen dsDNA assay kit (Life Technologies). Neurospheres were plated in ECM coated 48 well plates (n=6) at a density of 25 neurospheres/cm^2 with and without SDF-1α supplementation (1 μg/mL). At specified end point (0, 3 and 6 days), plates were scratched and neurospheres were lysed for 72 hours in humid conditions at 37°C in Proteinase K buffer and DNA was extracted with the DNeasy kit following manufacturer's instructions (Qiagen, Venlo, Limburg) prior to double strand DNA quantification with the Quant-iT PicoGreen dsDNA assay kit. Both λ DNA and cell standards were run and a cell count was

calculated for each well based on cell calibration curve. Experimental groups were normalized to their respective cell counts at day 0.

2.2.3.2. Proliferation Profile of Migrating Cells

Proliferation of migrated NPSCs was assessed with the Click-iT ® EdU Cell Proliferation Assay (Life Technologies). NPSCs that migrated through Millicell cell culture inserts as described previously were incubated with EdU for 4 hours in a humid environment at 37°C and visualized with fluorescent reporter AlexaFluor555 using an inverted fluorescent microscope (Leica, DMI4000 B, Wetzlar, Germany). Thresholded red channel images (n=6) were analyzed in MatLab for particle counts to obtain an EdU positive cell count for each experimental group.

2.2.4. NPSC Differentiation

2.2.4.1. Western Blot Analysis

NPSCs were cultured on ECM substrates for 3 and 6 days with or without SDF-1α supplementation. At the specified end point, NSPCs were lysed by mechanical agitation and incubation in cold RIPA lysis buffer (150mM NaCl, 50 mM Tris pH 8.0, 0.5% sodium deoxycholate, 1% NP-40, 1% protease inhibitor cocktail (all reagents from Sigma Aldrich)). Protein concentration was quantified by bicinchoninic acid protein assay (G-Biosciences, St. Louis, MO). SDS-PAGE gel electrophoresis and Western blotting were performed on 8% Bis-Acrylamide gels for the detection of phenotypic proteins indicative of NPSCs (rabbit anti-nestin, Abcam, ab27952, 177kDa) and young neurons (rabbit anti-β III tubulin, Millipore, MAB1637, 55kDa) and on 12% Bis-Acrylamide gels for the detection of astrocytes (mouse anti-GFAP, Millipore, MAB3402, 50kDa) and oligodendrocytes (mouse anti-Olig2, Millipore, AB9610, 32kDa). β-actin was used as an

internal control for all blots (rabbit anti-β-actin, LI-COR (Lincoln, NE), 926-42210, 45kDa). Goat anti-rabbit IRDye 800 (NC0217916, LI-COR) and goat anti-mouse IRDye 680 (926-32220, LI-COR) secondary antibodies were used appropriately. Membranes were blocked with 5% bovine serum albumin (BSA, Sigma Aldrich) in TBS-T (15.4mM Trizma-HCl (Sigma Aldrich), 137mM NaCl (Sigma Aldrich), 0.1% Tween 20(Bio-Rad, Hercules, CA)) and probed with the appropriate antibody dilutions in 2.5% BSA, TBS-T buffer. Band detection was performed using the LI-COR Odyssey far infrared scanner and Image Studio software (LI-COR) was used for band intensity quantification. Band intensity was normalized to β-actin expression.

2.2.4.2. Immunocytochemistry

NPSCs were cultured on ECM coated glass coverslips as described previously in 24-well plates (n=4 replicates per group) for 3 and 6 days with or without SDF-1α (1μg/mL), AMD3100 (5mM), and Y-27632 (25mM) supplementation every 48 hours. At specified end points, NPSCs were fixed with 3.7% paraformaldehyde (Sigma Aldrich), permeabilized with 0.1% Triton X 100 (Fisher Scientific), and probed for proteins indicative of astrocytes (rabbit anti-GFAP, Millipore, AB5804), young neurons (mouse anti-β III Tubulin, Millipore, MAB1637), NPSCs (rabbit anti-nestin, Abcam, ab27952), and oligodendrocytes (mouse anti-O4, Millipore, MAB345). AlexaFluor488-conjugated goat anti-rabbit (Invitrogen, A11034) and AlexaFluor555-conjugated goat anti-mouse (Invitrogen, A21422) secondaries were used appropriately. DAPI (Life Technologies) was used for visualization of cell nuclei. Samples were imaged at 10X via fluorescence microscopy (n=3 images per well; Leica, DMI4000 B).

2.2.5. Statistical Analysis

Statistical analysis was performed on all quantitative assays. The appropriate one-way or two-way ANOVA followed by Tukey post hoc tests were run to determine statistical significance with $p < 0.05$ considered significant (GraphPad Prism, La Jolla, CA). Multiplicity adjusted p-values reported for Tukey post hoc comparisons.

2.3. Results

2.3.1. SDF-1α-ECM crosstalk has a significant and synergistic effect on NPSC migration.

NPSC radial migration on gelatin, chondroitin 6 sulfate, heparin sulfate, collagen IV, and collagen I showed no significant increases compared to poly-L-lysine and fibronectin did not appear to act synergistically with SDF-1α; these substrates were therefore omitted from subsequent SDF-1α supplementation and inhibition studies (data not shown). With basal media treatment, radial NPSC migration significantly increased on Matrigel and laminin at all time points compared to poly-L-lysine controls ($p<0.0001$ for both Matrigel and laminin at all time points; Figure 2.1, 2.3). NPSC radial migration on vitronectin supplemented with SDF-1α significantly increased at all time points compared to poly-L-lysine controls (day 1: $p=0.021$; day 3: $p=0.0253$; day 6: $p<0.0001$). Significant and synergistic increases in NPSC radial migration were observed on Matrigel and laminin supplemented with SDF-1α at all time points compared to their appropriate substrate samples without SDF-1α supplementation as shown in Figures 2.1 and 2.3 (day 1: $p=0.0011$, 0.002; day 3: $p<0.0001$ for both; day 6: $p<0.0001$, $p=0.0152$ respectively). Moreover, upon the addition of CXCR4 antagonist (AMD3100), NPSC migration returned to basal substrate migration levels regardless of SDF-1α supplementation on Matrigel and laminin at all time points as shown in Figure 2.2 and

2.3. CXCR4 receptors are expressed on the membrane of NPSCs[136] and SDF-1α is its only known ligand[36] making the effects of its inhibition an indicator of SDF-1α-CXCR4 axis involvement in NPSC behavioral signaling. ROCK inhibition with Y-27632 appeared to increase NPSC radial migration on laminin at all days, significantly at day 3 (Figure 2.4, 2.5 p=0.0261**)**. However, Y-27632 in combination with SDF-1α supplementation was observed to significantly reduce radial NPSC migration back to basal levels on Matrigel, laminin, and vitronectin at days 3 and 6(Figure 2.4, 2.5**,** p=0.038, 0.0001 respectively**)**. Chemotactic migration results shown in Figure 2.6 further supported the radial migration data in which SDF-1α-ECM crosstalk significantly and synergistically increased NPSC chemotactic migration on Matrigel, laminin, and vitronectin at 3 days (p=0.0494, p<0.0001, p=0.0374 respectively) and on Matrigel and laminin at 6 days (p=0.0471, 0.001 respectively) compared to their respective substrate samples without SDF-1α supplementation. In comparison to poly-L-lysine controls, NPSC chemotactic migration in the presence of SDF-1α on Matrigel, laminin, and vitronectin was significantly increased at 3 days (p<0.0001,p<0.0001, p=0.0012 respectively) and this was maintained on Matrigel and laminin out to 6 days (p=0.0471, 0.0003 respectively).

2.3.2. SDF-1α significantly affects NPSC proliferation.

NPSC total proliferation as measured with PicoGreen significantly increased on poly-L-lysine, Matrigel, and laminin substrates supplemented with SDF-1α at 3 days compared to the appropriate substrate samples without SDF-1α supplementation (Figure 2.7, p=0.0076; 0.0009; 0.0064 respectively); this trend was also observed at 6 days however was not significant. The Millicell culture insert chemotactic migration assay allowed for analysis of the proliferation profile of the migrating subset of cells. Proliferation of migrated NPSCs on Matrigel coated culture inserts was significantly

increased when supplemented with SDF-1α at both days 3 and 6 compared to poly-L-lysine controls ($p<0.0001$; $p=0.0163$ respectively) and to Matrigel samples without SDF-1α supplementation ($p<0.0001$; $p=0.0163$ respectively) as shown in Figure 2.7. Similarly to total NPSC proliferation observations, the migrating subset of NPSCs on Matrigel, laminin, and vitronectin supplemented with SDF-1α appeared to support increased proliferation compared to samples without SDF-1α supplementation at day 3, however these differences were insignificant.

2.3.3. SDF-1α-ECM crosstalk significantly and synergistically alters differentiation profiles of NPSCs.

Neuronal differentiation was enhanced on laminin-based substrates (Matrigel and laminin) supplemented with SDF-1α compared to the appropriate substrate samples without SDF-1α. Western blotting demonstrated significant and synergistic increases in β III tubulin production on Matrigel and laminin supplemented with SDF-1α at day 3 (Figure 2.8, $p=0.0342$, 0.006 respectively). Increases in β III tubulin production with the addition of SDF-1α were observed for all samples at day 6 however they were not significant. Similar findings were observed in the quantification of immunocytochemistry where β III tubulin normalized positive area was significantly increased with the addition of SDF-1α on Matrigel at 3 days (Figure 2.9, 8A, $p=0.0004$); an increase was also observed on laminin at 3 days however insignificant (Figure 2.9, 8A, $p=0.0938$). This effect was abrogated with the addition of AMD3100 on Matrigel ($p=0.0007$) and laminin at 3 days. The synergistic increase in neuronal differentiation appeared to be acute in nature as significance was lost for all samples at day 6. Astrocyte and stem cell phenotypes did not differ significantly regardless of substrate, supplementation, or time point as indicated both by normalized positive GFAP and

nestin staining in ICC samples (Figures 2.9, 2.10, 2.11) and by protein expression in Western blotting (Figure 2.8 A, C, & E). A significant increase in oligodendrocyte differentiation at day 3 was observed on vitronectin supplemented with SDF-1α in Western blotting samples probed for Olig2 (Figure 2.8 A,D, $p=0.0435$). Insignificant acute increases in O4 positive staining were observed on vitronectin with and without SDF-1α supplementation as well (Figure 2.10C, 2.11).

2.4. Discussion

Following TBI, endogenous NPSCs migrate towards the site of injury in close proximity to vasculature[46]. Similarly, Kokovay et al. demonstrated that exogenous NPSCs transplanted into the SVZ associate with SVZ vasculature, potentially mediated by SDF-1α release from ependymal cells within the niche[48]. These vasophilic NPSC tendencies *in vivo* reflect the observations we identified in the present study regarding NPSC migration on laminin-based substrates supplemented with SDF-1α. Previous studies investigating the recruitment of endogenous NPSC after neural injury have established that the SDF-1α-CXCR4 axis plays a critical role in *in vivo* NPSC homing[48]. SDF-1α -ECM synergy has been observed in populations of thymocytes by Yanagawa et al.[39], but the data reported here are the first, to our knowledge, to investigate the combinatorial effects of NPSC association with the ECM in response to SDF-1α gradients similar to those established in the context of neural injury. A greater understanding of the driving forces behind NPSC behavior following neural injury may open the door to regenerative therapies which allow for greater control over the fate of endogenous NPSCs.

Regenerative strategies for neural injury/disease also include stem cell transplantation paradigms; however, such approaches are plagued with low cell survival

rates and high percentages of glial differentiation with minimal neuronal differentiation[137,138]. Laminin is well known to induce NPSC neuronal differentiation *in vitro*[139,140]. Laminin's role as a guidewire for NPSC migration after injury raises questions regarding its role in the integration of endogenous NPSCs recruited to the site of injury such as that observed by Hou et al. in their stroke model and Magavi et al. following induced cortical neuron apoptosis[43,44]. Therefore, the synergistic increase in neuronal differentiation observed on laminin-based substrates with SDF-1α supplementation is of great interest to the field both in its elucidation of NPSC behavior following neural injury and the opportunity it provides for increasing the neuronal differentiation NPSC transplantation therapy. However given the acute nature of SDF-1α-ECM mediated enhancement of neuronal differentiation, it is possible that other signaling factors are needed to sustain this level of neuronal differentiation. We also observed differences in the spatial distribution of neuronal differentiation relative to the core neurosphere in samples supplemented with SDF-1α compared to those without, specifically on laminin-based substrates. More new neurons on the periphery of the central neurosphere were observed on laminin-based substrates supplemented with SDF-1α and to a lesser extent on vitronectin samples supplemented with SDF-1α. We postulate that NPSCs underwent neuronal differentiation at higher rates peripherally to the neurosphere due to increased exposure to both integrin and SDF-1α signaling than those remaining within the neurosphere, a notion supported by the high concentration of nestin positive cells within the center of the neurosphere (Figure 2.9). Furthermore, previous research inducing neuronal differentiation of adult human neural progenitor cells and adult and neonatal rat stem cells found that laminin substrates increased efficacy compared to tissue culture or poly-L-lysine substrates due to cell spreading and the resultant uniformity of exposure to neuronal induction factors[45-47]. Within the

SVZ niche, laminin is closely associated with ependymal cells, fibroblast, and macrophages all of which secrete factors regulating NPSC migration and differentiation[141]. As mentioned previously, ependymal cells in close proximity to SVZ vasculature release SDF-1α which may also serve as a regulator of NPSC migration, differentiation, and proliferation[48]. However, the effect of SDF-1α-ECM crosstalk on neuronal differentiation in any cell lines has yet to be investigated and as such our findings build motivation for a myriad of investigations into the effect of this crosstalk on the differentiation of other stem/progenitor cell lines.

Alongside increasing neuronal differentiation and integration, increasing proliferation may be a potent mechanism to enhance the number of NPSCs at the site of injury both in endogenous and transplantation systems. The increases we observed in total proliferation across several substrates support data reported by other groups in which SDF-1α appeared to play a critical role in stimulating NPSC proliferation[55] as well as the proliferation of other cell types[50,51]. While SDF-1α plays a role in stimulating NPSC proliferation, this effect does not have a synergistic relationship with ECM signaling to the extent observed in migration or differentiation experiments. We observed higher proliferation on poly-L-lysine and vitronectin samples compared to those on laminin-based substrates due to the minimal NPSC migration out of the neurosphere on said substrates. Spatial observations of the immunocytochemistry staining for nestin indicate that the majority of nestin positive cells were confined within the center of the neurosphere, which provides a vastly different NPSC microenvironment than that external to the neurosphere. The inherent differences between environments within and external to the neurosphere are of interest to the field and are being investigated by other groups[52-55]. For example, Bez et al. reported neurospheres plated on Matrigel resulted in a higher density of BrdU positive cells within the

neurosphere center compared to the distal edges of the neurosphere[53]. In the context of the niche wherein maintenance of a stem cell phenotype is positively correlated with proliferation, these observations are coherent. NPSC proliferation within the SVZ is maintained mainly by soluble signaling factors EGF and FGF and also by Noggin; these factors in combination are largely responsible for the maintenance of multipotency of NPSCs in the SVZ [34,72]. Given the dual role of these signaling factors, inducing increases in both proliferation and neuronal differentiation is inherently problematic. Thus furthering the notion that low levels of NPSC proliferation external to the neurosphere on laminin-based samples is due to increased neuronal differentiation.

To evaluate the potential effect of SDF-1α – ECM crosstalk on proliferation independent of the neurosphere microenvironment, we also investigated the proliferation profile of NPSCs in a chemotactic Millicell insert assay. Interestingly, we observed significant increases in migrated NPSC proliferation only on Matrigel when supplemented with SDF-1α. BD Matrigel used in these experiments was comprised largely of laminin and collagen IV as well as heparin sulfate proteoglycans, and enactin[59]. It also contains levels of transforming growth factor-beta (TGF-β), epidermal growth factor (EGF), insulin-like growth factor, fibroblast growth factor (FGF), tissue plasminogen activator, and other growth factors naturally occurring in the Engelbreth-Holm-Swarm mouse tumor[60,61]. These growth factors present in Matrigel may have contributed to the synergistic increase of migrated NPSC proliferation since no such increase was observed on laminin, an abundant protein in Matrigel. Our observations of minimal NPSC migration on collagen IV and heparin sulfate and the known effects of TGF-β, EGF, and FGF on cellular proliferation further support this conclusion (data not shown)[142,143].

The mechanistic crosstalk implicated in our observations may be due to direct regulation of the SDF-1α/CXCR4 axis by integrin signaling and/or vice versa. Direct communication between axes has been observed in other cell types, however investigations into such a hypothesis have not yet been pursued in the context of NPSCs. In pancreatic cancer cells, Grzesiak et al. demonstrated that laminin-1 binding results in the upregulation of CXCR4[65]. Conversely, exposure of prostate cancer cells to SDF-1α has been shown to increase αvβ3 expression, an integrin which binds to fibronectin and vitronectin[66]. These findings taken together with our reported findings may point towards a similar means of protein regulation, which may play a role in the synergistic NPSC migration response we observed on laminin-based substrates.

From a mechanistic perspective, we observed that the RhoA/ROCK signaling pathway may not play a critical role in regulating the synergistic effects on SDF-1α/ECM directed NPSC migration or differentiation. The inhibition of ROCK with Y-27632 has previously been shown to increase NPSC neurite outgrowth[67,68]. Our radial migration results support this finding in the absence of SDF-1α, but were then abrogated with the addition of SDF-1α and Y-27632. Radial migration measurement is a common means of monitoring NPSC migration out of neurospheres[65], however, it does not account for significant variability among cell morphologies and as such, immunostaining was performed to better visualize the effect of ROCK inhibition on NPSC morphology. Increases in neurite outgrowth on samples supplemented with Y-27632 are visible in immunocytochemistry samples, which may aid in the interpretation of radial migration results. Previous studies focusing on ROCK signaling demonstrated that this signaling molecule plays a key role in regulating cellular migration through the dissolution of actin stress fibers at the retracting edge and the increase in integrin interactions at the leading edge of migrating cells[67,71,72]. In the context of the neurosphere, increases in leading

edge integrin interactions to a certain degree may serve to enhance migration out of the center of the neurosphere when exposed to an ECM substrate. In this light, the increase in NPSC radial migration on laminin supplemented with ROCK inhibitor Y-27632 is a consistent result. However, we hypothesize that in the presence of both SDF-1α and Y-27632, further potential increases in integrin interactions due to both SDF-1α and Y-27632 may serve only to immobilize NPSCs which have left the neurosphere, yielding comparable NPSC radial migration to that observed on laminin-based substrates without any supplementation[73]. While ROCK signaling is well known to be involved in actin cytoskeleton reorganization[33], its role in SDF-1α-ECM crosstalk may be restricted to regulating the cytoskeleton and may be minimally influenced by SDF-1α signaling. Other groups have found that Akt and MAPK pathways may play a critical role in SDF-1α/CXCR4-mediated NPSC migration[74,75]. Historically, Akt and MAPK pathways have a larger regulatory influence on proliferation, differentiation, and gene expression than on actin cytoskeleton reorganization[30,31] reinforcing the notion that ROCK-mediated cytoskeleton reorganization may not play a critical regulatory role in the observed SDF1-1α-ECM crosstalk phenomena. Akt and MAPK pathways may be activated by integrin interactions as well[76,77] and as such, data reported by Li et al. and Ganju et al. taken together with our findings suggests that SDF-1α-ECM crosstalk may be acting largely through regulation of DNA-based cellular activities rather than through actin cytoskeleton reorganization.

2.5. Conclusion

Endogenous NPSCs are known to associate with vasculature during recruitment up SDF-1α gradients towards the site of a neural injury. However, our results indicate that the relationship between these two mediators of NPSC recruitment is synergistic

rather than combinatorial in its effect on NPSC migration and neuronal differentiation. SDF-1α-ECM crosstalk does not appear to have a synergistic effect on NPSC proliferation, however SDF-1α alone increases proliferation in NPSCs. Moreover, the most significant results were observed on laminin-based substrates, which complements the *in vivo* behavior of NPSCs following neural injury. These results have implications in better understanding the mechanisms behind the endogenous repair response as well as improving current approaches to stem cell transplantation as a therapy for neural injury and neurodegenerative diseases.

2.6 Figures

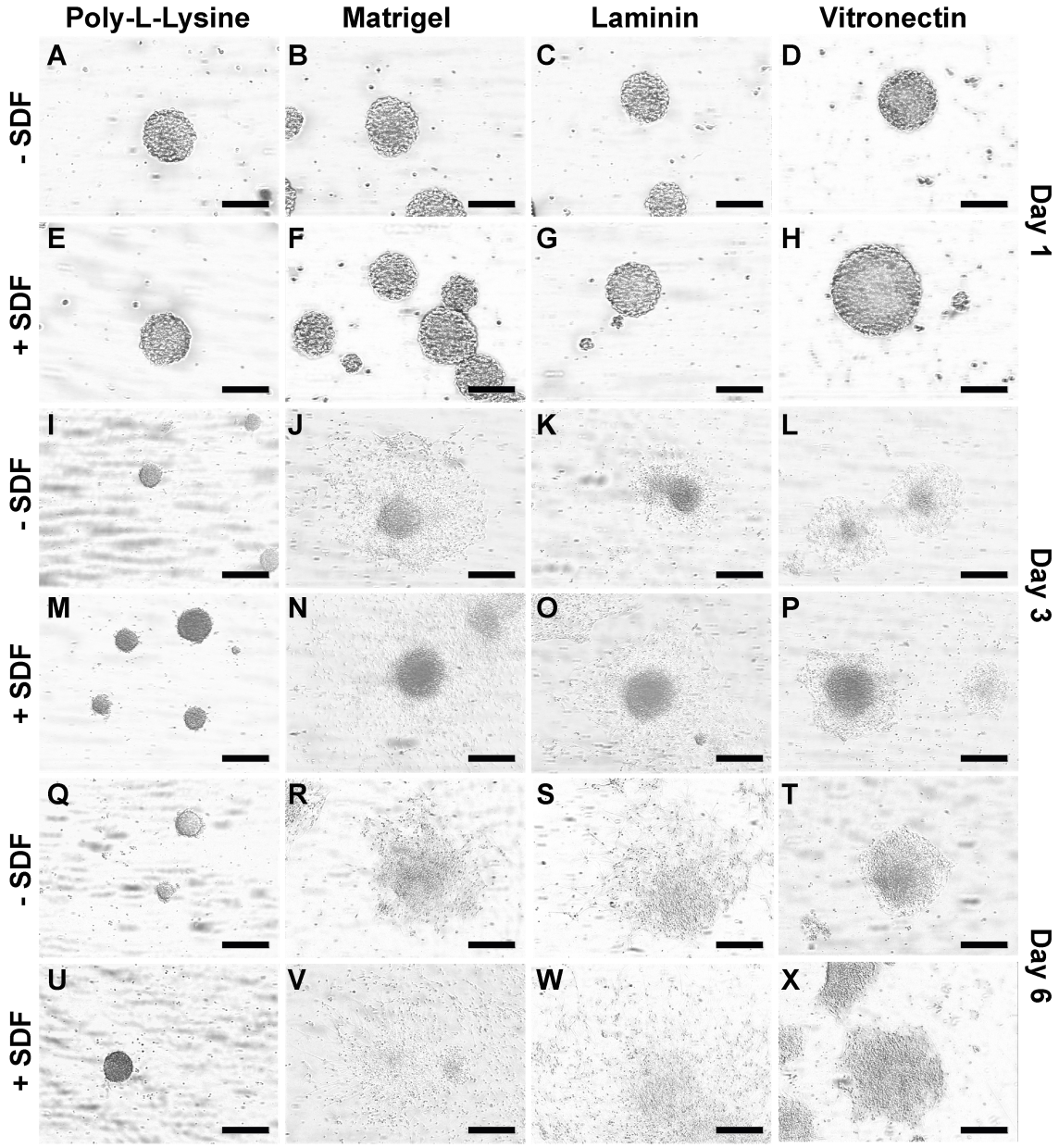

Figure 2.1: Morphology of migrating NPSCs supplemented with and without SDF-1α. NPSCs supplemented without SDF-1α migrating at day 1 (A-D), day 3 (I-L) and day 6 (Q-T) compared to those supplemented with SDF-1α at day 1 (E-H), day 3 (M-P), and day 6 (U-X). Scale bar is 250 μm.

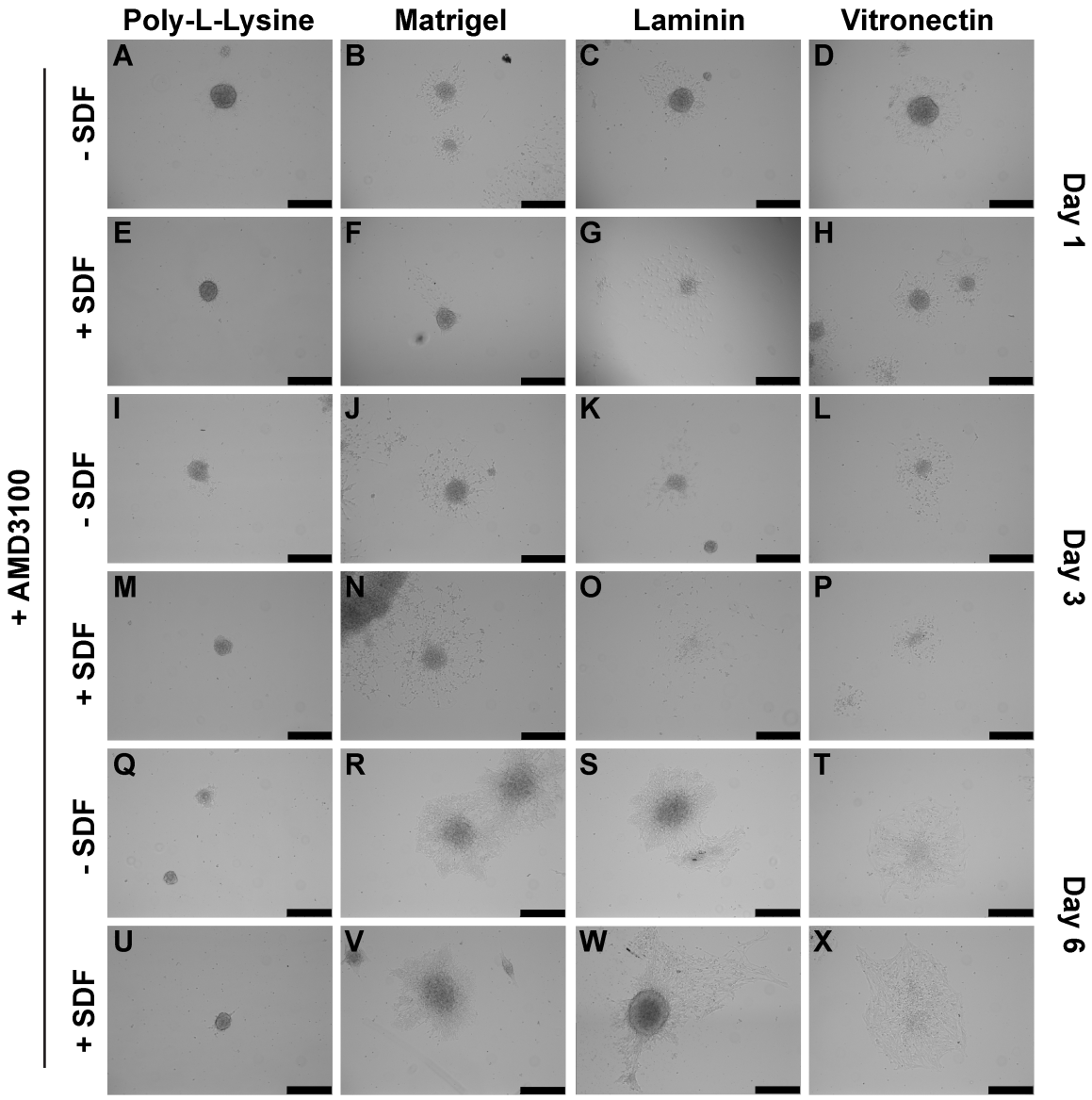

Figure 2.2: Morphology of migrating NPSCs on extracellular matrix substrates with or without SDF-1 α or AMD3100 supplementation. NPSCs supplemented AMD3100 without SDF-1α migrating at day 1 (A-D), day 3 (I-L) and day 6 (Q-T) compared to those supplemented with AMD3100 and SDF-1α at day 1 (E-H), day 3 (M-P), and day 6 (U-X). Scale bar is 250 μm.

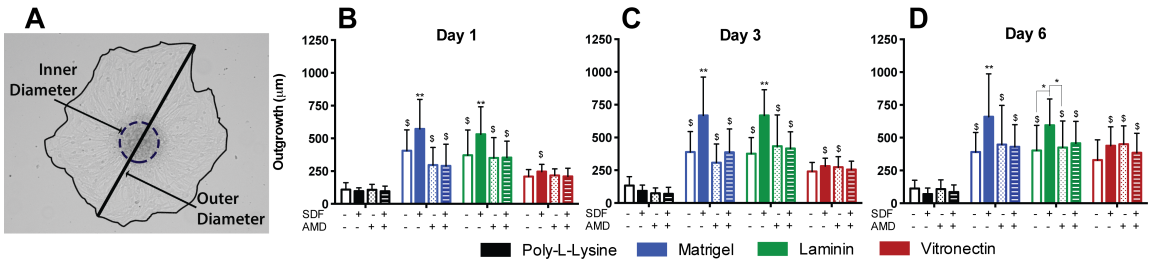

Figure 2.3: NPSC radial migration with and without SDF-1α or AMD3100 supplementation. Radial NPSC migration was determined by the longest outer diameter of neurosphere migration normalized to inner sphere diameter and reported in microns (A). Direct comparisons of NPSC radial migration on poly-L-lysine, Matrigel, laminin, and vitronectin with and without SDF-1α or AMD3100 supplementation at days 1, 3, and 6 (B-D). $p<=0.01 compared to poly-L-lysine controls; *p<=0.05;**p<=0.01 compared to all other supplementation within substrate groups unless specified otherwise.

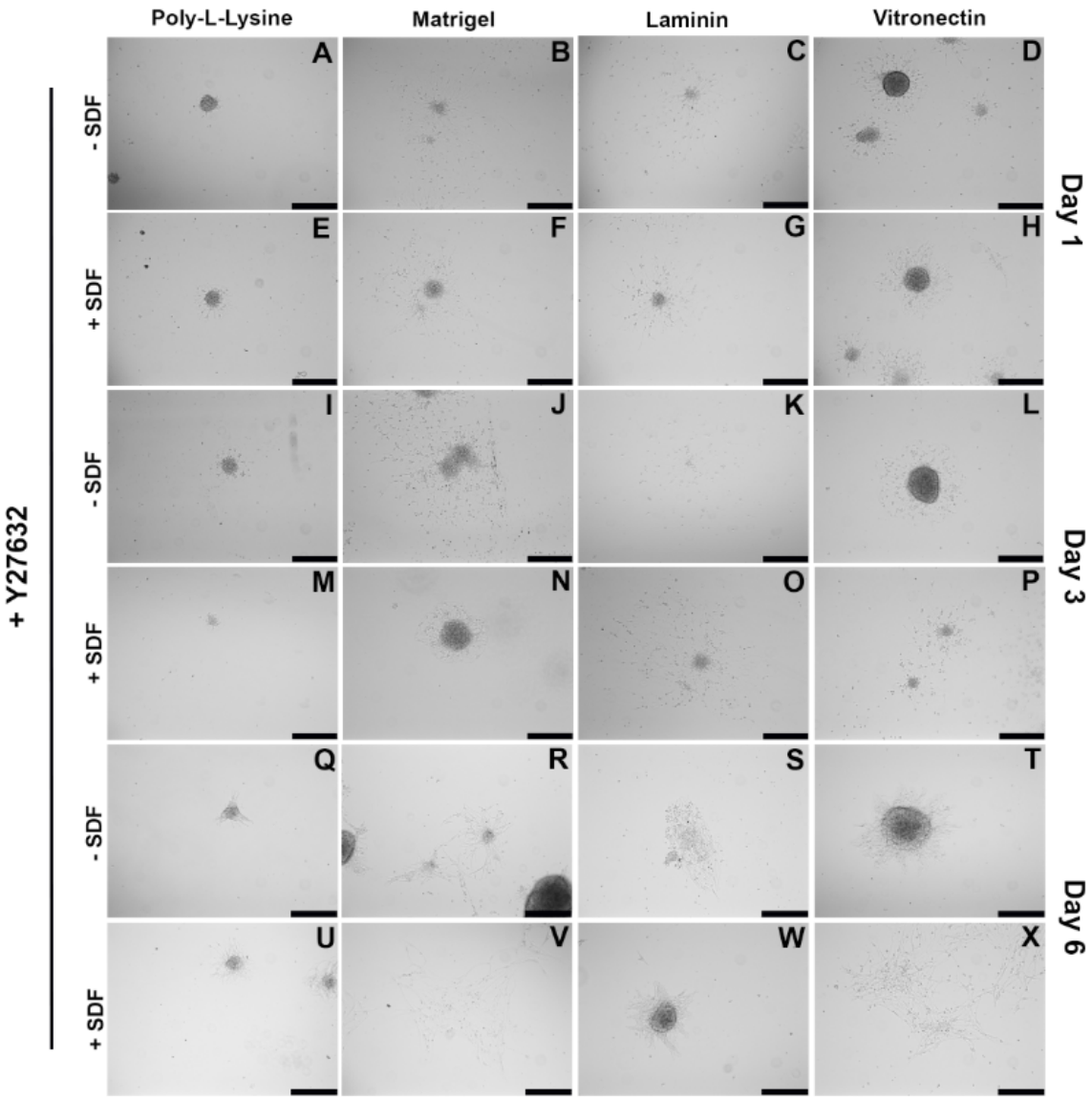

Figure 2.4: Morphology of migrating NPSCs supplemented with Y-27632 and with and without SDF-1α. NPSCs supplemented with Y-27632 without SDF-1α migrating at day 1 (A-D), day 3 (I-L) and day 6 (Q-T) compared to those supplemented with Y-27632 and SDF-1α at day 1 (E-H), day 3 (M-P), and day 6 (U-X). Scale bar is 250 μm.

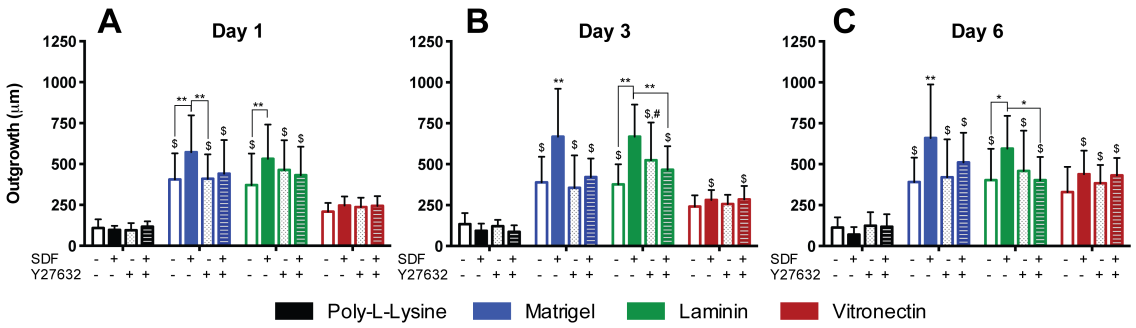

Figure 2.5: NPSC radial migration with and without SDF-1α or Y-27632 supplementation. Direct comparisons of NPSC radial migration on poly-L-lysine, Matrigel, laminin, and vitronectin with and without SDF-1α or Y-27632 supplementation at days 1, 3, and 6 (B-D). $p<=0.01 compared to poly-L-lysine controls; *p<=0.05;**p<=0.01 compared to all other supplementation within substrate groups unless specified otherwise.

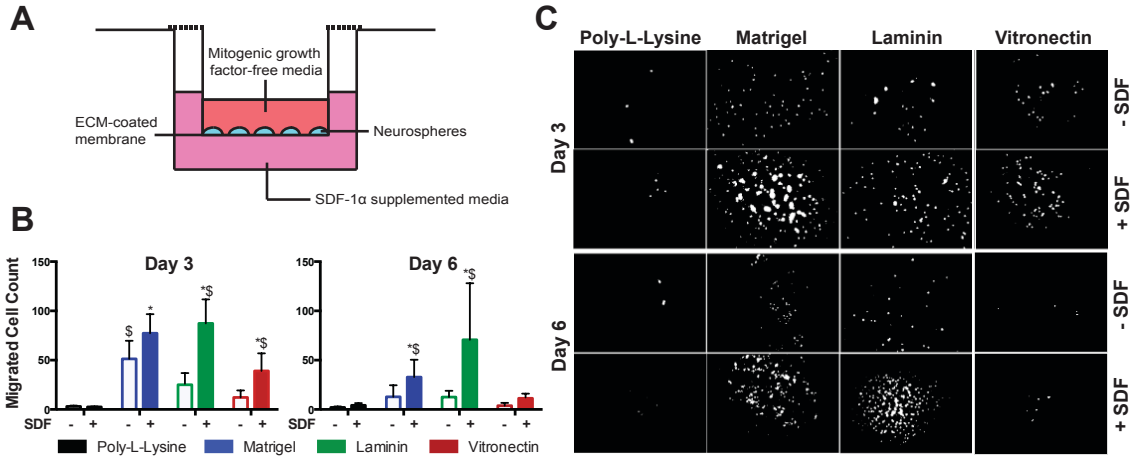

Figure 2.6: Chemotactic NPSC Migration on poly-L-lysine, Matrigel, laminin, and vitronectin with and without SDF-1α supplementation. Schematic depicting Millicell culture insert experimental set-up for chemotactic migration and migrated NSPC proliferation studies (A). Migrated cell counts were quantified by the particle counter in MatLab (B) for thresholded images of DAPI positive cells on the underside of the

Millicell culture insert membrane(C). $p<=0.01 compared to poly-L-lysine controls; *p<=0.05 compared to appropriate substrate groups without SDF-1α supplementation.

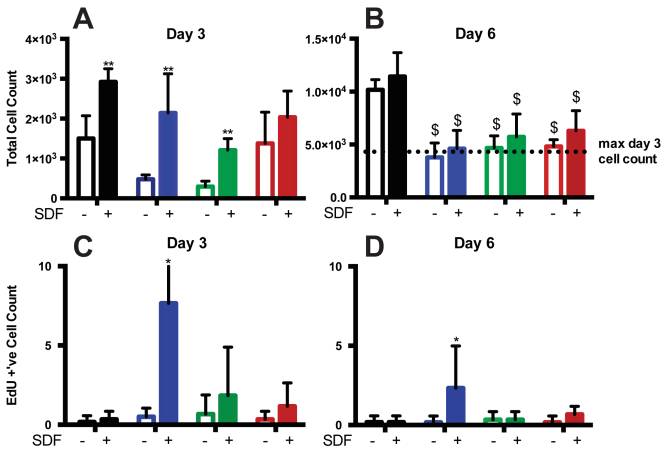

Figure 2.7: The effect of SDF-1α on proliferation of NPSCs cultured on poly-L-lysine, Matrigel, laminin, and vitronectin. Total NPSC proliferation was determined using the PicoGreen dsDNA quantification kit to calculate total cell number at days 3 and 6 (A, B respectively). NPSCs which migrated through Millicell culture inserts towards an SDF-1α sink (1μg/mL) were incubated with EdU for 4 hrs. Thresholded images of EdU positive cells were analyzed using the particle counter in MatLab for number of cells at 3 and 6 days (C, D respectively). $p<=0.05 compared to poly-L-lysine controls; *p<=0.05; **p<=0.01 compared to appropriate substrate groups without SDF-1α supplementation.

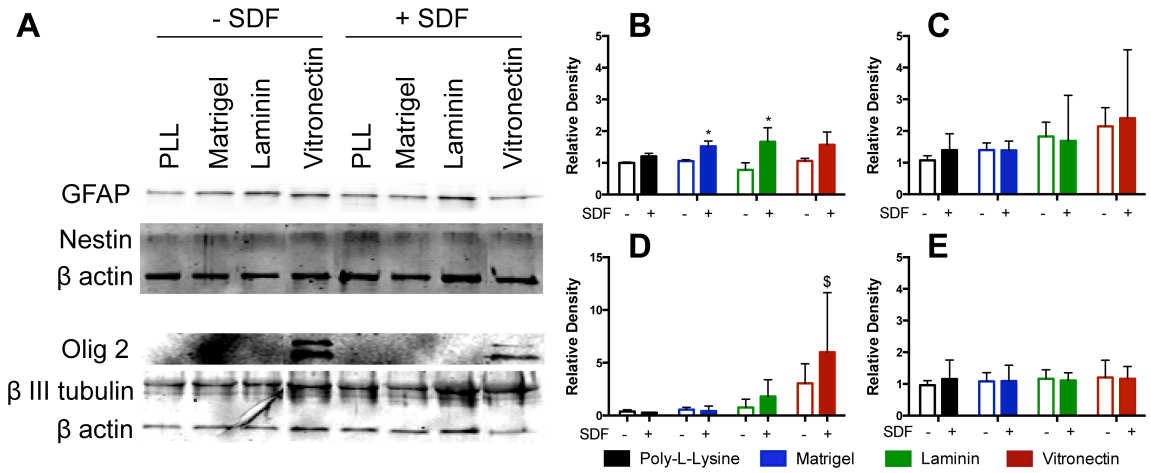

Figure 2.8: Western blot analysis of relative protein expression in NPSCs cultured on poly-L-lysine, Matrigel, laminin, and vitronectin. Phenotypic probes included β III tubulin (A,B), GFAP (A,C), Olig2 (A,D), and nestin (A,E), proteins indicative of young neurons, astrocytes, oligodendrocytes and NPSCs, respectively. Bands were analyzed using the LI-COR ImageStudio software for relative density and normalized to β-actin controls (B-E). $p<=0.05 compared to poly-L-lysine controls; *p<=0.05 compared to appropriate substrate groups without SDF-1α supplementation. Note that representative Western Blots for NPSC lysates presented were truncated to exclude extraneous sample groups (A).

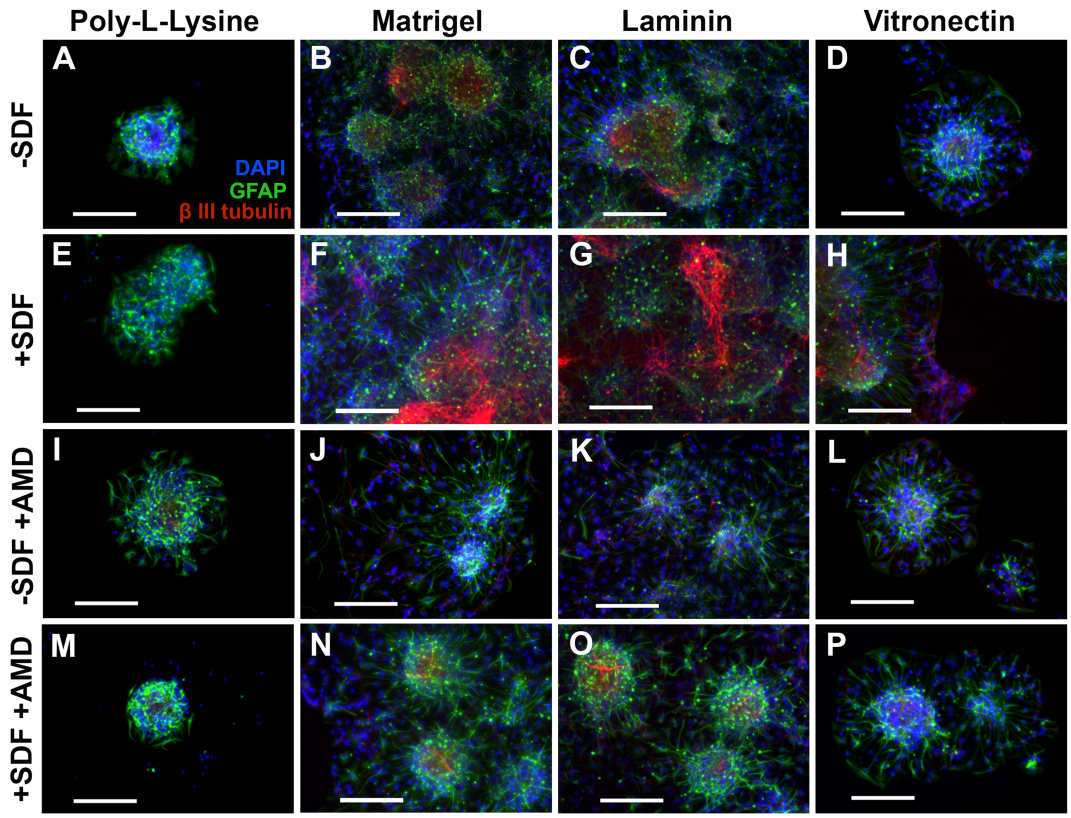

Figure 2.9: Immunocytochemistry for astrocytes and new neurons at day 3. Samples were probed for GFAP (green channel) and β III tubulin (red channel) indicative of astrocytes and young neurons, respectively. NPSCs were cultured on poly-L-lysine, Matrigel, laminin, and vitronectin without any supplementation (A-D); with SDF-1α (E-H); with AMD3100 (I-L); or with SDF-1α and AMD3100 (M-P). All scale bars are 100 μm.

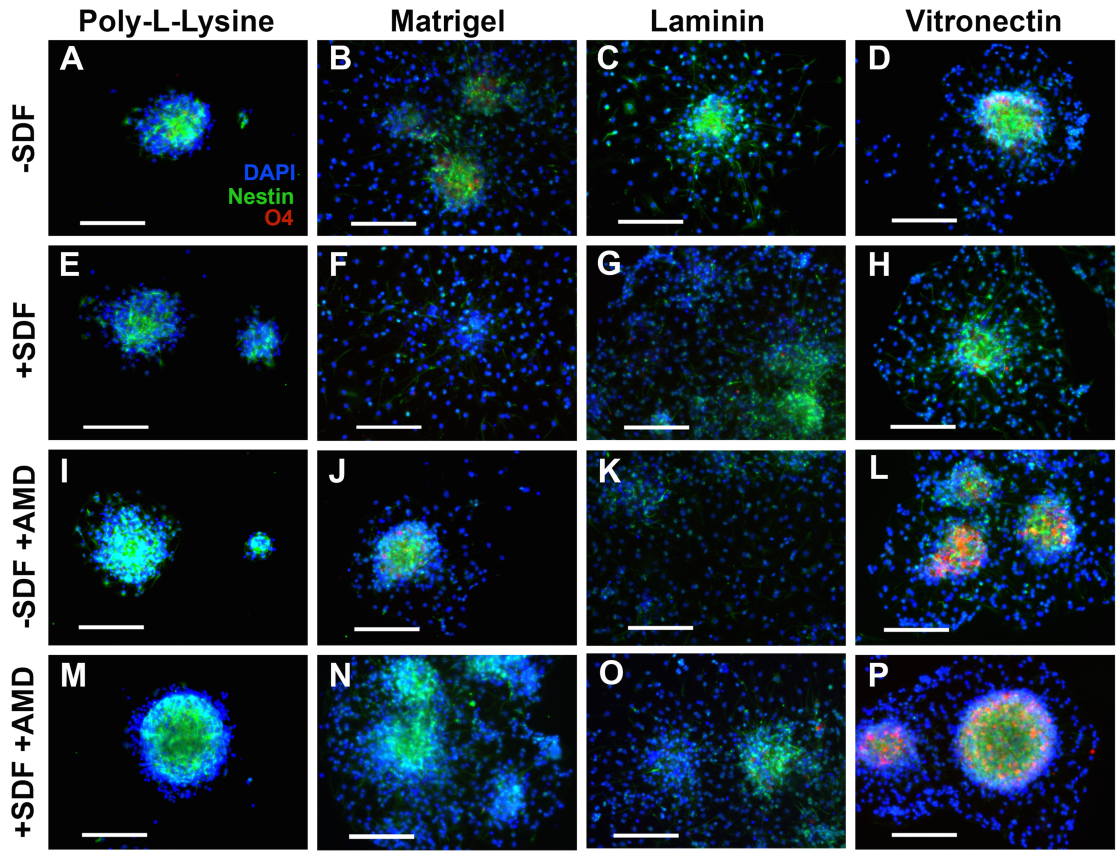

Figure 2.10: Immunocytochemistry for oligodendrocytes and NPSCs at day 3. Samples were probed for O4 (red channel) and nestin (green channel) indicative of oligodendrocytes and NPSCs, respectively. NPSCs were cultured on poly-L-lysine, Matrigel, laminin, and vitronectin without any supplementation (A-D); with SDF-1α (E-H); with AMD3100 (I-L); or with SDF-1α and AMD3100 (M-P). All scale bars are 100 μm.

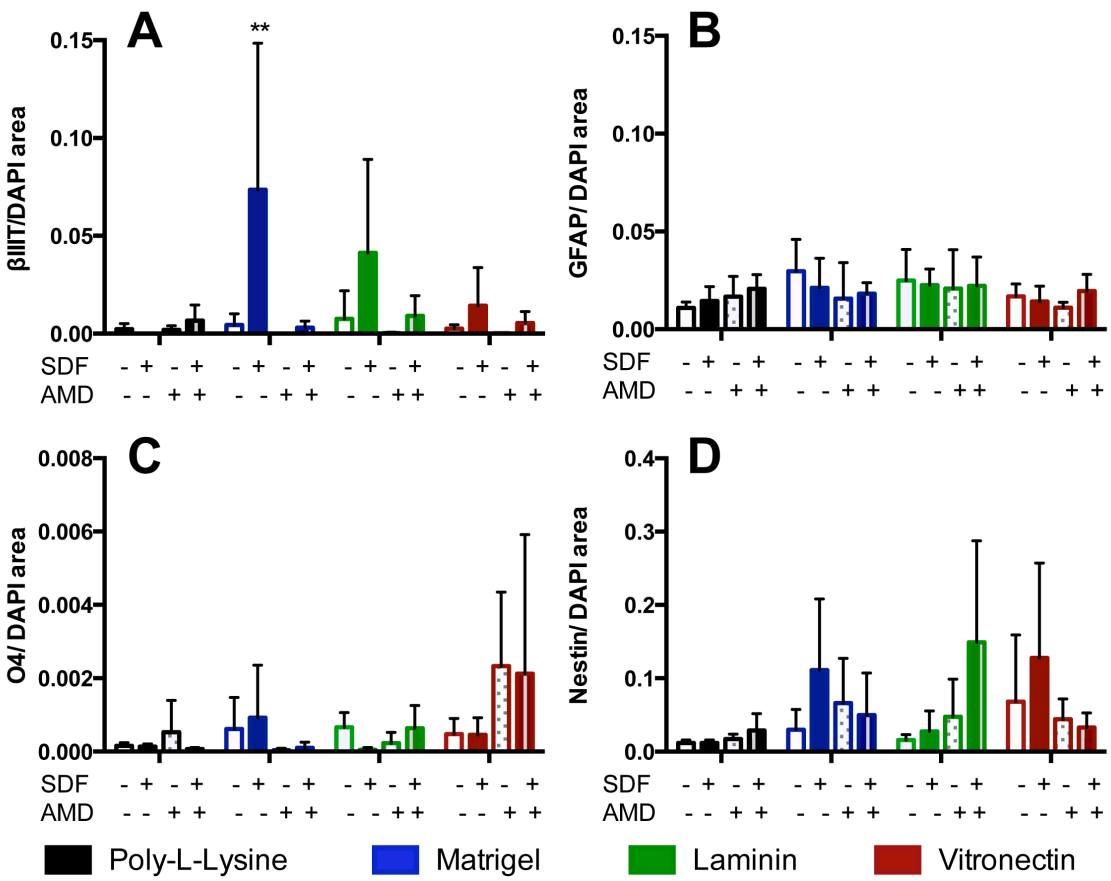

Figure 2.11: Quantification of immunocytochemistry positive staining. Thresholded images of independent color channels were quantified by summation of pixel value of the channel of interest and normalized to DAPI (blue channel) to determine relative levels of positive staining for β III tubulin (A), GFAP (B), O4 (C), and nestin (D). **p<=0.01 compared to all other supplementation within substrate group.

CHAPTER 3

ENHANCING NEURAL STEM CELL RESPONSE TO SDF-1α THROUGH HYALURONIC ACID-LAMININ HYDROGELS

3.1 Introduction

The impact of traumatic brain injury (TBI) has only recently garnered recognition from many social and healthcare communities despite its long-standing prevalence in the U.S. Approximately 1.7 million people sustain a TBI annually and the costs associated with TBI create a $76.5 billion strain on the American healthcare system and economy [4,6,144]. Long-term dysfunctions associated with TBI (e.g. chronic traumatic encephalopathy and motor impairment) [131,145,146] are largely due to the secondary, biochemical injury that follows the primary, mechanical insult; however, no clinical treatments directly target these underlying pathologies associated with TBI. Pre-clinical studies have investigated stem cell transplantation as a means to mitigate the effects of the secondary injury, but have suffered from staggeringly low rates of cell survival and engraftment (2-4%) [104-106,137]. This major limitation is mainly attributed to the cytotoxic injury microenvironment created by a systemic and neural inflammatory response, which is mediated by inflammatory cells that infiltrate the blood brain barrier and locally activated glia, respectively [20,22,147]. Activated glia also secrete factors that promote the endogenous repair response including the chemokine stromal cell-derived factor 1α (SDF-1α), which has been shown to play a critical role in recruitment of endogenous neural progenitor/stem cells (NPSCs) to the site of injury [53,55]. Exploiting this endogenous SDF-1α signaling paradigm for exogenous transplant strategies may serve to increase NPSC migration and engraftment into the surrounding tissue following

transplantation. As such, we aimed to develop a neurotransplantation platform that promotes exogenous cell response to injury-relevant SDF-1α signaling.

Tissue-engineered constructs have been used previously in an attempt to create a permissive transplant microenvironment; often in the form of hydrogels as their mechanical and cellular adhesion properties are easily tuned to mimic native neural tissue. The extracellular matrix (ECM) of native brain tissue is largely comprised of proteoglycans (e.g. lecticans), hyaluronic acid and tenascin C and R [148,149]. Specifically, the glycosaminoglycan hyaluronic acid (HA) is prominently expressed near neural stem cell niches and neuroblast migration routes (within the subventricular zone and rostral migratory stream, respectively) [125]. HA-based hydrogels are therefore a natural extension into mimicking the native neural ECM, and numerous groups have reported that HA-based hydrogels support survival, differentiation and proliferation of neural cell types *in vitro* and *in vivo*[129,150-152]. However, the effect of HA on NPSC migration remains largely unexplored despite the knowledge that normal physiological NPSC migration *in vivo* follows an HA-rich route [125]. Given these findings, the benefit of elucidating the relationship between HA and NPSC migration becomes evident.

Recent cell signaling studies have identified crosstalk between HA and the injury-related chemokine SDF-1α in mesenchymal (MSCs)[153] and hematopoietic stem cells (HSCs)[154,155] that resulted in heightened responsiveness to SDF-1α gradients. For example, MSCs cultured on HA substrate upregulate the SDF-1α receptor CXCR4, indicative of signaling crosstalk between HA and SDF-1α-axes [153]. The probability for similar HA-SDF-1α crosstalk mechanisms to exist in NPSCs is high, as NPSCs inherently express CXCR4 and the primary HA receptor CD44 [156,157]. Previous HA hydrogel platforms for neural tissue engineering considered HA a “blank slate” where tethered

protein or peptide-binding motifs serve as the primary cellular interfacing domains. However, we postulate that rather than serving as a "blank slate", HA will actively contribute to promoting NPSC chemotactic migration through HA-SDF-1α crosstalk.

Knowledge of HA-SDF-1α crosstalk will significantly inform next generation hydrogel systems capable of biochemically priming neurotransplants to dynamically respond to the local injury environment. We acknowledge that HA alone, however, is not sufficient to promote NPSC adhesion and migration effectively[130]. Thus, incorporation of an ECM protein known to support NPSC migration may provide the appropriate infrastructure for NPSCs to respond to SDF-1α gradients. We have previously reported that laminin and SDF-1α work synergistically to increase NPSC migration *in vitro* [2]. Therefore, in this work we have investigated a dual-purpose hydrogel system comprised of both HA (to modulate CXCR4 expression) and laminin (to provide adhesive cues). We hypothesize that HA-laminin hydrogels will 1. increase NPSC responsiveness to SDF-1α gradients and 2. provide a substrate that facilitates NPSC migration in response to injury relevant SDF-1α gradients, thereby equipping NPSCs with tools to dynamically respond to the neural injury environment.

3.2 Experimental Methods

3.2.1. Materials for polymer synthesis

3,3 Dithiopropionic acid (DTPA), anhydrous methanol, anhydrous ethanol, hydrazine hydrate (HH), hexane, concentrated sulfuric acid, ethyl ether, hydrochloric acid (HCl), sodium hydroxide (NaOH), sodium chloride (NaCl), hyaluronic acid sodium salt (HA) from Streptococcus equi, N-3-dimethylaminopropyl-N′-ethylcarbodiimide hydrochloride (EDC), 5,5'-dithiobis-2-nitrobenzoic acid (Ellman's reagent), and laminin-111 were purchased from Sigma Aldrich (St. Louis, MO, USA). Dithiothreitol (DTT) was

purchased from Gold Biotechnology (St. Louis, MO, USA). Poly(ethylene glycol) divinyl sulfone (PEGDVS) 5 kDa was purchased from JenKem Technology USA (Allen, TX, USA).

3.2.2. HA-Lm Gel Formation

Dithiopropionic dihydrazide (DTPH) was synthesized from DTPA and HH in a two-step reaction as previously described [158]. High molecular weight HA was functionalized with thiol groups through conjugation of the terminal hydrazides on DTPH to the carboxyl groups on HA using EDC chemistry and subsequent reduction of disulfide bonds using DTT as previously described [159]. ^{1}H NMR spectra was collected in D_2O (400 MHz Varian liquid state NMR, Agilent Technologies, Santa Clara, CA, USA), and Ellman's reagent test was used to quantify the concentration of conjugated thiols [160]. HA-S was sterilized by ethylene oxide gas and stored at -20°C.

HA-S hydrogels were formed via Michael-type addition crosslinking with PEGDVS as previously reported[116]. Briefly, PEGDVS was dissolved in media at a concentration that yielded an equimolar ratio of thiol-reactive groups to thiols present on the HA-S. HA-S was dissolved in pH 3 mitogenic growth factor-free culture media (formulation described under section 2.2 NPSC isolation and culture) and titrated between pH 7 and pH 8 with 1 M NaOH using phenol red as a colorimetric indicator of pH. The HA-S solution was mixed with an equal volume of crosslinker solution and vortex mixed for 15 seconds prior to plating.

Laminin was determined to have free thiols available for binding by Ellman's reagent test, presumably from its cysteine-rich β chain (data not shown). Laminin was conjugated to PEGDVS via Michael addition at 0.01 wt% and 0.10 wt% respectively in PBS for 15 minutes at room temperature. The solution was purified by dialysis against Tris-buffered saline to remove unbound PEGDVS and freeze dried. Capacity for covalent

immobilization of laminin was evaluated by ^{1}H NMR spectra in D_2O. Spectra were analyzed for ratio of PEG groups to vinyl groups and compared to non-reacted PEGDVS spectra to observe differences in vinyl groups available for binding. Based on data presented in section 3.1, laminin was incorporated within the gel at pre-determined concentrations by mixing with PEGDVS media solution and allowed to react 15 minutes at room temperature prior to mixing with HA-S solution, where PEGDVS concentration was adjusted to account for laminin incorporation.

3.2.3. NPSC isolation and culture

NPSCs were isolated from the medial and lateral germinal eminences of E14.5 C57BL/6 mice based on previously published protocols[135] and in accordance with a protocol approved by the Institutional Animal Care and Use Committee at Arizona State University. Briefly, mice were anesthetized at 3% isoflurane, rapidly decapitated, and fetuses were extracted from both uterine horns. Fetal tissue was rinsed in cold Leibovitz medium (Life Technologies, Carlsbad, CA) at each stage of the germinal eminence dissection. The germinal eminences were rinsed with sterile, cold Leibovitz medium before mechanical dissociation in working NPSC medium (glucose (6 mg/mL, Acros Organics, Geel, Belgium), HEPES buffer (5mM), progesterone (62.9 ng/mL), putrescine (9.6 μg/mL), heparin (1.83μg/mL), B27 growth supplement (1X, Life Technologies), epidermal growth factor (20 ng/mL), fibroblast growth factor (5 ng/mL), insulin (5 μg/mL), transferrin (5 μg/mL), sodium selenite (5 ng/mL) in Dulbecco's Modified Eagle Medium (Life Technologies), reagents from Sigma Aldrich unless otherwise specified) and plated at a density of 10^4 cells/mL in a humidified incubator at 37°C, 20% O_2, and 5% CO_2. NPSCs were cultured as non-adherent neurospheres in working NPSC medium, passaged by mechanical dissociation, and utilized for experiments between passages 3 through 6.

3.2.4. NPSC Response to Varied HA-Lm Gel Formulations

Gels were varied in HA and laminin concentration (Table 3.1) and optimized based on cellular response—i.e. NPSC viability, density and chain formation. HA concentrations (1.75 wt%, 2.00 wt%, 2.25 wt%) were selected based on previously reported rheological data for HA-PEGDVS gels [116] to mimic the stiffness of native neural tissue (0.2-1.0kPa) [117] and on observations that gels below 1.75 wt% HA did not support effective NPSC encapsulation necessary for transplantation. Laminin concentrations (0%, 0.005%, 0.01%, 0.015%) were selected based on hydrogels in the literature and as an extrapolation of our 2D ECM culture model[2,159,161]. HA-Lm gel films (100 μm thickness) were formed in 24-well plates (occupying approximately 85% of the well bottom) at 37 °C for 15 hours, and single cell NPSC suspensions ($2x10^3$ cells/well) were seeded directly on top of the gel. NPSCs were incubated for 1 hour to allow for adherence to the HA-Lm gel prior to the addition of 500 μL of mitogenic growth factor-free NPSC media to each well. NPSCs were cultured for 72 hours prior to analysis of viability, density, and chain formation.

3.2.4.1. Cell Density and Viability

After rinsing HA-Lm gels with sterile phosphate buffered saline, NPSCs were stained with Live/Dead assay (Biotium, Hayward, CA). Live cell counts were used to calculate cell density (cells/cm^2) as a measure of cell attachment to the HA-Lm gel. Fluorescent red (dead) and green (live) channel images (n=6 gels per goup, n=3 ROI per gel) were analyzed for number of positively stained cells using the particle counter plugin for Image J (NIH, Bethesda, MD) and reported as percent viability.

3.2.4.2. Chain Length

It was observed that gel formulations that supported high cell density and viability also supported the formation of chain-like NPSC assemblies as defined by two or more NPSCs visibility connected by continuous outgrowth in a linear fashion. Therefore, NPSC chain length was measured in MatLab as a tertiary metric for gel formulation optimization after 72 hours of culture on HA-Lm gels. Live cell images (n=6 gels per goup, n=3 ROI per gel) were analyzed for longest linear chain length in each frame.

3.2.5. Physical Properties of HA-Lm Gel

3.2.5.1. HA-Lm gel stiffness

Parallel plate rheological measurements were used to determine the storage and loss moduli of HA-Lm gels during gelation (Physica MCR101, Anton Paar, Graz, Austria). Briefly, 500 μL HA-Lm solutions were pipetted onto the fixed plate immediately following mixing and the moving plate was lowered to a height of 0.5mm. The gels were tested at 0.5 % strain with an oscillatory frequency of 1 Hz. The stage was heated to 37°C and maintained within a humid environmental chamber. Storage and loss moduli measurements were taken continuously for 6 hrs.

3.2.5.2. HA-Lm gel porosity and microstructure

HA-Lm gels (7 mm thickness) were formed in 96 well plates for 15 hours, dehydrated through immersion in a series of ethanol washes and subsequently dried with the Balzers CPD020 critical point dryer (Balzers Union Ltd., Liechtenstein) using liquid carbon dioxide as the transition solvent. Samples were cut open to expose interior microstructures, sputter coated with gold/palladium (60:40) using a Technics Hummer

Sputter Coater (Anatech Ltd., Alexandria, VA) and imaged via scanning electron microscopy (SEM) on an XL30 ESEM-FEG (FEI, Hillsboro, OR) with a 5kV beam and spot size of 3. Images were analyzed in Matlab for pore diameter and aspect ratio (n=3 images, 90-120 pores quantified per image).

3.2.6. NPSC CXCR4 Expression on HA-Lm Gel

3.2.6.1. Temporal CXCR4 Expression

HA-Lm gel films (Low HA/Moderate Lm, 100 μm thickness) were formed in the bottom of 6 well plates and allowed to gel for 15 hours in humid conditions at 37°C (n=3). NPSCs were seeded in mitogenic growth factor-free media as single cell suspension (5 x 10^5 cells/mL) directly on top of the films. NPSCs seeded on poly-L-lysine coating (PLL, 10μg/cm², MP Biomedicals, Solon, OH) or maintained in non-adherent conditions served as controls. NPSCs were allowed to adhere for 1 hour prior to taking baseline samples (time 0). After culture for 0, 24, 48 and 72 hours, cells were lysed by mechanical agitation in cold RIPA buffer (Bioworld, Dublin, OH) containing proteinase inhibitor cocktail (50 mM Tris-HCl, 150 mM NaCl, 1 mM EDTA1, % NP-40, 0.5% Sodium Deoxycholate, 0.1% SDS, 0.1% protease inhibitor cocktail (Sigma)). Protein concentration was determined by bicinchoninic acid assay (G-Biosciences, St. Louis, MO) prior to SDS-PAGE electrophoresis in 12% bis-acrylamide gels and western blotting for NPSC CXCR4 expression using β-actin to control for loading variability (rabbit anti-CXCR4, 39 kDa, cat no: 2074, Abcam, Cambridge, England; mouse anti-β-actin, 45 kDa, cat no: 926-42212, LI-COR, Lincoln, NE). The Odyssey Infrared Imaging System (LI-COR) was used to visualize bands stained with appropriate secondary antibodies (donkey anti-rabbit IRDye 800; donkey anti-mouse IRDye 680, LI-COR). Band density was quantified with the Image Studio software (LI-COR), normalized internally to β-

actin and externally to non-adherent control culture samples and reported as relative density.

3.2.6.2. Mechanistic CXCR4 Expression

HA-Lm gels were formed as in the temporal CXCR4 expression experiments. NPSCs (5 x 10^5 cells/mL) were seeded on HA-Lm gels or on HA only gels. Prior to seeding, NPSCs were either pre-treated with anti-CD44 (100μg/mL) to inhibit HA interactions or its isotype control for 45 minutes at 37°C (rat anti-CD44, Millipore, Darmstadt, Germany; rat IgG1 κ isotype control, BioLegend, San Diego, CA) or received no pre-treatment. NPSCs were cultured for 0 and 48 hours, lysed and analyzed by western blotting for CXCR4 expression as reported for temporal CXCR4 expression experiments (rabbit anti-CXCR4, Abcam; mouse anti-beta actin, LI-COR).

3.2.7. Chemotactic NPSC Migration

HA-Lm gels (1 mm thickness) were formed at the bottom of 24 well plate 8 μm pore size Transwell inserts (Corning Inc., Corning, NY) and allowed to gel for 15 hours at 37°C in humid conditions (n=3 per group). Groups included HA only gels, HA-Lm gels only or HA-Lm gels impregnated with the CXCR4 antagonist AMD3100 (5 μg/mL; Santa Cruz Biotechnology, Santa Cruz, CA), rat anti-CD44 (100 μg/mL; Millipore), or an anti-CD44 isotype control (100 μg/mL; rat IgG1 κ BioLegend). NPSCs were then seeded directly on top of the gels (10^5 cells/mL) and cultured for 24 and 48 hours in mitogenic growth factor-free media. NPSCs seeded onto impregnated gels were incubated with their respective supplementation at the appropriate concentration for 45 minutes at 37 °C prior to seeding. HA-only or HA-Lm gels were exposed to no SDF-1α, uniform SDF-1α or a gradient of SDF-1α. Uniform SDF-1α gels were allowed to saturate with SDF-1α (1 μg/mL; PeproTech Inc., Rocky Hill, NJ) prior to NPSC seeding and supplemented with 1

μg/mL SDF-1α in both the top and bottom Transwell chambers, while gradient SDF-1α gels were not pre-saturated and the gradient was maintained out to 48 hours. SDF-1α concentration of 1 μg/mL was determined based on previous studies in NPSCs[2]. Effective SDF-1α gradient maintenance out to 48 hours was validated by enzyme-linked immunosorbent assay (ELISA, Figure 3.8). Briefly, gels were formed in Transwell inserts and exposed to SDF-1α gradients as in chemotactic experiments for 12, 24 or 48 hours (n=3 per time point). SDF-1α concentration of both the lower chamber (donor) and upper chamber (receptor) of the Transwell insert (Figure 3.8) were determined by ELISA. At 24 and 48 hours, NPSCs that had migrated through the gel to the Transwell membrane were stained with DAPI and counted using the cell counter ImageJ plugin (NIH, Bethesda, MD).

3.2.8. Statistical Analysis

Two-way ANOVA with Tukey's post hoc test was performed for all experiments where statistical analysis was used (NPSC density, viability, chain length, temporal CXCR4 expression and mechanistic CXCR4 expression), where $\alpha=0.05$ in Prism 6 (GraphPad, Inc., La Jolla, CA).

3.3. Results

3.3.1. Formation of HA-Lm Gel Components

Successful thiolation of HA was evidenced by the appearance of thiol peaks (2.5 and 2.7 ppm) in the ^{1}H NMR spectrum of HA-S compared to that of HA prior to thiolation (Figure 3.1A). Moreover, covalent immobilization of laminin to PEG-DVS was apparent through both the appearance of peptide peaks in the NMR spectrum of PEG-DVS (Figure 3.1B) and the reduction of free vinyl groups relative to PEG groups in PEG-

DVS (Figure 3.1C). Collectively, these data indicate that our methods for formulating HA-Lm gel components enable the covalent immobilization of laminin within an HA hydrogel.

3.3.2. NPSCs Survive and Spread on HA-Lm Gels at 72 hours

NPSC density after 72 hours of culture on HA-Lm gels was found to be significantly higher on gels with lower HA concentrations and higher laminin concentrations (Low HA/ Moderate and High Lm) compared to all other groups, as illustrated in Figure 3.2A and Figure 3.3 ($p<0.0001$). Moreover, Low HA/ Moderate and High Lm gels were the only gels to support NPSC density increase above the initial plating density (Figure 3.2A). In quantifying percent viability, groups with low cell density yielded high variance in percent viability; therefore, groups with a coefficient of variance above 30% were omitted from statistical analysis (omitted groups included High HA gels and No Lm gels). NPSC viability was significantly higher on gels with lower HA concentrations and higher Lm concentrations (Low HA/Moderate and High Lm) compared to all other groups ($p=0.0177$, 0.0026, respectively). Moreover, NPSC chain length was significantly higher on gels that supported high NPSC density and viability (Low HA/ Moderate and High Lm) as compared to all other groups ($p<0.0001$) and on Moderate HA/ High Lm gels compared to all other Moderate HA gels ($p=0.0016$; Figure 3.4). Overall, Low HA/Moderate and High Lm gels supported the highest NPSC density and viability and longest NPSC chain length. The Low HA/Moderate Lm gel formulation was chosen for subsequent experimentation to minimize laminin reagent consumption.

3.3.3. HA-Lm Gel Physical Properties are Relevant to Native Neural Tissue

The storage modulus of HA-Lm gels (Low HA/Moderate Lm) was measured as 1.02 kPa by rheology after gelation for 6 hours (G', Figure 3.5A), which mimics the stiffness of native neural tissue (0.2-1kPa) [117]. Gelation time was 24 minutes at 37°C in humid conditions as indicated by the increase in storage modulus over the loss modulus (Figure 5A). SEM images illustrated a highly porous microstructure within the HA-Lm gel with pore size ranging from 2-17 μm and an average aspect ratio of 2.12 (Figure 3.5B), providing appropriate porosity for cellular infiltration.

3.3.4. HA-Lm Gel Upregulates NPSC CXCR4 Protein Expression

NPSC CXCR4 expression was significantly increased after 48 hours of culture on HA-Lm gel compared to NPSCs cultured on poly-L-lysine (PLL) at all time points ($p=0.0408$) and to NPSCs cultured on HA-Lm gel for 24 ($p=0.0145$) and 72 hours ($p=0.0097$). After 72 hours of culture, CXCR4 expression on HA-Lm gel returned to basal PLL CXCR4 expression levels (Figure 3.6). The significant increase in CXCR4 expression observed at 48 hours on HA-Lm gel was abrogated by inhibiting HA interactions with anti-CD44 (Figure 3.7A,B). CXCR4 expression after 48 hours of culture on HA-Lm gel impregnated with anti-CD44 was significantly reduced compared to that on HA-Lm gel without supplementation ($p<0.0001$) and was not significantly different from CXCR4 expression on PLL at 48 hours (Figure 3.7B). Moreover, this reduction was due to HA interaction inhibition and not simply to antibody supplementation as CXCR4 expression on gels impregnated with anti-CD44 isotype control was not significantly different from that on HA-Lm gels without supplementation (Figure 3.7B). NPSC adherence, and subsequently cell lysate protein concentration, was too low on HA only gels to allow for visualization of CXCR4 expression by western blotting.

3.3.5. HA-Lm Gel Promotes NPSC Chemotactic Migration in Response to SDF-1α Gradients

The Transwell culture set-up successfully maintained an SDF-1α concentration gradient throughout the experiment, as determined by ELISA. After 48 hours, the SDF-1α concentration in the donor (lower chamber) was 1.6-fold higher than that in the receptor (upper chamber) (Figure 3.8). Correspondingly, NPSC migration in response to SDF-1α gradient was significantly increased at 48 hours when compared either to 24 hours of migration in a gradient, or to any time point in response to uniform SDF-1α concentration or no SDF-1α (Figure 3.9A-C,J; $p=0.0067$,<0.0001 respectively). A 3.8-fold increase in migration over uniform and no SDF-1α was also observed at 24 hours, however it was not significant ($p=0.0676$). Moreover, SDF-1α gradients play a critical role in mediating this response as evidenced by the reduction of NPSC migration to basal levels with the addition of the CXCR4 antagonist AMD3100 (Figure 3.9D,H). The addition of AMD3100 significantly reduced NPSC migration compared to HA-Lm gels without AMD3100 at both 24 and 48 hours (Figure 3.9J, $p=0.0299$, <0.0001 respectively). Conversely, NPSC migration in HA-Lm gels+AMD3100 was not significantly different from uniform and no SDF-1α groups at either 24 or 48 hours.

3.3.6. Enhanced NPSC Chemotactic Response in HA-Lm Gel Requires both HA and Lm

NPSC chemotactic migration was attenuated when laminin was excluded from the gel and abrogated when HA interactions were blocked with an antibody against HA receptor CD44 (Figure 3.10). At both 24 and 48 hours, NPSC chemotactic migration was significantly reduced on HA-only gels compared to HA-Lm gels ($p=.0085$,<0.0001 respectively). Interestingly, in HA-only gels NPSC migration at 48 hours increased 4.7-fold over that at 24 hours, although the difference was not statistically significant. While

a low level of chemotactic migration was preserved in the absence of laminin, inhibiting HA interactions with anti-CD44 abrogated NPSC chemotactic migration such that it was 10- and 8-fold less than NPSC chemotactic migration on HA-Lm gels at 24 and 48 hours, respectively. This significant decrease in NPSC migration in HA-Lm+anti-CD44 gels compared to HA-Lm gels at 24 and 48 hours ($p=0.0046$, <0.0001 respectively) was specifically due to HA interaction inhibition rather than to antibody supplementation as the isotype control for anti-CD44 did not affect NPSC migration.

3.4 Discussion

Historically, neural progenitor/stem cell (NPSC) transplantation following TBI has been plagued by low survival rates (2-4%) and poor engraftment into the surrounding tissue, which has impeded the full realization of NPSC transplant potential as a therapeutic intervention following TBI[25,102,106]. Some groups have turned to tissue engineered scaffolding to improve cell transplant survival and engraftment following TBI[122,124,162], while others have primed transplants biochemically for the injury microenvironment (i.e. CXCR4-overexpressing transplants) and observed increased viability and engraftment in the surrounding tissue[112,163]. While both approaches have yielded moderate improvements in transplant survival and engraftment, a dual-purpose hydrogel that simultaneously primes NPSC transplants for the injury microenvironment and provides the appropriate ECM infrastructure could offer the benefits of a multi-component transplant system while minimizing complexity.

Neural tissue engineered scaffolds have largely focused on mimicking the neural niche environment so as to provide cell transplants with an environment permissive to NPSC survival and engraftment. The mechanical properties of the niche are most often re-created in hydrogels for neural tissue engineering as they can be tuned to mimic the

stiffness of native neural tissue. Our HA-Lm gel has mechanical properties similar to the neural niche (1.02 kPa storage modulus[117], Figure 3.5), providing the appropriate mechanical cues to NPSCs. This point is reflected in the significantly higher NPSC viability and density observed on low HA gels compared to moderate and high HA gels (Figure 3.2). Given that HA content correlates with gel stiffness [116], it can be postulated that the mechanical properties of the low HA gels are better suited for maintenance of NPSC culture than those of the higher HA content gels. However, the niche provides more than just mechanical cues to its resident NPSCs; it also provides critical ECM and soluble signals.

Others have looked at incorporating peptide binding motifs (i.e. RGD or laminin binding domain[130,151]) and ECM proteins (i.e. fibronectin, collagen I, laminin[118,120,124,164]) within hydrogels to promote cell adhesion, however peptide binding motifs may not fully capture the functionality of the ECM protein they are intended to mimic and fibronectin and collagen I are not native to neural tissue. The vascular basement membrane protein laminin provides relevant ECM signaling to NPSCs in the subventricular niche where endogenous NPSCs have been shown to leave and home to the site of injury by way of the surrounding vasculature[32,48,165,166]. In our system, the inclusion of laminin significantly increased NPSC density, viability and chain formation compared to HA gels without laminin (Figures 3.2 and 3.4). Moreover, we have previously observed that signaling crosstalk between laminin and SDF-1α synergistically increases NPSC chemotactic migration[2]. Collectively, these data illustrate the significant role that laminin plays in regulating NPSC migratory behaviors in response to injury-relevant signaling.

Laminin alone does not comprise the niche and, as such, will not fully recapitulate the niche ECM environment for NPSC transplants. Within the subventricular niche, the glycosaminoglycan hyaluronic acid (HA) has been found at higher concentrations than elsewhere in the adult brain [125,126]. Interestingly, evidence of signaling crosstalk between the HA receptor CD44 and laminin was observed by Deboux et al., in which CD44-overexpressing NPSCs plated on laminin were observed to increase spreading and outgrowth [167], suggesting that the roles of laminin and HA in regulating NPSC fate within the niche environment may be more interconnected than previously described. Our data illustrate the critical individual roles that laminin and HA play in providing NPSCs with a substrate to support adherence and migration (laminin) and a substrate to regulate the NPSC receptor expression profile (HA). Upon inhibiting HA interactions, NPSCs remained adhered to the HA-Lm gel but their CXCR4 protein expression was significantly attenuated whereas excluding laminin abrogated NPSC adherence, leaving the system irrelevant for transplantation applications (Figure 3.6). CXCR4 protein expression within the adult brain is restricted to NPSCs, as such, maintenance of this phenotypic marker without compromising NPSC adhesion and migration may be attributed to the specialized microenvironment of the niche [136]. Therefore, we postulate that the ECM signals provided to NPSCs by the HA-Lm gel are more comprehensive in their recapitulation of the niche ECM environment than previously developed hydrogel systems.

Increases in CXCR4 protein expression on the HA-Lm gel directly correlated with increased NPSC chemotactic migration in response to gradients of the injury-relevant chemokine SDF-1α. Inhibiting NPSC interaction with either component of the gel significantly reduced chemotactic migration in response to SDF-1α gradients indicating the synergistic effect that HA and laminin have on promoting NPSC chemotactic

response to SDF-1α (Figure 3.10). Previous studies on NPSC migration in response to SDF-1α gradients when plated on laminin in 2D yielded data similar to that observed here for HA-Lm gels impregnated with anti-CD44 [2]. Increased NPSC chemotactic migration on HA-Lm gels is critically dependent on SDF-CXCR4 interactions as inhibition of this signaling axis with CXCR4 antagonist AMD3100 reduced NPSC migration to levels comparable to that on HA-Lm gel with either uniform or no SDF-1α (Figure 3.10); however, it is important to consider alternative mechanisms that may contribute to increased NPSC migration within the HA-Lm gel. CD44 interaction with HA has been observed to precede and facilitate the formation of focal adhesions in other cell types [168,169] and it is thought that CD44 works closely with integrin β1 to promote transmigration of intravenously injected NPSCs as they migrate towards regions of neural injury [167,170]. Therefore, the role of HA within the HA-Lm gel may not only be to promote CXCR4 expression but also to promote adhesion and migration on laminin. To this end, the results of using of laminin peptide sequences instead of full-length laminin could raise interesting questions regarding the distinct roles of HA and laminin within the gel. Given the mechanistic ambiguity surrounding potential crosstalk between HA and laminin, we feel that the inclusion of full-length laminin may more effectively allow these signaling events to occur. However, future mechanistic studies investigating the distinct role of laminin within the gel may utilize such peptides.

Interestingly, NPSC chemotactic response to SDF-1α was not completely abrogated after 48 hours of culture on HA-only gels (Figure 3.10). NPSCs cannot form focal adhesions to HA alone as HA interactions are mediated by receptor CD44 and the hyaluronan-mediated motility receptor (RHAMM), not by integrins [171]. Given that NPSC migration in 2D is typically focal adhesion-dependent[172,173], the chemotactic migration of NPSCs within an HA-only gel was a very intriguing finding. Moreover,

NPSC adherence to HA only gels in the absence of SDF-1α was minimal (Figure 3.7), leading us to suspect an interaction between HA and SDF-1α that may alter NPSC adhesion and migration behaviors. We postulate two potential scenarios in which NPSCs may migrate through HA-only gels in the presence of SDF-1α: 1. HA may promote NPSC ECM production and 2. NPSCs may exhibit migratory mode plasticity dependent on environmental conditions. HA has been observed to induce the production of integrin-binding osteopontin and collagens in other cell types [174,175]. Moreover, astrocytes are known to secrete ECM *in vitro* [176] and given the heterogeneous nature of the neurosphere assay [177,178], there may be a subset of NPSCs capable of secreting ECM within the HA only gel. NPSC migration through HA only gels was only observed after 48 hours, thus it is feasible that matrix is being produced on which the NPSCs are then able to migrate in a more typical focal adhesion-mediated manner, however further investigation is necessary to elucidate the potential formation of focal adhesions in this context, particularly in light of low NPSC adherence to HA only gels in the absence of SDF-1α. Alternatively, NPSC migration mechanisms may be more adaptive than previously described as environment-dependent migration mode plasticity has been observed in other cell types (i.e. 2D versus 3D [179,180]). In 3D, cells do not appear to form stable focal adhesions during migration but may instead depend on pseudopodia to move through the ECM [181,182]. Transient cell-matrix and cell-cell adhesion is also found in NPSCs migrating by chain migration mechanisms through the rostral migratory stream (RMS), an area with high concentrations of HA in the adult brain [125]. While chain migration on HA in the RMS draws an interesting conceptual parallel with data presented here, NPSC chain migration has been observed to be dependent on β1 integrin signaling and as such would still require a substrate that supports β1 integrin binding [39]. Interestingly, Avigdor et al. have proposed that SDF-1α may function to increase

CD44 avidity to HA in HSCs, allowing for increased HSC retention in SDF-1α rich niches independent of integrin anchoring[155]. Investigating HA-SDF-1α interaction by this mechanism and probing for the formation of focal adhesions in NPSCs migrating on HA-only gels in response to SDF-1α gradients would enlighten these postulations and provide insight into the mechanisms by which NPSCs are migrating in this context.

Regardless of mechanism, the capacity of NPSCs to migrate through the bulk of the HA-Lm gel, as opposed to on top of it or along an interface, indicates the relevancy of the gel to *in vivo* transplantation applications as these cells would be tasked with migration through the bulk of the gel into the surrounding tissue post-transplantation. Thus, NSPC migration through the HA-Lm gel provides motivation for future work investigating its effects after neural injury.

3.5 Conclusion

Given the local increases in SDF-1α after brain injury and the critical role that others have found SDF-1α to play in regulating NPSC fate after brain injury, increasing NPSC response to SDF-1α may serve as a viable approach to improving NPSC transplant efficacy following TBI. We have shown here that our HA-Lm gel both biochemically primes NPSCs for the injury microenvironment by upregulating the SDF-1α receptor CXCR4 and provides the appropriate ECM cues to promote migration in response to SDF-1α. Therefore, this platform may serve to improve transplant efficacy by providing transplants with the tools to dynamically respond to the injury microenvironment.

3.6 Figures

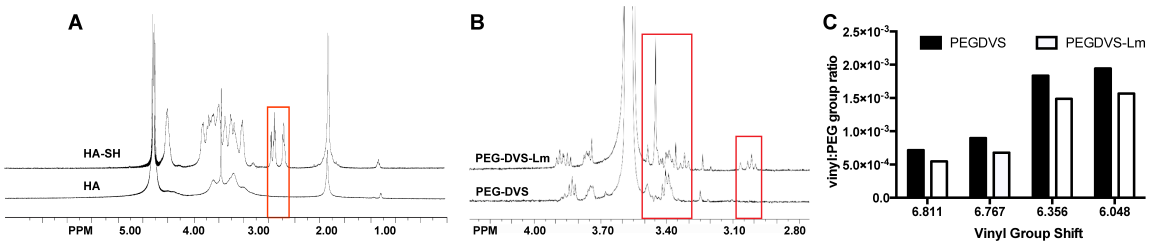

Figure 3.1: Gel formulation proof of concept. Successful HA thiolation was evidenced by the appearance of thiol group peaks (red rectangle) in the NMR spectra of HA-S compared to HA (A). Laminin was covalently immobilized to PEGDVS as evidenced by the appearance of peptide peaks (red rectangles) in the NMR spectra of PEGDVS-Lm compared to PEGDVS (B). The PEGDVS-Lm spectra had a marked reduction in the ratio of free vinyl groups to PEG groups compared to PEGDVS (C), indicative of vinyl groups having bound to laminin free thiols.

Table 3.1: HA-Lm gel formulation naming convention. NPSC response was studied on all combinations of HA and laminin w/v percentages. Gel formulations will be referenced according to labels that provide relative descriptions of HA and laminin content. For example, a 1.75% HA/0.010% Lm gel will be referenced as a Low HA/Moderate Lm gel throughout the text.

Label	HA w/v%	Laminin w/v%
No	N/A	0.000
Low	1.75	0.005
Moderate	2.00	0.010
High	2.25	0.015

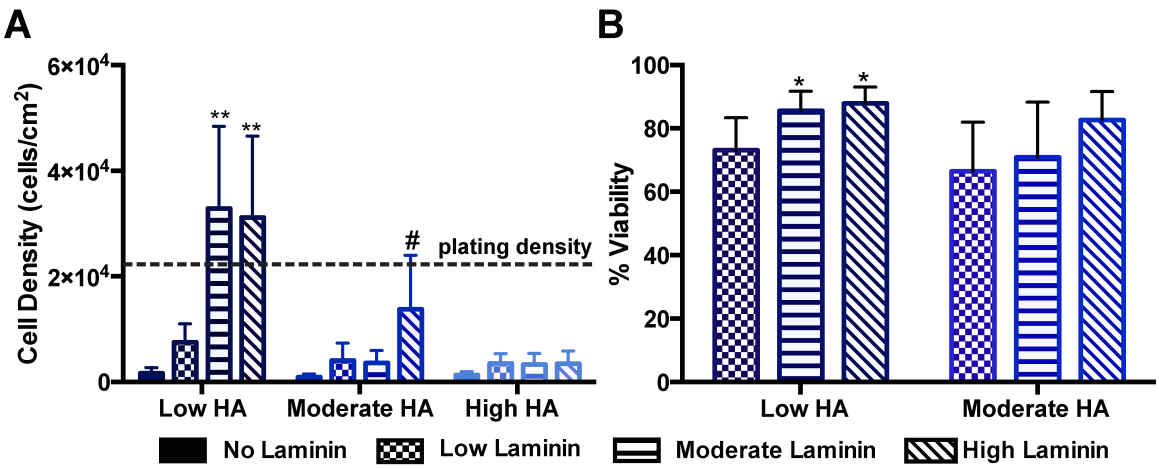

Figure 3.2: NPSC density and viability after 72 hours of culture on a spectrum of gel formulations. NPSC density was significantly higher on gels with low HA and moderate and high Lm content compared to all other gels formulations and these were the only formulations in which density increased over the plating density (A). Moderate HA/High Lm supported significantly higher NPSC density than other moderate HA formulations, but it did not exceed the initial plating density. Low HA/Moderate and High Lm gels supported significantly higher NPSC viability compared to the Low HA/Low Lm gel and to the Moderate HA/Low and Moderate Lm gels (B). **$p<0.01$ compared to Low HA/No and Low Lm gel, all Moderate and High HA gels; #$p<0.05$ compared to other Moderate HA gels;*$p<0.05$ compared to all Low Lm gels and Moderate HA/Moderate Lm gel.

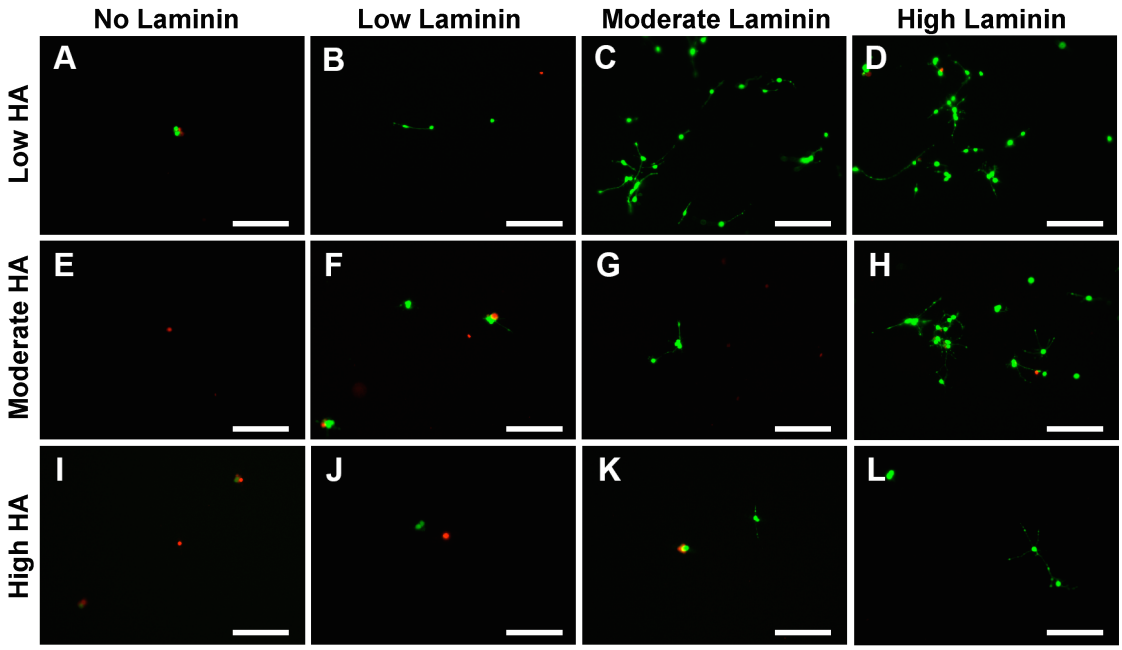

Figure 3.3: NPSC viability and density after 72 hours of culture on a spectrum of gel formulations. Live/dead assay images of Low HA gels (A-D), Moderate HA gels (E-H) and High HA gels (I-L) with No laminin (A,E,I), Low laminin (B,F,J), Moderate laminin (C,G,K) and High laminin (D,H,L). Density and viability are notably higher on Low HA/Moderate and High Lm gels and on Moderate HA/High Lm gels. Scale bars are 150 microns.

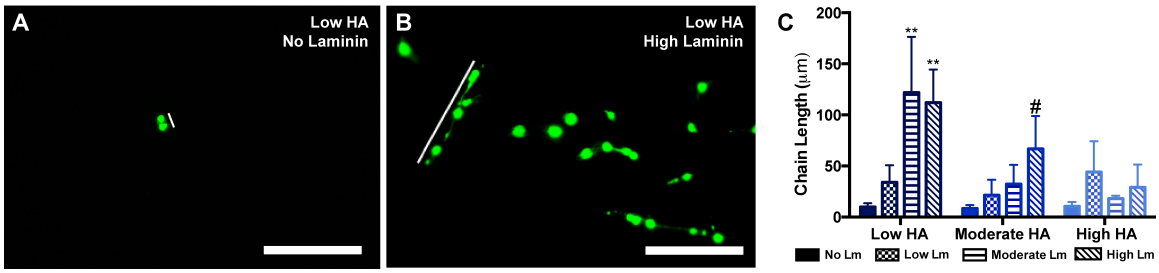

Figure 3.4: NPSC chain length after 72 hours of culture on a spectrum of gel formulations. Chain length was measured in Matlab as a tertiary metric for gel optimization, where chainlike assemblies were defined as one or more NPSCs

continuously connected via neurite outgrowth in a linear fashion (A,B). Chain length on low HA/Moderate and High Lm gels was significantly longer compared to all other gel formulations (C). Chain length on Moderate HA/High Lm gels was significantly longer than all other Moderate HA gels. **p<0.01 compared to Low HA/No and Low Lm gel, all Moderate and High HA gels; #p<0.05 compared to other Moderate HA gels. Scale bar is 100 microns.

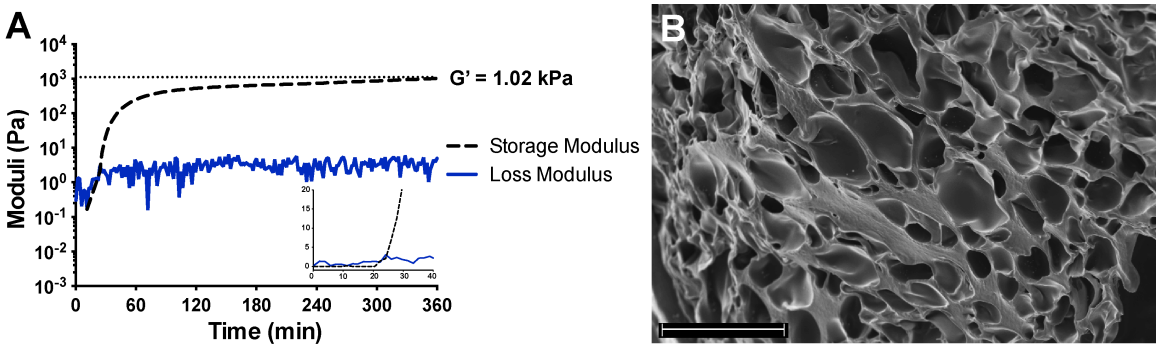

Figure 3.5: Physical properties of the Low HA/Moderate Lm gel. HA-Lm gel storage modulus was 1.02 kPa, which is similar to that to native neural tissue (0.2-1.0 kPa) and gelation time was 24 minutes(A). SEM images illustrate that the microstructure is highly porous with interconnected pores ranging from 2-17 μm with an average aspect ratio of 2.12. Scale bar is 20 μm

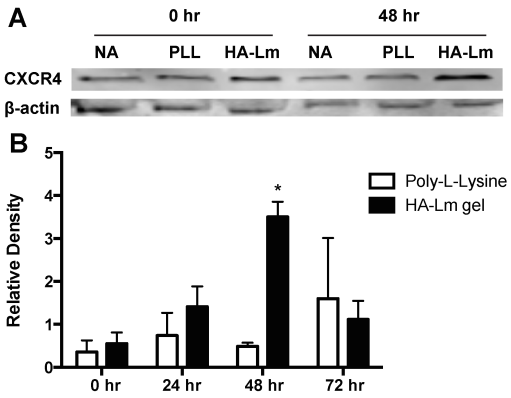

Figure 3.6: HA-Lm gel promotes NPSC CXCR4 upregulation after 48 hours of culture. As determined by western blotting, NPSC CXCR4 protein expression on HA-Lm gel (Low HA/Moderate Lm) is significantly increased compared to PLL at all time points and to HA-Lm gel at all other times points (A,B). CXCR4 expression normalized internally to beta-actin expression and externally to CXCR4 expression in non-adherent culture (NA). *p<0.05 compared to all other time points and culture conditions.

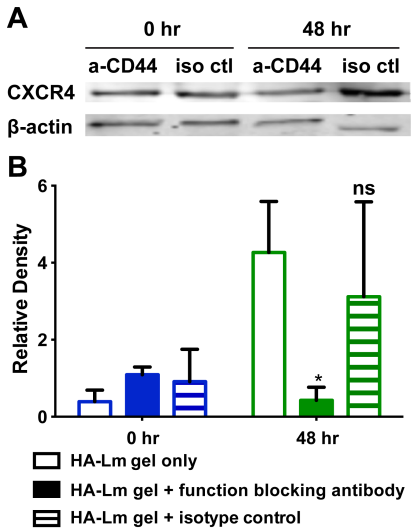

Figure 3.7: HA-Lm gel-mediated NPSC CXCR4 upregulation is critically dependent on HA. Inhibition of HA with function blocking anti-CD44 abrogates CXCR4 upregulation at 48h (A,B). These differences were specifically due to HA inhibition as CXCR4

expression with isotype control supplementation was not significantly different from HA-Lm gel at 48h (B). Exclusion of Lm within the gel did not allow for sufficient adherence of NPSCs to the gel and thus protein levels were too low for effective detection by western blotting, leaving the system irrelevant for transplantation. *p<0.05 compared to HA-Lm gel at 48 hr; ns = not significantly different from HA-Lm gel at 48 hr.

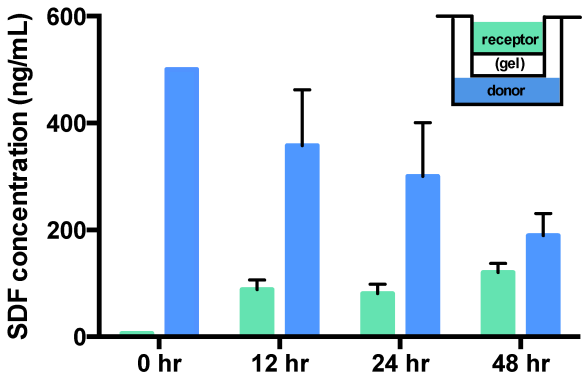

Figure 3.8: SDF-1α gradient maintenance in Transwell set up out to 48 hours. SDF-1α was allowed to diffuse across the gel within the Transwell set up and SDF-1α concentration within the donor (lower chamber) and receptor (upper chamber) was measured by ELISA at 0, 12, 24, and 48 hours (inset). SDF-1α concentration after 48 hours remained 1.6-fold higher in the donor compared to receptor.

Table 3.2: Experimental groups used to characterize NPSC chemotactic migration through the HA-Lm gel. NPSCs were either exposed to no SDF-1α (Group 1), uniform SDF-1α (Group 2) or a gradient of SDF-1α (Groups 3-7). NPSCs were seeded on either an HA-Lm gel (Groups 1-6) or an HA only gel (Group 7). Moreover, NPSCs exposed to a gradient of SDF-1α and seeded on an HA-Lm gel were supplemented with either AMD3100 (Group 4), anti-CD44 (Group 5), or an isotype control (Group 6).

Group	Gel	SDF-1α Exposure	Inhibitor Supplementation
1	HA-Lm	None	None
2	HA-Lm	Uniform	None
3	HA-Lm	Gradient	None
4	HA-Lm	Gradient	AMD3100
5	HA-Lm	Gradient	anti-CD44
6	HA-Lm	Gradient	anti-CD44 isotype control
7	HA only	Gradient	None

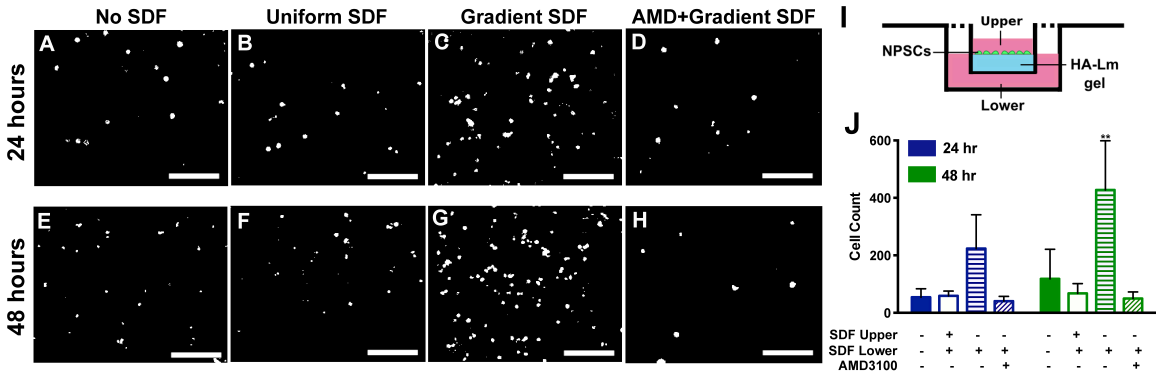

Figure 3.9: HA-Lm gel supports NPSC chemotactic migration in response to SDF-1α gradients. NPSC migration within Transwell set up (I) is not significantly different in the absence of SDF-1α (A,E) compared to uniform SDF-1α concentration (B,F) at 24 and 48 h. In response to a SDF-1α gradient, NPSC migration increases at 24 h and significantly increases at 48 h compared to NPSCs not exposed to a SDF-1α gradient (J). This response is specifically mediated by SDF-1α as inhibiting its activity with AMD3100

reduced NPSC migration to levels observed in the absence of SDF-1α gradients. Scale bar is 150 microns, **p<0.01 compared to all other groups.

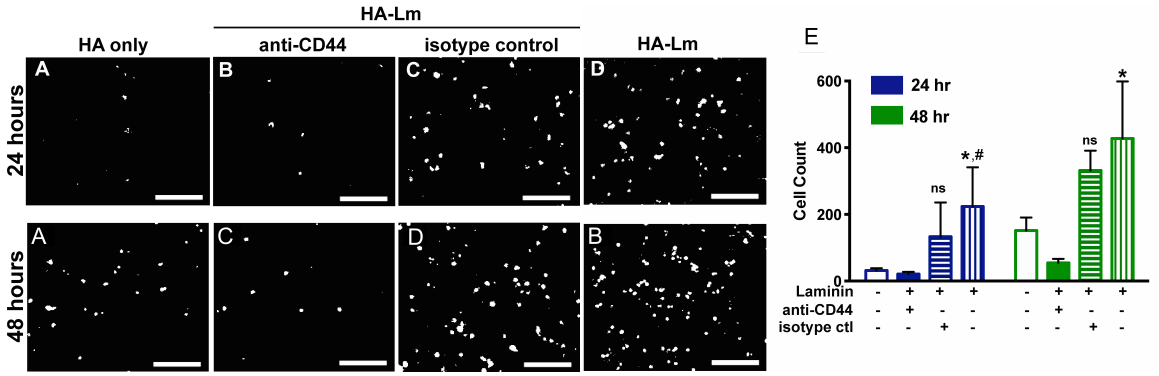

Figure 3.10: NPSC chemotactic migration within HA-Lm gel is critically dependent on both HA and laminin. NPSC migration is significantly decreased on HA only gels compared to on HA-Lm gels at both 24 (A,D) and 48 hours(E,H). Moreover, NPSC migration is significantly decreased when HA signaling is inhibited with anti-CD44 at 24 (B) and 48 (F) hours compared to migration on HA-Lm gel (I). Reduced NPSC migration is due specifically to CD44 inhibition as the appropriate isotype control does not significantly affect NPSC migration. Scale bar is 150 microns, *p<0.01 compared to other groups of same time point, #p<0.005 compared to HA-Lm at 48 hours, ns = not significantly different from HA-Lm gel group of same time point.

CHAPTER 4

INCREASING NEURAL STEM CELL TRANSPLANT REPONSE TO SDF-1α GRADIENTS AFTER TRAUMATIC BRAIN INJURY

4.1. Introduction

Traumatic brain injury (TBI) is a significant public health concern in the U.S., where approximately 1.7 million Americans sustain a TBI annually, leading to an estimated 52,000 deaths and creating a significant strain on the U.S. healthcare and economy[4-6]. TBI is characterized by a primary, mechanical insult that results in an expansive biochemical insult at the cellular and subcellular levels, known collectively as the secondary injury[8]. The secondary injury creates a highly cytotoxic injury microenvironment in which pro-inflammatory and excitotoxic signals as well as reactive oxygen species are secreted by the surrounding activated astrocytes and microglia[13,183]. Moreover, breakdown of the blood-brain barrier after TBI allows for infiltration of inflammatory cells types that further exacerbate the injury[14]. Taken together, this creates a microenvironment that is not supportive of stem cell transplants.

This is reflected in the low rates of stem cell survival, retention and engraftment following transplantation into an injury environment. Previous preclinical transplantation paradigms have shown moderate success after injury; however the full potential of these therapies has yet to be realized. Harting et al. reported a 1.9% retention rate at 48 hours after subacute transplantation into a controlled cortical impact model of TBI[106]. Similarly, Tate et al. reported survival rates of 2-3% at 1 week after NPSC subacute transplantation after controlled cortical impact[124]. We postulate that a viable approach to increasing transplant retention and engraftment may be increasing transplant responsiveness to the endogenous repair signaling that occurs parallel to the secondary injury.

Specifically, the chemokine stromal cell-derived factor-1α (SDF-1α) has been shown to play a critical role in recruiting endogenous neural progenitor/stem cells (NPSCs) to the site of injury[48,184,185]. In stroke models, SDF-1α has been shown to be upregulated by activated astrocytes and microglia within the injury penumbra, creating a chemoattractive source for endogenous NPSCs[55,56,186]. Simlarly, Itoh et al. have observed increased SDF-1α within the injury penumbra after TBI; however, the mechanism of increase in this context was not explicated identified[53]. As such, some groups have looked to capitalize on this endogenous SDF-1α source by transplanting cells that overexpress the receptor for SDF-1α, CXCR4. Studies to-date in CXCR4 overexpression for transplantation have all been in mesenchymal stem cells (MSCs) as these cells are known to respond to SDF-1α, yet lose their CXCR4 expression in culture. Systemically administered CXCR4-transduced MSCs have been shown to improve homing within the brain as well as promote neuroprotective and anti-inflammatory effects after TBI[112]. Similarly in a stroke model, Yu et al. observed improved transplant retention and motor function recovery after CXCR4-transfection in MSC transplants[163]. These studies have shown improvement in transplant efficacy, however they've utilized time- and cost-prohibitive techniques (i.e. transfection, transduction), which may create obstacles in scaling up technologies for clinical use. Moreover, while MSCs may be capable of differentiation down a neural lineage, NPSCs are inherently more inclined to give rise to neural cell types than MSCs and may be less inclined to form masses within the brain as has been observed with transplanted MSCs[98,187,188].

These technologies are also void of an equivalently promising approach to improving transplant efficacy: providing structural support to transplants. Increased NPSC transplant survival and enhanced distribution within the host tissue was observed by Tate et al. as a function of transplanting NPSCs within extracellular matrix (ECM)

scaffolds after TBI[124]. Alternatively, transplant scaffolding decorated with ECM peptides have been shown by Cheng et al. to increase NPSC transplant neuronal differentiation after TBI[123]. Therefore, providing the benefits of both CXCR4 overexpression and structural support in one transplantation platform would minimize technological complexity.

For these reasons, we have previously developed a dual-purpose hyaluronic acid-laminin (HA-Lm) hydrogel that serves to 1. increase NPSC sensitivity to SDF-1α gradients by upregulating CXCR4 and 2. provide the appropriate infrastructure to support NPSC migration[3]. The design of this hydrogel was driven by mechanistic data illustrating the effect of its individual components, hyaluronic acid (HA) and laminin, on NPSC response to SDF-1α gradients. We found that the HA component induced CXCR4 upregulation in NPSCs[3], while the laminin component engaged in a signaling crosstalk with SDF-1α that synergistically increased NPSC migration[2].

Based on previous studies indicating the critical role of SDF-1α in promoting endogenous NPSC recruitment and studies illustrating the benefit of transplanting CXCR4-overexpressing MSCs after TBI, we postulate that transplanting CXCR4-overexpressing NPSCs will enhance transplant efficacy after TBI. Specifically, we hypothesize that transplanting NPSCs within the HA-Lm gel will enhance their response to local SDF-1α signaling, thereby increasing transplant retention and migration into the surrounding host tissue after injury.

4.2. Experimental Methods

4.2.1. HA-Lm Gel Formation

HA-Lm gel was formed as previously described[3]. Briefly, dithiopropionic dihydrazide (DTPH) was synthesized from DTPA and HH in a two-step reaction as previously described [158]. High molecular weight HA was functionalized with thiol

groups through conjugation of the terminal hydrazides on DTPH to the carboxyl groups on HA using EDC chemistry and subsequent reduction of disulfide bonds using DTT as previously described [159]. ^{1}H NMR spectra was collected in D_2O (400 MHz Varian liquid state NMR, Agilent Technologies, Santa Clara, CA, USA), and Ellman's reagent test was used to quantify the concentration of conjugated thiols [160](data not shown). HA-S was sterilized by ethylene oxide gas and stored at -20°C.

HA-S hydrogels were formed via Michael-type addition crosslinking with PEGDVS as previously reported[3,116]. Briefly, PEGDVS was dissolved in media at a concentration that yielded an equimolar ratio of thiol-reactive groups to thiols present on the HA-S. HA-S was dissolved in pH 3 mitogenic growth factor-free culture media (formulation described under section 2.2 NPSC isolation and culture) and titrated between pH 7 and pH 8 with 1 M NaOH using phenol red as a colorimetric indicator of pH. The HA-S solution was mixed with an equal volume of crosslinker solution and vortex mixed for 15 seconds prior to plating.

Laminin was determined to have free thiols available for binding by Ellman's reagent test, presumably from its cysteine-rich β chain (data not shown). Laminin was conjugated to PEGDVS via Michael addition at 0.01 wt% and 0.10 wt% respectively in PBS for 15 minutes at room temperature. Based on previous experiments[3], laminin was incorporated within the gel at 1.75 wt/v% by mixing with PEGDVS media solution and allowed to react 15 minutes at room temperature prior to mixing with HA-S solution, where PEGDVS concentration was adjusted to account for laminin incorporation.

4.2.2. NPSC Isolation and Culture

NPSCs were isolated from the medial and lateral germinal eminences of E14.5 C57BL/6 mice based on previously published protocols[135] and in accordance with a protocol approved by the Institutional Animal Care and Use Committee at Arizona State

University. Briefly, mice were anesthetized at 3% isoflurane, rapidly decapitated, and fetuses were extracted from both uterine horns. Fetal tissue was rinsed in cold Leibovitz medium (Life Technologies, Carlsbad, CA) at each stage of the germinal eminence dissection. The germinal eminences were rinsed with sterile, cold Leibovitz medium before mechanical dissociation in working NPSC medium (formulation described in Section 2.2) and plated at a density of 10^4 cells/mL in a humidified incubator at 37°C, 20% O_2, and 5% CO_2. NPSCs were cultured as non-adherent neurospheres in working NPSC medium, passaged by mechanical dissociation, and utilized for experiments between passages 3 through 6.

4.2.3. NPSC and SDF-1α dual injections into an intact brain

All transplantation studies were performed in accordance with the Arizona State University Institutional Animal Care and Use Committee. Immediately prior to transplantation, NPSCs were labeled with QTracker 655 according to the manufacturer protocol (Life Technologies). Labeling with QTracker 655 did not adversely affect NPSC viability, proliferation, migration or capacity for differentiation as determined by Live/Dead assay, MTT assay, a radial migration assay and immunocytochemistry, respectively (data not shown). For all experiments, NPSCs were transplanted at a density of 3×10^4 cells/μL.

Transplantation into an intact brain was performed to determine the efficacy of the HA-Lm gel in promoting NPSC response to exogenous SDF-1α gradients without confounding effects from a TBI. For these experiments, adult male C57/BL 6 mice (n=3 per group) were anesthetized and a craniotomy performed as in the CCI procedure and 2 μL of NPSC suspension was transplanted bolus, within the HA-Lm gel, or within the HA-Lm gel impregnated with the CXCR4 antagonist AMD3100 at 1.5 mm anterior of

bregma, 1.5 mm lateral of midline and a depth of 0.8 mm. Immediately following NPSC transplantation, 2 μL of exogenous SDF-1α (100 μg/mL) was injected 0.5 mm away from the NPSCs (at 1.5 mm anterior to bregma, 2.0 mm lateral of midline) at a depth of 0.8 mm. Separate 5 μL Hamilton syringes were used for bolus NPSC and SDF-1α injections and a 25 μL Hamilton syringe was used for HA-Lm gel injections to accommodate the higher viscosity of the HA-Lm solution (Hamilton, Reno, NV). The needle was stereotaxically placed before lowering 0.5 mm into the cortical tissue at a rate of 0.15 mm/min, held for 1 min, retracted to 0.3 mm and syringe contents injected at 0.5 μL/min and held again for 1 min before retracting, where the entire injection occurred over a span of 10 minutes per injection. At 1, 3, and 7 days post-injection, the mice were sacrificed by pericardial perfusion and post-fixed in 4% paraformaldehyde.

4.2.4. NPSC Retention and Chemotactic Migration in an Intact Brain

Following fixation, intact brains mice that received NPSC and SDF-1α dual injections were saturated with 30% sucrose, frozen and serially sectioned. Sections were blocked with goat serum, but not permeabilized, to maintain QTracker 655 retention within the transplanted NPSCs. Sections were stained for SDF-1α (rabbit anti-SDF-1α, Abcam; AlexaFluor-488 conjugated anti-rabbit, Life Technologies) and visualized using fluorescence microscopy (DMI6000B, Leica). Specifically, for each section both needle tracks and the area between them were imaged by taking three 40X tile scan images of 0.23 mm width each to span the entire injection area as illustrated in Figure 4.2 (n=6 per animal). Images were analyzed for retention within the brain and chemotactic migration away from their injection site and towards the exogenous SDF-1α injection site. Cell retention was defined as the labeled NPSC count per section for all three tile scans, while migrating NPSCs were defined as the labeled NPSCs per section within the central tile

scan only (excluding cells remaining within the needle track), as illustrated in Figure 4.2B,C. Conditions for counting labeled NPSCs were set to minimize the incidence of false positives where a DAPI stained nuclei was required to be less than 10 μm away from two or more positive punctate 655 signals that were greater than 1 pixel in size. Moreover, if the positive 655 signal within one cell was sharing a border with a second cell, then it was only counted as a single labeled cell. Examples of NPSCs that do and do not satisfy the conditions for being counted are shown in Figure 4.3.

4.2.5. Controlled Cortical Impact Model

The controlled cortical impact model (CCI) was used to impart unilateral frontoparietal cortex contusions in mice in accordance with the Arizona State University Institutional Animal Care and Use Committee[189]. Briefly, adult male C57/BL 6 mice were anesthetized using isoflurane and immobilized in a stereotaxic frame (Leica, Wetzlar, Germany). A 3 mm diameter craniotomy was performed using a biopsy punch, keeping the dura mater intact, centered 1.5 mm anterior of bregma and 1.5 mm lateral of midline. Following craniotomy, a 2 mm diameter electromagnetically driven piston was centered 1.5 mm anterior of bregma and 1.5 mm lateral of midline and impacted 1 mm into the cortical tissue at a velocity of 6 m/s for a duration of 200 ms (ImpactOne, Leica). Bleeding was stopped using a cellulose sponge prior to closing the incision.

4.2.6. Spatial and Temporal Distribution of SDF-1α after CCI

The brains of mice that received CCI only were used to determine the spatial and temporal distribution of SDF-1α after injury. Animals were sacrificed at 1, 3 and 7 days after CCI by pericardial perfusion. Following fixation, brains were saturated with 30% sucrose, frozen and serially sectioned. Sections were blocked with 8% goat serum and permeabilized with Triton-X 100(Fisher Scientific, Houston, TX) prior to staining

against SDF-1α (rabbit anti-SDF-1α, Abcam, Cambridge, England; AlexaFluor-555 conjugated anti-rabbit, Life Technologies, Carlsbad, CA) and visualized via fluorescence microscopy (DMI6000B, Leica).

4.2.7. NPSC transplantation into an injured brain

A CCI was administered to adult male C57/BL 6 mice as described previously. Three days after injury, mice (n=4 per group) were anesthetized and stabilized using a stereotaxic frame before receiving 4 μL of either vehicle (mitogenic growth-factor free NPSC media), bolus NPSCs or HA-Lm gel only. Transplantations were stereotaxically oriented at 1.5 mm anterior to bregma, 1.5 mm lateral of midline and a depth of 0.3 mm. As during transplantation into an intact brain, separate Hamilton syringes were used for each group (5 μL syringes for vehicle and bolus groups; 25 μL for gel only and NPSC in gel groups), where the needle was lowered 0.5 mm into the cortical tissue at 0.15 mm/min, held for 1 min, retracted to 0.3 mm, syringe contents expelled at 0.5 μL/min and held again for 1 min before retracting, where the entire injection occurred over 15 minutes. At 1, 3, and 7 days post-transplantation, mice were sacrificed by pericardial perfusion and post-fixed in 4% paraformaldehyde.

4.2.8. NPSC Survival and Migration into Host Tissue in an Injured Brain

Injured brains that received bolus or HA-Lm gel encapsulated NPSCs were processed and stained as those used in Section 4.2.6. The injury penumbra was divided into 3 regions of 0.23 mm width each that were categorized as the proximal, medial and distal regions relative to the lesion. Within each region, 40X images were acquired (n=4 per region) and analyzed for number of labeled NSPCs. NPSC transplant survival was assessed by TUNEL staining for apoptotic cells.

4.2.9. Statistical Analysis

One-tailed t-tests were performed to compare bolus to HA-Lm encapsulated NPSCs in all studies where $\alpha=0.05$ and the null hypothesis was that HA-Lm gel encapsulation would not increase NPSC retention/chemotactic migration. Error was reported as standard error of the mean and all statistical analysis was performed in Prism 6 (GraphPad Inc., La Jolla, CA)

4.3. Results

4.3.1. SDF-1α is Acutely Upregulated Within the Injury Penumbra after CCI

Qualitative assessment of SDF-1α expression within the injury penumbra indicated that SDF-1α expression increased acutely after the CCI mouse model of TBI. Local, penumbral increase in SDF-1α peaked at 1 day after CCI compared to sham (Figure 4.1A,D). Increased SDF-1α expression was sustained at 3 days after CCI compared to sham brains; however, the spatial distribution of SDF-1α was concentrated within the cortical tissue along the edge of the injury lesion rather than directly ventral of the lesion within the penumbra as seen in day 1(Figure 4.1B,D). Both day 1 and day 3 ispilateral SDF-1α expression increased compared to appropriate contralateral controls (Figure 4.1A,B,E,F). At 7 days after CCI, increased SDF-1α expression was more diffuse in nature compared to at days 1 and 3 and appeared to have minimally increased compared to contralateral SDF-1α expression levels(Figure 4.1C,G). However, SDF-1α expression at day 7 did remain elevated compared to sham brains(Figure 4.1C,D,G,H).

4.3.2. HA-Lm gel significantly increases NPSC transplant acute retention within intact brain

Average NPSC transplant retention was significantly higher at 1 and 3 days when transplanted in the HA-Lm gel compared to bolus transplantation (p=0.0029,.0296 respectively, Figure 4.4, 4.5A). By day 7, there was no significant difference between bolus and HA-Lm gel transplanted NPSCs (p=0.2461, Figure 4.4, 4.5A). NPSC count per mm^2 when transplanted bolus was 293.0±39.11, 372.5±3.62, and 418.6±19.11 at days 1, 3, and 7, respectively. When transplanted within the HA-Lm gel, NPSC count per mm^2 was 572.6±32.60, 572.6±88.53, and 454.1±35.62 at days 1, 3, and 7, respectively.

4.3.3. HA-Lm gel significantly increases NPSC transplant acute chemotactic migration within intact brain

NPSC migration out of the transplantation site towards the exogenous SDF-1α injection site was significantly increased at days 1 and 3 when transplanted within the HA-Lm gel compared to bolus (p= 0.0432, 0.0081, respectively, Figure 4.5B). NPSC transplant chemotactic migration was not significantly different by day 7 between HA-Lm gel and bolus transplants (p=0.2627, Figure 4.5B). When transplanted as bolus injection, migrating NPSC count per mm^2 was 100.7±15.73, 122.3±2.71, and 151.2±11.34 at days 1, 3, and 7, respectively. When transplanted within the HA-Lm gel, migrating NPSC count per mm^2 was 166.7±3.10, 187.7±16.14, and 160.0±3.04 at 1, 3, and 7 days, respectively.

4.3.4. HA-Lm gel did not mitigate NPSC transplant apoptosis after 7 days

Based on morphological observations of NPSC transplants at 7 days after transplantation, it appeared that NPSCs were undergoing apoptosis in both the bolus

and HA-Lm gel transplant groups (Figure 4.6). Specifically, a large portion of labeled NPSC transplants at the 7 day time point had a multi-nucleated morphology, as illustrated in Figures 4.3D and 4.6. Both the bolus and HA-Lm gel groups displayed an increase in multi-nucleated cells with positive QTracker 655 labeling at 7 days after transplantation compared to 1 and 3 days after transplantation.

4.4. Discussion

The need for improved therapies following TBI is evidenced by the high percentage of patients suffering long-term dysfunction after injury[7]. Current stem cell transplantation paradigms have demonstrated that cell therapy may be a viable approach to mitigating the deleterious effects of the secondary injury; however, transplants suffer from low rates of survival and engraftment[25,106,124,137]. To this end, researchers have looked to increase transplant efficacy through several means. One approach is to utilize the transplants as delivery devices where transplants are engineered to constitutively overexpress growth and/or trophic factors (i.e. fibroblast growth factor, brain-derived neurotrophic factor)[110,111,190]. While this approach has shown improvement in transplant engraftment and increased extracellular levels of their respective protein it does not enable dynamic transplant interaction with and response to the injury microenvironment. Given the transient and dynamic nature of injury-induced signaling, the capacity to dynamically respond to the injury microenvironment may prove beneficial to transplants. One approach that provides transplants with the means to respond to the injury microenvironment is enhancing transplant responsiveness/sensitivity to endogenous signaling factors within the injury environment, typically through genetic manipulation (i.e. transfection, transduction)[112,163]. Alternatively, transplants may be provided a scaffold environment as a tool to enable their retention and survival after injury. Transplant

scaffolds will also serve to modulate transplant response to the injury; however, scaffolding is typically not thought to do so through biochemical priming of transplants to enhance responsiveness/sensitivity to the injury environment. Rather, the main mechanism of benefit of scaffolding has previously been viewed as its capacity to create a permissive transplant environment that provides structural support and beneficial insoluble signaling to transplants[191]. Our approach has been to investigate scaffolding as a means to enhance transplant responsiveness to endogenous repair signaling within the injury microenvironment. In this way we have looked to provide transplants with a dual-purpose tool that combines the benefits of a permissive scaffolding environment with increased capacity to dynamically respond to injury-induced signaling.

Specifically, enhancing NPSC transplant responsiveness to the chemokine SDF-1α may prove beneficial based on its critical role in mediating NPSC behavior after neural injury[48,53,55] and based on previous studies in CXCR4-overexpressing MSCs[112,163]. Our data demonstrate that the HA-Lm gel does enhance NPSC transplant chemotactic migration in response to SDF-1α gradients *in vivo*. These findings illustrate the feasibility of using a transplant scaffold to modulate NPSC responsiveness to injury-relevant signaling. However, in order for our transplantation platform to be effective in the context of an injury, transplants need exposure to SDF-1α signaling.

To this end, we observed a prominent increase in SDF-1α positive stain within the injury penumbra after our small animal model of TBI. Specifically, SDF-1α expression within the injury penumbra peaked at 1-3 days after injury and remained elevated out to 7 days. These findings have been validated by unpublished quantitative enzyme-linked immunosorbent assay data within our lab. Previous work by Shear et al. demonstrated

that transplanting 2-7 days after injury yielded the highest rates of transplant survival, illustrating a temporal "window" for transplantation[25]. This temporal transplant window is framed by a robust inflammatory response within the first 24 hours after injury and by the onset of glial scar formation at 7-14 days after injury[103,192]. Therefore, SDF-1α upregulation within the range of 2-7 days after injury demonstrates that SDF-1α will be available within a time frame that is relevant to NPSC transplantation.

Another critical component of the transplant microenvironment is the inflammatory response. Our system may be interacting with the inflammatory response in a manner that could be contributing to enhanced transplant retention and chemotactic migration. Specifically, high molecular weight HA, such as that used to form the HA-Lm gel, serves an anti-inflammatory purpose within the brain and may also serve to reduce the formation of the glial scar after TBI[193,194]. Moreover, as we move towards transplantation after TBI it will be critical to consider that the transplants themselves have the capacity to modulate inflammation. This modulation of the injury environment has been called the "bystander effect," in which transplants do not actively replace cells, but rather provide support to host cells through trophic and/or growth factor signaling and reducing pro-inflammatory signaling[195,196].

To this end, an unexpected observation included the apoptotic transplant morphology seen at day 7 in both the bolus and HA-Lm gel NPSC transplants; however, apoptotic staining (i.e. TUNEL) will need to be performed to confirm these observations. At 7 days after transplantation, we observed positively labeled, multi-nucleated cells as illustrated in Figure 4.3D, 4.6. These observations may be indicative that the HA-Lm gel does not enhance NPSC transplant survival at a subacute, 7 day time and/or that by 7

days the QTracker 655 gets expelled from transplants and phagocytosed by multi-nucleated inflammatory cell types. TUNEL staining will elucidate the survival of NPSC transplants as a function of the HA-Lm gel platform.

In this light, a more robust method for tracking cells (i.e. GFP labeling) may help to minimize confusion regarding label retention moving forward. The NPSCs used in these studies were primary fetal-derived cells, which are highly sensitive to their extracellular environment. This, taken together with our need to maintain labeling out to 7 days, restricted available labeling methods. Of the available labeling methods, QTracker 655 yielded the highest NPSC viability without adverse effects on NPSC migration, proliferation and capacity for differentiation. GFP-labeled NPSCs would allow for monitoring transplant morphology and would eliminate the need for the cell counting conditions currently required to minimize incidences of false positives with QTracker 655.

4.5. Conclusion

While several questions remain open-ended regarding the effect of the HA-Lm gel on NPSC transplants, specifically within the context of an injury environment, the HA-Lm gel acutely enhanced NPSC transplant retention and chemotactic migration in response to SDF-1α gradients as was its design goal. We look forward to data illustrating the effect of the HA-Lm gel on NPSC transplants after TBI.

4.6. Figures

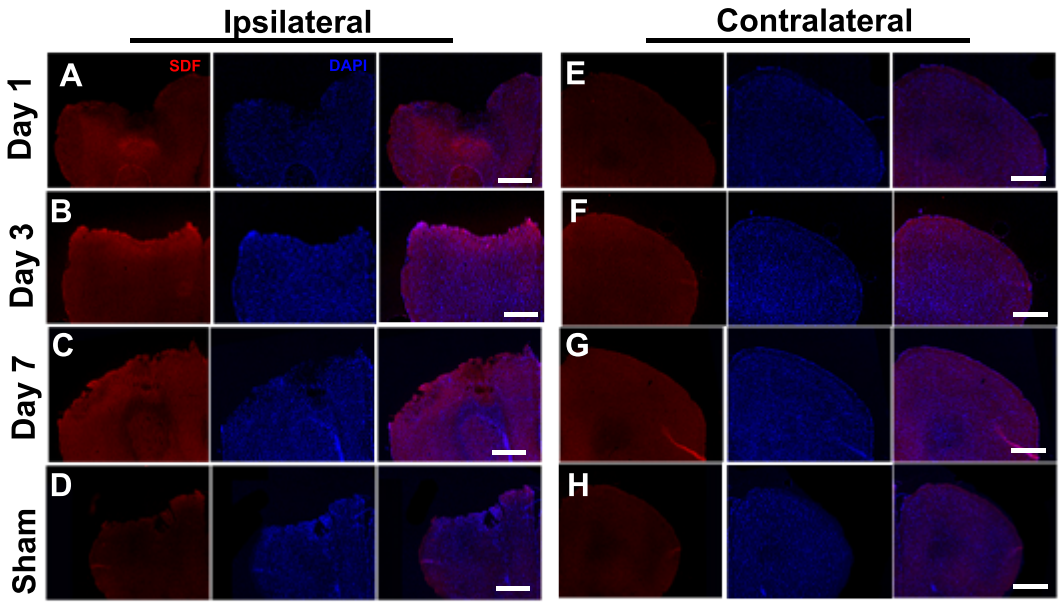

Figure 4.1: Qualitative assessment of the spatial and temporal distribution of SDF-1α after CCI. Prominent increases in SDF-1α expression were observed within the injury penumbra after CCI at 1 and 3 days (A,B) compared to the contralateral cortex (E,F,) and to sham brains (D,H). A diffuse increase was maintained at 7 days after CCI in both the ipsilateral (C) and contralateral cortices (G) compared to sham brains (D,H).

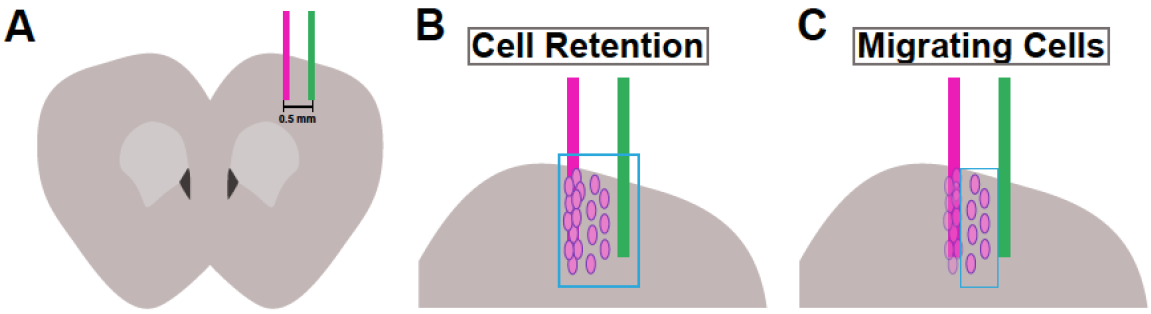

Figure 4.2: Schematic illustrating the spatial transplantation parameters and NPSC counting regions. NPSCs were transplanted 0.5 mm medial to the exogenous SDF-1α injection site(A). NPSC retention was calculated by counting both the NPSCs retained

within their injection site and the NPSCs migrate towards the SDF-1α injection site (B). Migrating NPSCs were counted as only those NPSCs migrating away from their injection site towards the exogenous SDF-1α injection site(C).

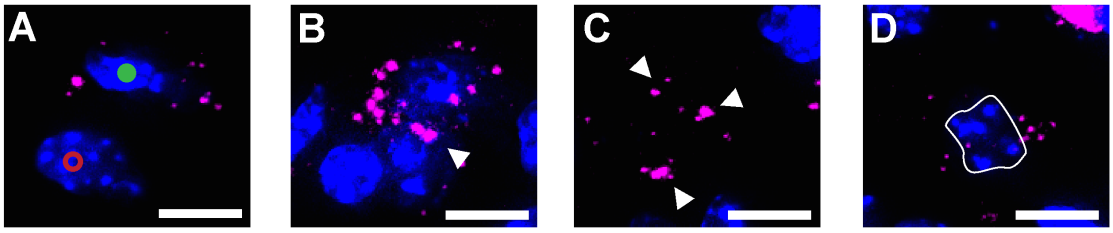

Figure 4.3: Examples illustrating the different criteria for counting labeled NPSC transplants. An example of a labeled cell (•) next to an unlabeled cell (°) based on the criteria outlined in section 4.2.4.(A). An example of a labeled NPSC sharing a boundary with another NPSC, counting as only one labeled cell (arrowhead indicates boundary, B). An example of extracellular QTracker 655 that is not affiliated with an NPSC transplant (arrowheads, C). An example of a labeled, but multi-nucleated cell, indicating that it is apoptotic or an inflammatory cell type has phagocytosed extracellular QTracker 655 (white boundary, D).

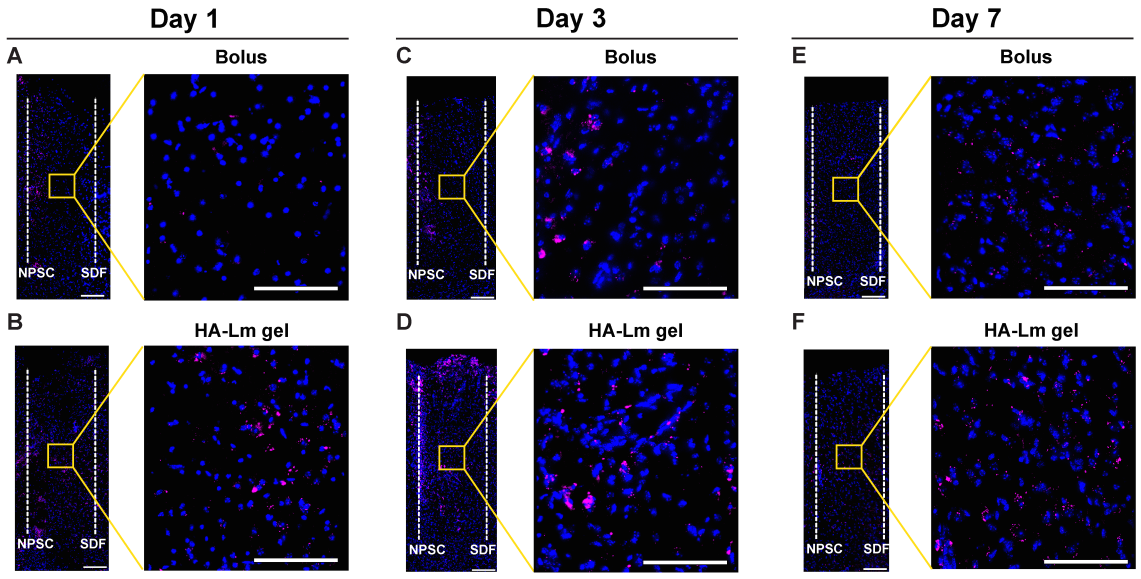

Figure 4.4: NPSC transplant retention and migration within an intact brain. At days 1 and 3 there was enhanced QTracker 655 positive transplant retention (overview)

and migration (inset) when transplanted within the HA-Lm gel (B,D) as compared to the bolus transplants (A,C). Differences between retention and migration at 7 days post-transplant in the bolus (E) and HA-Lm gel (F) groups are less robust. Moreover, the QTracker 655 positive signal appears to be less concentrated within cells and there are visible multi-nucleated cells with positive QTracker 655 signal. Overview scale bar is 250 μm; inset scale bar is 100 μm.

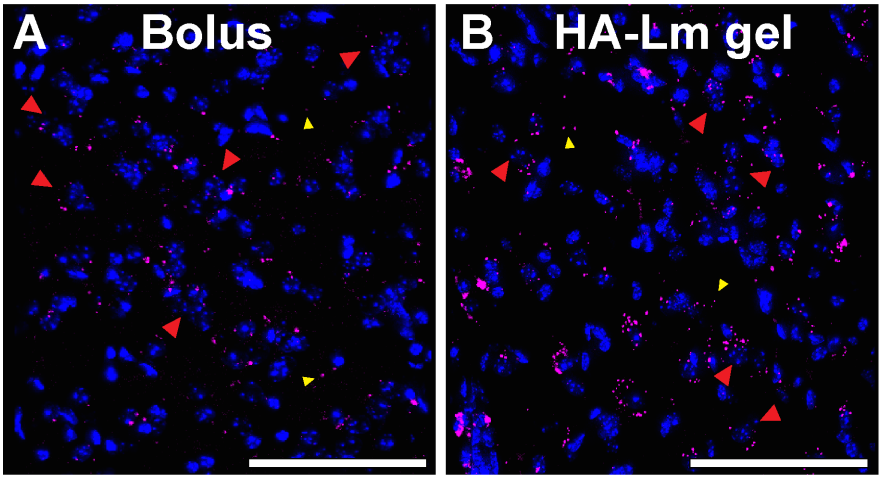

Figure 4.5: NPSC transplant apoptotic morphology at 7 days. Insets of bolus (A) and HA-Lm gel (B) transplants within the active migration region displaying multi-nucleated DAPI staining (red arrowheads) and increased extracellular QTracker 655 positive signal (yellow arrowheads). Scale bar is 100 μm.

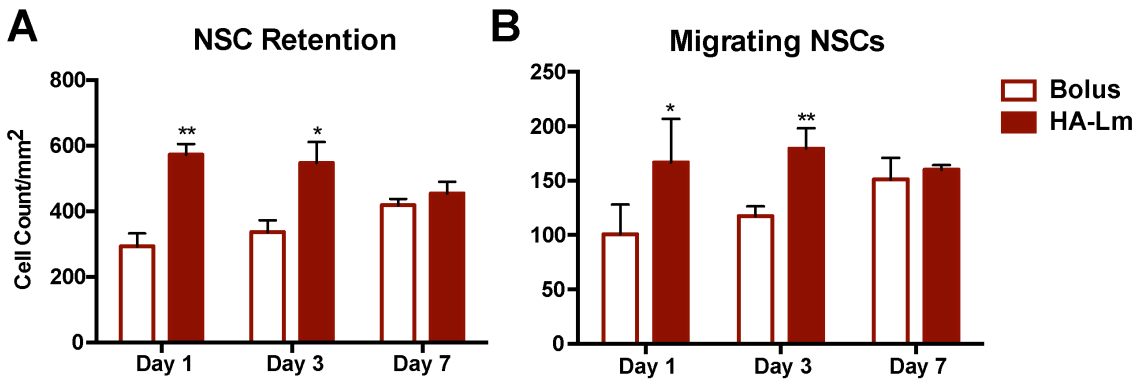

Figure 4.6: Quantification of NPSC transplant retention and migration within an intact brain. Transplantation within the HA-Lm gel significantly increased NPSC transplant retention (A) and chemotactic migration (B) compared to bolus transplant controls at 1 and 3 days. *,**$p<0.05$, 0.01, respectively, compared to bolus of same time point.

CHAPTER 5

SUMMARY AND FUTURE WORK

5. 1. Summary of Findings

5.1.1. Aim 1: Determine the critical ECM migratory cues that mediate NPSC response to injury-relevant chemokine gradients.

We determined that the vascular basement membrane protein laminin engages in a signaling crosstalk with the injury-relevant chemokine, SDF-1α, that significantly and synergistically increased NPSC migration. SDF-1α-laminin crosstalk also significantly increased neuronal differentiation of NPSCs, however it did not have a synergistic effect on NPSC proliferation. SDF-1α enhanced NPSC proliferation regardless of extracellular matrix substrate. The most robust effect of SDF-1α-ECM crosstalk was observed in increased NPSC migration and as such, the remaining work was focused on enhancing NPSC chemotactic migration.

5.1.2. Aim 2: Develop a neurotransplantation system that promotes NPSC response to critical chemotactic signals.

A hydrogel comprised of hyaluronic acid and laminin (HA-Lm gel) was developed and characterized that induced the upregulation of SDF-1α receptor CXCR4 in NPSCs. This upregulation was critically dependent on the HA component of the gel as blocking NPSC interaction with HA abrogated CXCR4 upregulation. Without the laminin component, NPSCs could not effectively adhere to the gel making both gel components critical for *in vivo* relevancy. Moreover, NPSC chemotactic migration through the HA-Lm gel was significantly enhanced in response to SDF-1α in a manner that was critically dependent on the SDF-1α gradient, HA, and laminin. Therefore, the HA-Lm gel represented a scaffolding transplantation platform capable of enhancing NPSC response to injury-relevant signaling.

5.1.3. Aim 3: Determine the efficacy of transplanting CXCR4 overexpressing NPSCs for enhancing NPSC migration in response to injury-relevant chemotactic signaling.

The HA-Lm gel served to acutely increased NPSC transplant retention within an intact brain compared to bolus NPSC transplants. Moreover, transplantation within the HA-Lm gel significantly increased NPSC transplant migration towards an exogenous source of SDF-1α compared to bolus NPSC transplant chemotactic migration. Our animal model of TBI was found to increase SDF-1α expression within the injury penumbra at equivalent time points post-injury. Therefore, our TBI model can serve as a viable source for SDF-1α to NPSC transplants in ongoing studies post-injury.

5. 2. Discussion

The mechanisms behind NPSCs response to and mitigation of the secondary injury of TBI remain poorly understood. As such, many groups are actively working to understand the signals that attract endogenous NPSCs to the injury. We've chosen to investigate combinations of soluble and insoluble signaling pathways as mediators of NPSC recruitment. This research direction was derived from the migratory route undertaken by endogenous NPSCs; specifically, the tendency by NPSCs to affiliate with vasculature as they leave the neural niche and home to the injury environment[47,48]. By migrating along the vasculature, NPSCs are taking advantage of the unique extracellular matrix (or insoluble signaling) of the vascular basement membrane. Previous studies in the literature had also illustrated the critical dependence of endogenous NPSC recruitment on injury-induced SDF-1α upregulation (or soluble signaling)[55]. Taken together, these findings led us to hypothesize that there may be something specific about the interaction between soluble SDF-1α signaling and insoluble vascular basement membrane signaling that modulates NPSC behavior. Indeed, we found that there was a signaling crosstalk between SDF-1α and vascular basement

membrane protein laminin that significantly and synergistically increased NPSC migration. For our purposes, this data informed the focus of our transplantation platform development to enhance migration. For the field, this data served as valuable information regarding the mechanism of endogenous repair by NPSC recruitment to the site of injury.

We used this information to guide the development of a novel transplantation platform that served to both increase the expression of the SDF-1α receptor, CXCR4, and to provide the laminin signaling previously determined to be an insoluble signal that mediated NPSC response to SDF-1α. In looking to develop a novel neurotransplantation platform, we looked to the neural niche for guidance and inspiration. The niche is highly vascularized (providing further motivation to expose transplants to laminin signaling) and also contains the glycosaminoglycan hyaluronic acid (HA) at higher concentrations than elsewhere in the adult brain[125,126]. Previous work in the literature indicated that HA increased responsiveness and/or sensitivity to SDF-1α in other stem cell types (i.e. MSCs, HSCSs)[154,155,197]. Therefore, we investigated the capacity of HA to increase NPSC responsiveness to SDF-1α and found that interaction with an HA hydrogel induces NPSC upregulation of the SDF-1α receptor CXCR4. Other methods for increasing NPSC responsiveness/sensitivity to SDF-1α were explored (i.e. hypoxic preconditioning, transfection); however, interaction with an HA hydrogel was the most appealing approach due to its relative simplicity and capacity to serve as a hydrogel transplantation scaffold. While hypoxic preconditioning has been shown to upregulate CXCR4, it may also have detrimental side effects on other cell signaling pathways. Transfection would allow for targeted CXCR4 overexpression; however, this option is time- and cost-prohibitive when considering translation to the clinic. The complexity represented by these two methods (from the cell signaling and technological perspectives, respectively)

was avoided by modulating the extracellular environment with HA. Moreover, HA allowed us to combine the benefits of biochemical priming with the benefits of a transplantation scaffold into one comparably simple technology. Therefore, the HA hydrogel enabled us to probe an outside-in signaling mechanism to modulate CXCR4 expression in NPSCs.

Our first *in vivo* study aimed to evaluate the efficacy of the HA-laminin hydrogel in the absence of an injury microenvironment. The many confounding variables of an injury microenvironment would complicate our ability to directly evaluate the efficacy of our gel in promoting migration in response to SDF-1α signaling specifically. Therefore, the success of the HA-Lm gel in promoting NPSC migration in response to exogenous SDF-1α signaling in an intact brain indicates that the hydrogel platform is effective in its design and we are currently looking at its effect on NPSC transplants in the context of an injury microenvironment. By first evaluating the HA-laminin transplantation system in a more simplistic intact brain model, results with a pre-clinical small animal model of TBI will be informative to the field regardless of the outcome. In this way, observing no effect of the HA-Lm gel on NPSC transplants in an injury context will indicate that the field needs to look towards a therapy that is able to respond to multiple dynamic variables within the injury microenvironment.

Alternatively, future studies with the HA-Lm gel as a transplant platform may require that the focus shift away from enhanced chemotactic migration as a means to enhance engraftment and promote survival. An interesting alternative may be that the HA-Lm gel promotes chemotactic migration in an attempt to enhance cellular “cargo” delivery. Specifically, the aforementioned bystander effect may prove to be more widely distributed and effective if NPSC transplants are able to leave the transplantation site with enhanced efficacy at acute time points. Given that the HA-Lm gel may not have

been able to mitigate subacute transplant apoptosis, its mechanism of benefit within the injury environment may be to encourage NPSC migration into the surrounding tissue prior to releasing their growth and/or trophic factor "cargo."[195]

Since the onset of this work, the volume of work on HA scaffolding for neural stem cells within the field has significantly increased, specifically HA-laminin hydrogels, as evidenced by recent conference papers (Society for Biomaterials 2015, Biomedical Engineering Society 2015, abstracts unpublished). As such, our work contributes meaningful knowledge to an emerging area of interest within the biomaterials and neural tissue engineering communities.

Moreover, this work has applications in many other fields of inquiry, as SDF-1α signaling is not exclusive to the neural injury environment. The SDF-1α -CXCR4 axis has been shown to play a complex role in the development of several pathologies including atherosclerosis[198,199] and subsequently, myocardial infarctions[200], and most notably tumor growth, vascularization and metastasis[201-203]. SDF-1α has also been implicated as a critical mediator of bone marrow-derived progenitor/stem cell homing to regions of stress and injury[204-208]. In these pathological contexts, the HA-Lm gel represents a tool to both develop a therapeutic intervention and to probe disease pathophysiology and progression.

For example, following myocardial infarction (MI), SDF-1α is acutely upregulated within the infarct and border regions out to 3 days[209-211]. In this context, SDF-1α plays a critical role in recruiting systemic mesenchymal stem cells (MSCs) to aid in remodeling after MI[209,210]. The development of the HA-Lm gel was based, in part, on literature demonstrating that HA interactions induce CXCR4 overexpression in MSCs[153]. Therefore, the benefit of developing the HA-Lm gel for use as an MSC transplant scaffold post-MI is self-evident. Based on the roles of SDF-1α after MI

established in the literature, it is hypothesized that the HA-Lm gel may serve to 1) increase MSC transplant retention and survival 2) improve SDF-1α-induced re-vascularization within the infarct region and 3) facilitate SDF-1α-mediated remodeling of the infarct region. Delivery of the HA-Lm gel without cell cargo may also be beneficial in itself after MI as it may serve to enhance responsiveness to local SDF-1α signaling in both local cardiac stem cell populations[212,213] and systemic MSC populations.

However, the function of SDF-1α signaling extends beyond pathologies and as such, our HA-Lm gel may also be useful in probing and/or enhancing the homeostatic roles for SDF-1α. Specifically, SDF-1α -CXCR4 signaling plays critical roles in maintaining bone marrow and neural stem cell niches [214-217] and mediating inflammation[218-220] under normal physiological conditions. In this homeostatic context, the HA-Lm gel may be optimized for use as an artificial niche with the goal of probing niche dynamics. A more thorough understanding of stem cell niche dynamics would inform therapies that aim to enhance the endogenous stem cell response to injury. While our work has been focused on the development of a platform to facilitate repair following traumatic brain injury, we believe the HA-Lm gel to be relevant to a broader scientific community given the diverse nature of SDF-1α signaling.

5.3. Future Work

5.3.1. NPSC Transplant Response to Injury-Induced SDF-1α Gradients

Our completed data sets have demonstrated the efficacy of the HA-Lm gel in enhancing transplant retention and migration in response to exogenous SDF-1α gradients *in vivo*. Based on data obtained in Aim 1, we focused our efforts on enhancing NPSC transplant chemotactic migration towards SDF-1α and were successful in doing so without the confounding variables of the injury microenvironment. However, a more complete recapitulation of the injury microenvironment is necessary in moving this

technology towards clinical relevancy. Therefore, current studies are investigating the efficacy of our HA-Lm gel transplant system in an animal model of TBI.

Methods outlined in Section 4.2 describe an ongoing study that employs a controlled cortical impact model of TBI to model the injury microenvironment prior to transplantation. This study will determine the effect of the HA-Lm gel on transplant retention and migration into the surrounding tissue as a function of endogenous, local SDF-1α signaling. Moreover, we will also investigate how the HA-Lm gel affects inflammation after TBI. Recent work within the field indicates that transplants may contribute to repair after TBI through the "bystander effect" (i.e. modulation of inflammation and local trophic signaling) rather than cell replacement. Therefore, probing inflammatory metrics may provide a more complete understanding of the ways in which our transplantation system is interacting with and modulating the injury microenvironment.

5.3.2. Human Induced Pluripotent Stem Cells as an Alternative Cell Source for Transplantation

Our current body of work investigates NPSC transplant response to injury-relevant signaling after TBI as a function of transplant microenvironment with the long-term goal of clinical translation. However, this work was focused on the response of fetal-derived NPSCs, which does not represent a clinically relevant cell source. First, these cells cannot be sustainably sourced and appropriately scaled in a human model due to scarcity of tissue and ethical concerns. Second, the NPSC phentoype is heterogeneous and will give rise to all cell types of the central nervous system, creating an uncontrollable variable during transplantation. Therefore, we have looked to an alternative cell source with increased clinical relevancy.

Specifically, we have begun collaboration with Dr. David Brafman at ASU to investigate the behavior of human induced pluripotent stem cell-derived neural progenitor cells (hNPCs) within our novel transplantation platform. These cells can be sourced from patient fibroblasts, representing a cell source that is not only more sustainable and less ethically controversial, but also has the potential to be patient-specific. The combination of these traits (sustainability and patient specificity) makes this cell source an attractive candidate in moving towards a more clinically relevant stem cell transplantation population.

To this end, ongoing work is investigating 1. the level of expression of CXCR4 in hNPC populations and 2. the effect of SDF-1α-laminin crosstalk on hNPC migration. Preliminary data indicate a basal level of CXCR4 expression within the hNPC population and that there may be a synergistic relationship between SDF-1α and laminin that enhances hNPC migration. However, migration of hNPCs in this context is lower than that observed for mouse NPSCs. As such, work in the immediate future will focus on continued probing of the hNPC response to SDF-1α-laminin crosstalk. Longer-term work will look towards the behavior of hNPCs within the HA-Lm gel and its regulation of their CXCR4 expression.

REFERENCES

[1] C.P. Addington, A. Roussas, D. Dutta, S.E. Stabenfeldt, Endogenous repair signaling after brain injury and complementary bioengineering approaches to enhance neural regeneration, Biomark Insights. 10 (2015) 43–60.

[2] C.P. Addington, C.M. Pauken, M.R. Caplan, S.E. Stabenfeldt, The role of SDF-1α-ECM crosstalk in determining neural stem cell fate, Biomaterials. 35 (2014) 3263–3272.

[3] C.P. Addington, J.M. Heffernan, C.S. Millar-Haskell, E.W. Tucker, R.W. Sirianni, S.E. Stabenfeldt, Enhancing neural stem cell response to SDF-1α gradients through hyaluronic acid-laminin hydrogels, Biomaterials. 72 (2015) 11–19.

[4] V.G. Coronado, L.C. McGuire, K. Sarmiento, J. Bell, M.R. Lionbarger, C.D. Jones, et al., Trends in Traumatic Brain Injury in the U.S. and the public health response: 1995-2009, J Safety Res. 43 (2012) 299–307.

[5] V.G. Coronado, L. Xu, S.V. Basavaraju, L.C. McGuire, M.M. Wald, M.D. Faul, et al., Surveillance for traumatic brain injury-related deaths: United States, 1997-2007, (2011) 1-32.

[6] R.B. Arbour, Traumatic Brain Injury Pathophysiology, Monitoring, and Mechanism-Based Care, Crit Care Nurs Clin North Am. 25 (2013) 297–319.

[7] A.W. Selassie, E. Zaloshnja, J.A. Langlois, T. Miller, P. Jones, C. Steiner, Incidence of Long-term Disability Following Traumatic Brain Injury Hospitalization, United States, 2003, J Head Trauma Rehab. 23 (2008) 123–131.

[8] J.M. Silver, T.W. McAllister, S.C. Yudofsky, Textbook of Traumatic Brain Injury, American Psychiatric Pub, 2011.

[9] E.A. Finkelstein, P.S. Corso, T.R. Miller, Incidence and Economic Burden of Injuries in the United States, Oxford University Press, USA, 2006.

[10] M.C. LaPlaca, C.M. Simon, G.R. Prado, D.K. Cullen, CNS injury biomechanics and experimental models, Prog Brain Res. 161 (2007) 13–26.

[11] S.S. Margulies, L.E. Thibault, T.A. Gennarelli, Physical model simulations of brain injury in the primate, J Biomechanics. 23 (1990) 823–836.

[12] D.H. Smith, D.F. Meaney, Axonal damage in traumatic brain injury, The Neuroscientist. 6 (2000) 483–495.

[13] C. Werner, K. Engelhard, Pathophysiology of traumatic brain injury, Brit J Anaesth. 99 (2007) 4–9.

[14] E.M. Golding, Sequelae following traumatic brain injury: the cerebrovascular perspective, Brain Res Rev. 38 (2002) 377–388.

[15] R.L. Hayes, L.W. Jenkins, B.G. Lyeth, Neurotransmitter-mediated mechanisms of traumatic brain injury: acetylcholine and excitatory amino acids, J Neurotrauma. 9 (1992) S173–87.

[16] V. Parpura, P.G. Haydon, Physiological astrocytic calcium levels stimulate glutamate release to modulate adjacent neurons, P Natl Acad Sci. 97 (2000) 8629–8634.

[17] M.F. Anderson, F. Blomstrand, C. Blomstrand, P.S. Eriksson, M. Nilsson, Astrocytes and stroke: networking for survival? Neurochem Res. 28 (2003) 293–305.

[18] M. Pekny, M. Nilsson, Astrocyte activation and reactive gliosis, Glia. 50 (2005) 427–434.

[19] Z.Z. Chong, F. Li, K. Maiese, Oxidative stress in the brain: Novel cellular targets that govern survival during neurodegenerative disease, Prog Neurobiol. 75 (2005) 207–246.

[20] M.C. Morganti-Kossmann, M. Rancan, V.I. Otto, P.F. Stahel, T. Kossmann, Role of cerebral inflammation after traumatic brain injury: a revisited concept, Shock. 16 (2001) 165–177.

[21] J.M. Ziebell, M.C. Morganti-Kossmann, Involvement of pro-and anti-inflammatory cytokines and chemokines in the pathophysiology of traumatic brain injury, Neurotherapeutics. 7 (2010) 22–30.

[22] R.R. Hicks, V.B. Martin, L. Zhang, K.B. Seroogy, Mild experimental brain injury differentially alters the expression of neurotrophin and neurotrophin receptor mRNAs in the hippocampus, Exp Neurol. 160 (1999) 469–478.

[23] M.D. Norenberg, Astrocyte Responses to Cns Injury, J Neuropathol Exp Neurol. 53 (1994) 213–220.

[24] W.T. Norton, D.A. Aquino, I. Hozumi, F.C. Chiu, C.F. Brosnan, Quantitative aspects of reactive gliosis: a review, Neurochem Res. 17 (1992) 877–885.

[25] D.A. Shear, C.C. Tate, M.C. Tate, D.R. Archer, M.C. LaPlaca, D.G. Stein, et al., Stem cell survival and functional outcome after traumatic brain injury is dependent on transplant timing and location, Restor Neurol Neurosci. 29 (2011) 215–225.

[26] T.D. Palmer, J. Takahashi, F.H. Gage, The adult rat hippocampus contains primordial neural stem cells, Mol Cell Neurosci. 8 (1997) 389–404.

[27] J. Altman, G.D. Das, Postnatal neurogenesis in the guinea-pig, Nature. 214 (1967) 1098–1101.

[28] H.G. Kuhn, H. Dickinson-Anson, F.H. Gage, Neurogenesis in the dentate gyrus of the adult rat: age-related decrease of neuronal progenitor proliferation, J Neurosci. 16 (1996) 2027–2033.

[29] C. Lois, A. Alvarez-Buylla, Proliferating subventricular zone cells in the adult mammalian forebrain can differentiate into neurons and glia, P Natl Acad Sci. 90 (1993) 2074–2077.

[30] F. Doetsch, J.M. Garcı´a-Verdugo, A. Alvarez-Buylla, Cellular composition and three-dimensional organization of the subventricular germinal zone in the adult mammalian brain, J Neurosci. 17 (1997) 5046–5061.

[31] K. Jin, V. Galvan, Endogenous neural stem cells in the adult brain, J Neuroimmune Pharmacol. 2 (2007) 236–242.

[32] M. Tavazoie, L. Van der Veken, V. Silva-Vargas, M. Louissaint, L. Colonna, B. Zaidi, et al., A Specialized Vascular Niche for Adult Neural Stem Cells, Cell Stem Cell. 3 (2008) 279–288.

[33] Q. Shen, Y. Wang, E. Kokovay, G. Lin, S.-M. Chuang, S.K. Goderie, et al., Adult SVZ Stem Cells Lie in a Vascular Niche: A Quantitative Analysis of Niche Cell-Cell Interactions, Cell Stem Cell. 3 (2008) 289–300.

[34] F. Doetsch, A niche for adult neural stem cells, Curr Opin Genet Dev. 13 (2003) 543–550.

[35] Z. Mirzadeh, F.T. Merkle, M. Soriano-Navarro, J.M. Garcia-Verdugo, A. Alvarez-Buylla, Neural Stem Cells Confer Unique Pinwheel Architecture to the Ventricular Surface in Neurogenic Regions of the Adult Brain, Cell Stem Cell. 3 (2008) 265–278.

[36] Q. Shen, S.K. Goderie, L. Jin, N. Karanth, Y. Sun, N. Abramova, et al., Endothelial cells stimulate self-renewal and expand neurogenesis of neural stem cells, Science. 304 (2004) 1338–1340.

[37] R. Faigle, H. Song, Biochimica et Biophysica Acta, BBA-Gen Subjects. 1830 (2013) 2435–2448.

[38] J.S. Goldberg, K.K. Hirschi, Diverse roles of the vasculature within the neural stem cell niche, Regen Med. 4 (2009) 879–897.

[39] T.S. Jacques, J.B. Relvas, S. Nishimura, R. Pytela, G.M. Edwards, C.H. Streuli, Neural precursor cell chain migration and division are regulated through different beta1 integrins, Development. 125 (1998) 3167–3177.

[40] S. Ramaswamy, G.E. Goings, K.E. Soderstrom, F.G. Szele, D.A. Kozlowski, Cellular proliferation and migration following a controlled cortical impact in the mouse, Brain Res. 1053 (2005) 38–53.

[41] S. Chirumamilla, D. Sun, M.R. Bullock, R.J. Colello, Traumatic brain injury induced cell proliferation in the adult mammalian central nervous system, J Neurotrauma. 19 (2002) 693–703.

[42] G.M. Thomsen, J.E. Le Belle, J.A. Harnisch, W.S.M. Donald, D.A. Hovda, M.V. Sofroniew, et al., Traumatic brain injury reveals novel cell lineage relationships within the subventricular zone ☆ , Stem Cell Res. 13 (2014) 48–60.

[43] R. Zhang, Z. Zhang, L. Wang, Y. Wang, A. Gousev, L. Zhang, et al., Activated neural stem cells contribute to stroke-induced neurogenesis and neuroblast migration toward the infarct boundary in adult rats, J Cereb Blood Flow Metab. 24 (2004) 441–448.

[44] M. Ninomiya, T. Yamashita, N. Araki, H. Okano, K. Sawamoto, Enhanced neurogenesis in the ischemic striatum following EGF-induced expansion of transit-amplifying cells in the subventricular zone, Neurosci Lett. 403 (2006) 63–67.

[45] R.L. Zhang, M. Chopp, S.R. Gregg, Y. Toh, C. Roberts, Y. LeTourneau, et al., Patterns and dynamics of subventricular zone neuroblast migration in the ischemic striatum of the adult mouse, J Cereb Blood Flow Metab. 29 (2009) 1240–1250.

[46] T. Yamashita, Subventricular Zone-Derived Neuroblasts Migrate and Differentiate into Mature Neurons in the Post-Stroke Adult Striatum, J Neurosci. 26 (2006) 6627–6636.

[47] S. Bovetti, Y.C. Hsieh, P. Bovolin, I. Perroteau, T. Kazunori, A.C. Puche, Blood Vessels Form a Scaffold for Neuroblast Migration in the Adult Olfactory Bulb, J Neurosci. 27 (2007) 5976–5980.

[48] E. Kokovay, S. Goderie, Y. Wang, S. Lotz, G. Lin, Y. Sun, et al., Adult SVZ Lineage Cells Home to and Leave the Vascular Niche via Differential Responses to SDF1/CXCR4 Signaling, Cell Stem Cell. 7 (2010) 163–173.

[49] H. Hatic, M.J. Kane, J.N. Saykally, B.A. Citron, Modulation of transcription factor Nrf2 in an in vitro model of traumatic brain injury, J Neurotrauma. 29 (2012) 1188–1196.

[50] C. Iadecola, C.A. Salkowski, F. Zhang, T. Aber, M. Nagayama, S.N. Vogel, et al., The transcription factor interferon regulatory factor 1 is expressed after cerebral ischemia and contributes to ischemic brain injury, J Exp Med. 189 (1999) 719–727.

[51] A. Li, X. Sun, Y. Ni, X. Chen, A. Guo, HIF-1α Involves in Neuronal Apoptosis after Traumatic Brain Injury in Adult Rats, J Mol Neurosci. 51 (2013) 1052–1062.

[52] J. Ramos-Cejudo, M. Gutiérrez-Fernández, B. Rodríguez-Frutos, M. Expósito Alcaide, F. Sánchez-Cabo, A. Dopazo, et al., Spatial and Temporal Gene Expression Differences in Core and Periinfarct Areas in Experimental Stroke: A Microarray Analysis, PLoS ONE. 7 (2012) e52121.

[53] T. Itoh, T. Satou, H. Ishida, S. Nishida, M. Tsubaki, S. Hashimoto, et al., The relationship between SDF-1 α/CXCR4 and neural stem cells appearing in damaged area after traumatic brain injury in rats, Neurol Rese. 31 (2009) 90–102.

[54] Q. Xu, S. Wang, X. Jiang, Y. Zhao, M. Gao, Y. Zhang, et al., Hypoxia-induced astrocytes promote the migration of neural progenitor cells via vascular endothelial growth factor, stem cell factor, stromal-derived factor-1α and monocyte chemoattractant protein-1 upregulation *in vitro*, Clin Exp Pharmacol Physiol. 34 (2007) 624–631.

[55] J. Imitola, K. Raddassi, K.I. Park, F.-J. Mueller, M. Nieto, Y.D. Teng, et al., Directed migration of neural stem cells to sites of CNS injury by the stromal cell-derived factor 1α/CXC chemokine receptor 4 pathway, P Natl Acad Sci. 101 (2004) 18117–18122.

[56] W.D. Hill, D.C. Hess, A. Martin-Studdard, J.J. Carothers, J. Zheng, D. Hale, et al., SDF-1 (CXCL12) is upregulated in the ischemic penumbra following stroke: association with bone marrow cell homing to injury, J Neuropathol Exp Neurol. 63 (2004) 84–96.

[57] L. Xue, J. Wang, W. Wang, Z. Yang, Z. Hu, M. Hu, et al., The Effect of Stromal Cell-Derived Factor 1 in the Migration of Neural Stem Cells, Cell Biochem Biophys. 70 (2014) 1609–1616.

[58] T.R.M. Filippo, L.T. Galindo, G.F. Barnabe, C.B. Ariza, L.E. Mello, M.A. Juliano, et al., CXCL12 N-terminal end is sufficient to induce chemotaxis and proliferation of neural stem/progenitor cells, Stem Cell Res. 11 (2013) 913–925.

[59] P. Thored, A. Arvidsson, E. Cacci, H. Ahlenius, T. Kallur, V. Darsalia, et al., Persistent production of neurons from adult brain stem cells during recovery after stroke, Stem Cells. 24 (2006) 739–747.

[60] S. Nag, J.L. Takahashi, D.W. Kilty, Role of vascular endothelial growth factor in blood-brain barrier breakdown and angiogenesis in brain trauma, J Neuropathol Exp Neurol. 56 (1997) 912–921.

[61] A. Chodobski, I. Chung, E. Koźniewska, T. Ivanenko, W. Chang, J.F. Harrington, et al., Early neutrophilic expression of vascular endothelial growth factor after traumatic brain injury, Neuroscience. 122 (2003) 853–867.

[62] M.K. Sköld, C.V. Gertten, A.-C. Sandbergnordqvist, T. Mathiesen, S. Holmin, VEGF and VEGF receptor expression after experimental brain contusion in rat, J Neurotrauma. 22 (2005) 353–367.

[63] J.M. Krum, J.M. Rosenstein, VEGF mRNA and Its Receptor flt-1 Are Expressed in Reactive Astrocytes Following Neural Grafting and Tumor Cell Implantation in the Adult CNS, Exp Neurol. 154 (1998) 57–65.

[64] E. Papavassiliou, N. Gogate, M. Proescholdt, J.D. Heiss, S. Walbridge, N.A. Edwards, et al., Vascular endothelial growth factor (vascular permeability factor) expression in injured rat brain, J Neurosci Res. 49 (1997) 451–460.

[65] N. Mani, A. Khaibullina, J.M. Krum, J.M. Rosenstein, Vascular endothelial growth factor enhances migration of astroglial cells in subventricular zone neurosphere cultures, J Neurosci Res. 88 (n.d.) 248–257.

[66] N.O. Schmidt, D. Koeder, M. Messing, F.-J. Mueller, K.S. Aboody, S.U. Kim, et al., Vascular endothelial growth factor-stimulated cerebral microvascular endothelial cells mediate the recruitment of neural stem cells to the neurovascular niche, Brain Res. 1268 (2009) 24–37.

[67] H. Zhang, VEGF is a chemoattractant for FGF-2-stimulated neural progenitors, J Cell Biol. 163 (2003) 1375–1384.

[68] Y. Wang, K. Jin, X.O. Mao, L. Xie, S. Banwait, H.H. Marti, et al., VEGF-overexpressing transgenic mice show enhanced post-ischemic neurogenesis and neuromigration, J Neurosci Res. 85 (2007) 740–747.

[69] K. Jin, Y. Zhu, Y. Sun, X.O. Mao, L. Xie, D.A. Greenberg, Vascular endothelial growth factor (VEGF) stimulates neurogenesis in vitro and in vivo, P Natl Acad Sci. 99 (2002) 11946–11950.

[70] A. Schänzer, F.P. Wachs, D. Wilhelm, T. Acker, C. Cooper Kuhn, H. Beck, et al., Direct stimulation of adult neural stem cells in vitro and neurogenesis in vivo by vascular endothelial growth factor, Brain Pathol. 14 (2004) 237–248.

[71] N. Kawahara, K. Mishima, S. Higashiyama, N. Taniguchi, A. Tamura, T. Kirino, The gene for heparin-binding epidermal growth factor-like growth factor is stress-inducible: its role in cerebral ischemia, J Cereb Blood Flow Metab. 19 (1999) 307–320.

[72] F. Doetsch, L. Petreanu, I. Caille, J.M. Garcia-Verdugo, A. Alvarez-Buylla, EGF converts transit-amplifying neurogenic precursors in the adult brain into multipotent stem cells, Neuron. 36 (2002) 1021–1034.

[73] B.A. Reynolds, W. Tetzlaff, S. Weiss, A multipotent EGF-responsive striatal embryonic progenitor cell produces neurons and astrocytes, J Neurosci. 12 (1992) 4565–4574.

[74] D. Alagappan, D.A. Lazzarino, R.J. Felling, M. Balan, S.V. Kotenko, S.W. Levison, Brain injury expands the numbers of neural stem cells and progenitors in the SVZ by enhancing their responsiveness to EGF, Asn Neuro. 1 (2009) 95–111.

[75] A. Oyagi, N. Morimoto, J. Hamanaka, M. Ishiguro, K. Tsuruma, M. Shimazawa, et al., Forebrain specific heparin-binding epidermal growth factor-like growth factor knockout mice show exacerbated ischemia and reperfusion injury, Neurosci. 185 (2011) 116–124.

[76] J.L. Cook, V. Marcheselli, J. Alam, P.L. Deininger, N.G. Bazan, Temporal changes in gene expression following cryogenic rat brain injury, Mol Brain Res. 55 (1998) 9–19.

[77] S.A. Frautschy, P.A. Walicke, A. Baird, Localization of basic fibroblast growth factor and its mRNA after CNS injury, Brain Res. 553 (1991) 291–299.

[78] A. Logan, S.A. Frautschy, A.-M. Gonzalez, A. Baird, A time course for the focal elevation of synthesis of basic fibroblast growth factor and one of its high-affinity receptors (flg) following a localized cortical brain injury, J Neurosci. 12 (1992) 3828–3837.

[79] A. Logan, S.A. Frautschy, A. Baird, Basic fibroblast growth factor and central nervous system injury, Ann NY Acad Sci. 638 (1991) 474–476.

[80] S.P. Finklestein, P.J. Apostolides, C.G. Caday, J. Prosser, M.F. Philips, M. Klagsbrun, Increased basic fibroblast growth factor (bFGF) immunoreactivity at the site of focal brain wounds, Brain Res. 460 (1988) 253–259.

[81] A. Gritti, E.A. Parati, L. Cova, P. Frolichsthal, R. Galli, E. Wanke, et al., Multipotential stem cells from the adult mouse brain proliferate and self-renew in response to basic fibroblast growth factor, J Neurosci. 16 (1996) 1091–1100.

[82] S. Yoshimura, Y. Takagi, J. Harada, T. Teramoto, S.S. Thomas, C. Waeber, et al., FGF-2 regulation of neurogenesis in adult hippocampus after brain injury, P Natl Acad Sci. 98 (2001) 5874–5879.

[83] F. Agasse, C. Nicoleau, J. Petit, M. Jaber, M. Roger, O. Benzakour, et al., Evidence for a major role of endogenous fibroblast growth factor-2 in apoptotic cortex-induced subventricular zone cell proliferation, European J Neurosci. 26 (2007) 3036–3042.

[84] O. Lindvall, P. Ernfors, J. Bengzon, Z. Kokaia, M.-L. Smith, B.K. Siesjö, et al., Differential regulation of mRNAs for nerve growth factor, brain-derived neurotrophic factor, and neurotrophin 3 in the adult rat brain following cerebral ischemia and hypoglycemic coma, P Natl Acad Sci. 89 (1992) 648–652.

[85] J. Truettner, R. Schmidt-Kastner, R. Busto, O.F. Alonso, J.Y. Loor, W.D. Dietrich, et al., Expression of brain-derived neurotrophic factor, nerve growth factor, and heat shock protein HSP70 following fluid percussion brain injury in rats, J Neurotrauma. 16 (2015) 471–486.

[86] J. Sanchez-Ramos, S. Song, F. Cardozo-Pelaez, C. Hazzi, T. Stedeford, A. Willing, et al., Adult Bone Marrow Stromal Cells Differentiate into Neural Cells in Vitro, Exp Neurol. 164 (2000) 247–256.

[87] R.R. Hicks, S. Numan, H.S. Dhillon, M.R. Prasad, K.B. Seroogy, Alterations in BDNF and NT-3 mRNAs in rat hippocampus after experimental brain trauma, Mol Brain Res. 48 (1997) 401–406.

[88] A.K. Shetty, M.S. Rao, B. Hattiangady, V. Zaman, G.A. Shetty, Hippocampal neurotrophin levels after injury: Relationship to the age of the hippocampus at the time of injury, J Neurosci Res. 78 (2004) 520–532.

[89] P.E. Batchelor, G.T. Liberatore, J.Y. Wong, M.J. Porritt, F. Frerichs, G.A. Donnan, et al., Activated macrophages and microglia induce dopaminergic sprouting in the injured striatum and express brain-derived neurotrophic factor and glial cell line-derived neurotrophic factor, J Neurosci. 19 (1999) 1708–1716.

[90] M. Sieber-Blum, Role of the neurotrophic factors BDNF and NGF in the commitment of pluripotent neural crest cells, Neuron. 6 (1991) 949–955.

[91] A. Cheng, S. Wang, J. Cai, M.S. Rao, M.P. Mattson, Nitric oxide acts in a positive feedback loop with BDNF to regulate neural progenitor cell proliferation and differentiation in the mammalian brain, Dev Biol. 258 (2003) 319–333.

[92] S. Ahmed, B.A. Reynolds, S. Weiss, BDNF enhances the differentiation but not the survival of CNS stem cell-derived neuronal precursors, J Neurosci. 15 (1995) 5765–5778.

[93] M.B. Lachyankar, P.J. Condon, P.J. Quesenberry, N.S. Litofsky, L.D. Recht, A.H. Ross, Embryonic precursor cells that express Trk receptors: induction of different cell fates by NGF, BDNF, NT-3, and CNTF, Exp Neurol. 144 (1997) 350–360.

[94] B. Kirschenbaum, S.A. Goldman, Brain-derived neurotrophic factor promotes the survival of neurons arising from the adult rat forebrain subependymal zone, P Natl Acad Sci. 92 (1995) 210–214.

[95] X. Gao, J. Chen, Conditional Knockout of Brain-Derived Neurotrophic Factor in the Hippocampus Increases Death of Adult-Born Immature Neurons following Traumatic Brain Injury, J Neurotrauma. 26(2009) 1325–1335.

[96] M. Endres, G. Fan, L. Hirt, M. Fujii, K. Matsushita, X. Liu, et al., Ischemic brain damage in mice after selectively modifying BDNF or NT4 gene expression, J Cereb Blood Flow Metab. 20 (2000) 139–144.

[97] C. Qu, A. Mahmood, D. Lu, A. Goussev, Y. Xiong, M. Chopp, Treatment of traumatic brain injury in mice with marrow stromal cells, Brain Res. 1208 (2008) 234–239.

[98] N. Grigoriadis, A. Lourbopoulos, R. Lagoudaki, J.M. Frischer, E. Polyzoidou, O. Touloumi, et al., Variable behavior and complications of autologous bone marrow mesenchymal stem cells transplanted in experimental autoimmune enchepalitis, Exp Neurol. 230 (2011) 78–89.

[99] E.Y. Snyder, The risk of putting something where it does not belong: Mesenchymal stem cells produce masses in the brain, Exp Neurol. 230 (2011) 75–77.

[100] A. Mahmood, D. Lu, M. Lu, M. Chopp, Treatment of Traumatic Brain Injury in Adult Rats with Intravenous Administration of Human Bone Marrow Stromal Cells, Neurosurg. 53 (2003) 697–703.

[101] A. Mahmood, D. Lu, L. Wang, Y. Li, M. Lu, M. Chopp, Treatment of traumatic brain injury in female rats with intravenous administration of bone marrow stromal cells, Neurosurg. 49 (2001) 1196–1203.

[102] D.A. Shear, M.C. Tate, D.R. Archer, S.W. Hoffman, V.D. Hulce, M.C. LaPlaca, et al., Neural progenitor cell transplants promote long-term functional recovery after traumatic brain injury, Brain Res. 1026 (2004) 11–22.

[103] T.G. Bush, N. Puvanachandra, C.H. Horner, A. Polito, T. Ostenfeld, C.N. Svendsen, et al., Leukocyte infiltration, neuronal degeneration, and neurite outgrowth after ablation of scar-forming, reactive astrocytes in adult transgenic mice, Neuron. 23 (1999) 297–308.

[104] P. Riess, C. Zhang, K.E. Saatman, H.L. Laurer, L.G. Longhi, R. Raghupathi, et al., Transplanted neural stem cells survive, differentiate, and improve neurological motor function after experimental traumatic brain injury, Neurosurg. 51 (2002) 1043–1054.

[105] A. Wennersten, X. Meijer, S. Holmin, L. Wahlberg, T. Mathiesen, Proliferation, migration, and differentiation of human neural stem/progenitor cells after transplantation into a rat model of traumatic brain injury, J Neurosurg. 100 (2004) 88–96.

[106] M.T. Harting, L.A.E. Sloan, F. Jimenez, J. Baumgartner, C.S. Cox, Subacute Neural Stem Cell Therapy for Traumatic Brain Injury, J Surg Res. 153 (2009) 188–194.

[107] N. Kamei, N. Tanaka, Y. Oishi, T. Hamasaki, K. Nakanishi, N. Sakai, et al., BDNF, NT-3, and NGF released from transplanted neural progenitor cells promote corticospinal axon growth in organotypic cocultures, Spine. 32 (2007) 1272–1278.

[108] H.-J. Kim, J.-H. Lee, S.-H. Kim, Therapeutic effects of human mesenchymal stem cells on traumatic brain injury in rats: secretion of neurotrophic factors and inhibition of apoptosis, J Neurotrauma. 27 (2010) 131–138.

[109] X. Chen, M. Katakowski, Y. Li, D. Lu, L. Wang, L. Zhang, et al., Human bone marrow stromal cell cultures conditioned by traumatic brain tissue extracts: Growth factor production, J Neurosci Res. 69 (2002) 687–691.

[110] H. Ma, B. Yu, L. Kong, Y. Zhang, Y. Shi, Neural stem cells over-expressing brain-derived neurotrophic factor (BDNF) stimulate synaptic protein expression and promote functional recovery following transplantation in rat model of traumatic brain injury, Neurochem Res. 37 (2012) 69–83.

[111] Z. Wang, W. Yao, Q. Deng, X. Zhang, J. Zhang, Protective Effects of BDNF Overexpression Bone Marrow Stromal Cell Transplantation in Rat Models of Traumatic Brain Injury, J Mol Neurosci. 49 (2012) 409–416.

[112] Z. Wang, Y. Wang, Z. Wang, S. Gutkind, Z. Wang, F. Wang, et al., Engineered Mesenchymal Stem Cells with Enhanced Tropism and Paracrine Secretion of Cytokines and Growth Factors to Treat Traumatic Brain Injury, Stem Cells. 33 (2014) 456–467.

[113] O.Y. Bang, K.S. Jin, M.N. Hwang, H.Y. Kang, B.J. Kim, S.J. Lee, et al., The Effect of CXCR4 Overexpression on Mesenchymal Stem Cell Transplantation in Ischemic Stroke, Cell Med. 4 (2012) 65–76.

[114] J. Gao, D. Prough, D. McAdoo, J. Grady, M. Parsley, L. Ma et al., Transplantation of primed human fetal neural stem cells improves cognitive function in rats after traumatic brain injury, Exp Neurol. 201 (2006) 281–292.

[115] K.I. Park, Y.D. Teng, E.Y. Snyder, The injured brain interacts reciprocally with neural stem cells supported by scaffolds to reconstitute lost tissue, Nat Biotech. 20 (2002) 1111–1117.

[116] J.M. Heffernan, D.J. Overstreet, L.D. Le, B.L. Vernon, R.W. Sirianni, Bioengineered Scaffolds for 3D Analysis of Glioblastoma Proliferation and Invasion, Ann Biomed Eng. (2014).

[117] Y.-B. Lu, K. Franze, G. Seifert, C. Steinhäuser, F. Kirchhoff, H. Wolburg, et al., Viscoelastic properties of individual glial cells and neurons in the CNS, P Natl Acad Sci. 103 (2006) 17759–17764.

[118] C. Qu, A. Mahmood, X.S. Liu, Y. Xiong, L. Wang, H. Wu, et al., The treatment of TBI with human marrow stromal cells impregnated into collagen scaffold: Functional outcome and gene expression profile, Brain Res. 1371 (2011) 129–139.

[119] Y. Xiong, C. Qu, A. Mahmood, Z. Liu, R. Ning, Y. Li, et al., Delayed transplantation of human marrow stromal cell-seeded scaffolds increases transcallosal neural fiber length, angiogenesis, and hippocampal neuronal survival and improves functional outcome after traumatic brain injury in rats, Brain Res. 1263 (2009) 183–191.

[120] D. Lu, A. Mahmood, C. Qu, X. Hong, D. Kaplan, M. Chopp, Collagen scaffolds populated with human marrow stromal cells reduce lesion volume and improve functional outcome after traumatic brain injury, Neurosurg. 61 (2007) 596.

[121] A. Mahmood, H. Wu, C. Qu, S. Mahmood, Y. Xiong, D.L. Kaplan, et al., Suppression of neurocan and enhancement of axonal density in rats after treatment of traumatic brain injury with scaffolds impregnated with bone marrow stromal cells: Laboratory investigation, J Neurosurg. 120 (2015) 1147–1155.

[122] J. Guan, Z. Zhu, R.C. Zhao, Z. Xiao, C. Wu, Q. Han, et al., Transplantation of human mesenchymal stem cells loaded on colalgen scaffolds for the treatment of traumatic brain injury in rats, Biomaterials. 34 (2013) 5937–5946.

[123] T.Y. Cheng, M.H. Chen, W.H. Chang, M.Y. Huang, T.W. Wang, Neural stem cells encapsulated in a functionalized self-assembling peptide hydrogel for brain tissue engineering, Biomaterials. 34 (2013) 2005–2016.

[124] C.C. Tate, D.A. Shear, M.C. Tate, D.R. Archer, D.G. Stein, M.C. LaPlaca, Laminin and fibronectin scaffolds enhance neural stem cell transplantation into the injured brain, J Tissue Eng Regen Med. 3 (2009) 208–217.

[125] C. Lindwall, M. Olsson, A.M. Osman, H.G. Kuhn, M.A. Curtis, Selective expression of hyaluronan and receptor for hyaluronan mediated motility (Rhamm) in the adult mouse subventricular zone and rostral migratory stream and in ischemic cortex, Brain Res. 1503 (2013) 62–77.

[126] M. Preston, L.S. Sherman, Neural Stem Cell Niches: Critical Roles for the Hyaluronan-Based Extracellular Matrix in Neural Stem Cell Proliferation and Differentiation, Front Biosci (Scholar Edition). 3 (2012) 1165.

[127] Y. Liang, P. Walczak, J.W.M. Bulte, The survival of engrafted neural stem cells within hyaluronic acid hydrogels, Biomaterials. 34 (2013) 5521–5529.

[128] A.J. Mothe, R.Y. Tam, T. Zahir, C.H. Tator, M.S. Shoichet, Biomaterials, Biomaterials. 34 (2013) 3775–3783.

[129] W.M. Tian, S.P. Hou, J. Ma, C.L. Zhang, Q.Y. Xu, I.S. Lee, et al., Hyaluronic acid-poly-D-lysine-based three-dimensional hydrogel for traumatic brain injury, Tissue Eng. 11 (2005) 513–525.

[130] X.Z. Shu, K. Ghosh, Y. Liu, F.S. Palumbo, Y. Luo, R.A. Clark, et al., Attachment and spreading of fibroblasts on an RGD peptide-modified injectable hyaluronan hydrogel, J Biomed Mater Res. 68A (2003) 365–375.

[131] S. Nolan, Traumatic brain injury: a review, Crit Care Nurs Q. 28 (2005) 188–194.

[132] L. Wei, J.L. Fraser, Z.-Y. Lu, X. Hu, S.P. Yu, Transplantation of hypoxia preconditioned bone marrow mesenchymal stem cells enhances angiogenesis and neurogenesis after cerebral ischemia in rats, Neurobiol Dis. 46 (2012) 635–645.

[133] A.M. Turnley, Regulation of endogenous neural stem/progenitor cells for neural repair—factors that promote neurogenesis and gliogenesis in the normal and damaged brain, Front Cell Neurosci. 6 (2013) 1–18.

[134] T.K. McIntosh, K.E. Saatman, R. Raghupathi, D.I. Graham, D.H. Smith, V. Lee, et al., Review. The Dorothy Russell Memorial Lecture. The molecular and cellular sequelae of experimental traumatic brain injury: pathogenetic mechanisms, Neuropathol Appl Neurobiol. 24 (1998) 251–267.

[135] H. Azari, S. Sharififar, M. Rahman, S. Ansari, B.A. Reynolds, Establishing Embryonic Mouse Neural Stem Cell Culture Using the Neurosphere Assay, JoVE (2011) e2457.

[136] P.B. Tran, G. Banisadr, D. Ren, A. Chenn, R.J. Miller, Chemokine receptor expression by neural progenitor cells in neurogenic regions of mouse brain, J Comp Neurol. 500 (2006) 1007–1034.

[137] M.T. Harting, J.E. Baumgartner, L.L. Worth, L. Ewing-Cobbs, A.P. Gee, M.-C. Day, et al., Cell therapies for traumatic brain injury, Neurosurg FOCUS. 24 (2008) E18.

[138] R.M. Richardson, A. Singh, D. Sun, H.L. Fillmore, D.W. Dietrich III, M.R. Bullock, Stem cell biology in traumatic brain injury: effects of injury and strategies for repair: A review, J Neurosurg. 112 (2010) 1125–1138.

[139] D.S. Park, J.S. Park, D.S. Yeon, The effects of laminin on the characteristics and differentiation of neuronal cells from epidermal growth factor-responsive neuroepithelial cells, Yonsei Med J. 39 (1998) 130–140.

[140] L.A. Flanagan, L.M. Rebaza, S. Derzic, P.H. Schwartz, E.S. Monuki, Regulation of human neural progenitor cells by laminin and integrins, J Neurosci Res. 83 (2006) 845-856.

[141] T. Garzón-Muvdi, A. Quiñones-Hinojosa, Neural stem cell niches and homing: recruitment and integration into functional tissues, ILAR J. 51 (2010) 3–23.

[142] Q. Zhang, G. Liu, Y. Wu, H. Sha, P. Zhang, J. Jia, BDNF Promotes EGF-Induced Proliferation and Migration of Human Fetal Neural Stem/Progenitor Cells via the PI3K/Akt Pathway, Molecules, (2011) 1–11.

[143] F.P. Wachs, B. Winner, S. Couillard-Despres, T. Schiller, R. Aigner, J. Winkler, et al., Transforming growth factor-beta1 is a negative modulator of adult neurogenesis, J Neuropathol Exp Neurol. 65 (2006) 358–370.

[144] D. Thurman, J. Guerrero, Trends in hospitalization associated with traumatic brain injury, Jama. 282 (1999) 954–957.

[145] T.W. McAllister, Neurobiological consequences of traumatic brain injury, Dialog Clin Neurosci. 13 (2011) 287.

[146] A.C. McKee, R.C. Cantu, C.J. Nowinski, E.T. Hedley-Whyte, B.E. Gavett, A.E. Budson, et al., Chronic Traumatic Encephalopathy in Athletes, J Neuropathol Exp Neurol 68 (2009) 709–735.

[147] J.M. Ziebell, M.C. Morganti-Kossmann, Involvement of Pro- and Anti-Inflammatory Cytokines and Chemokines in the Pathophysiology of Traumatic Brain Injury, Neurotherapeutics. 7 (2010) 22–30.

[148] A. Bignami, M. Hosley, D. Dahl, Hyaluronic acid and hyaluronic acid-binding proteins in brain extracellular matrix, Anat Embryol (Berl). 188 (1993) 419–433.

[149] D. Bonneh-Barkay, C.A. Wiley, Brain Extracellular Matrix in Neurodegeneration, Brain Pathol. 19 (2009) 573–585.

[150] K. Brännvall, K. Bergman, U. Wallenquist, S. Svahn, T. Bowden, J. Hilborn, et al., Enhanced neuronal differentiation in a three-dimensional collagen-hyaluronan matrix, J Neurosci Res. 85 (2007) 2138–2146.

[151] Y.T. Wei, W.M. Tian, X. Yu, F.Z. Cui, S.P. Hou, Q.Y. Xu, et al., Hyaluronic acid hydrogels with IKVAV peptides for tissue repair and axonal regeneration in an injured rat brain, Biomed Mater 2 (2007) S142–S146.

[152] Y. Wang, Y.T. Wei, Z.H. Zu, R.K. Ju, M.Y. Guo, X.M. Wang, et al., Combination of hyaluronic acid hydrogel scaffold and PLGA microspheres for supporting survival of neural stem cells, Pharm Res 28 (2011) 1406–1414.

[153] G. Lisignoli, S. Cristino, A. Piacentini, C. Cavallo, A.I. Caplan, A. Facchini, Hyaluronan-based polymer scaffold modulates the expression of inflammatory and degradative factors in mesenchymal stem cells: Involvement of Cd44 and Cd54, J Cell Physiol 207 (2006) 364–373.

[154] B.P. Purcell, J.A. Elser, A. Mu, K.B. Margulies, J.A. Burdick, Synergistic effects of SDF-1α chemokine and hyaluronic acid release from degradable hydrogels on directing bone marrow derived cell homing to the myocardium, Biomaterials. 33 (2012) 7849–7857.

[155] A. Avigdor, CD44 and hyaluronic acid cooperate with SDF-1 in the trafficking of human CD34+ stem/progenitor cells to bone marrow, Blood. 103 (2004) 2981–2989.

[156] M. Naruse, K. Shibasaki, S. Yokoyama, M. Kurachi, Y. Ishizaki, Dynamic Changes of CD44 Expression from Progenitors to Subpopulations of Astrocytes and Neurons in Developing Cerebellum, PLoS ONE. 8 (2013) e53109.

[157] Y. Liu, S.S.W. Han, Y. Wu, T.M.F. Tuohy, H. Xue, J. Cai, et al., CD44 expression identifies astrocyte-restricted precursor cells, Dev Biol. 276 (2004) 31–46.

[158] K.P. Vercruysse, D.M. Marecak, J.F. Marecek, G.D. Prestwich, Synthesis and in vitro degradation of new polyvalent hydrazide cross-linked hydrogels of hyaluronic acid, Bioconjugate Chem. 8 (1997) 686–694.

[159] X.Z. Shu, Y. Liu, F. Palumbo, G.D. Prestwich, Disulfide-crosslinked hyaluronan-gelatin hydrogel films: a covalent mimic of the extracellular matrix for in vitro cell growth, Biomaterials. 24 (2003) 3825–3834.

[160] G.L. Ellman, Tissue sulfhydryl groups, Arch Biochem Biophys. 82 (1959) 70–77.

[161] X.Z. Shu, S. Ahmad, Y. Liu, G.D. Prestwich, Synthesis and evaluation of injectable, in situ crosslinkable synthetic extracellular matrices for tissue engineering, J Biomed Mater Res. 79A (2006) 902–912.

[162] T.-Y. Wang, J.S. Forsythe, D.R. Nisbet, C.L. Parish, Promoting engraftment of transplanted neural stem cells/progenitors using biofunctionalised electrospun scaffolds, Biomaterials. 33 (2012) 9188–9197.

[163] X. Yu, D. Chen, Y. Zhang, X. Wu, Z. Huang, H. Zhou, et al., Overexpression of CXCR4 in mesenchymal stem cells promotes migration, neuroprotection and angiogenesis in a rat model of stroke, J Neurol Sci. 316 (2012) 141–149.

[164] S. Suri, C.E. Schmidt, Cell-laden hydrogel constructs of hyaluronic acid, collagen, and laminin for neural tissue engineering, Tissue Eng Part A. 16 (2010) 1703–1716.

[165] K. Beck, I. Hunter, J. Engel, Structure and function of laminin: anatomy of a multidomain glycoprotein, FASEB J. 4 (1990) 148-160.

[166] R. Timpl, H. Rohde, P.G. Robey, S.I. Rennard, J.M. Foidart, G.R. Martin, Laminin - a glycoprotein from basement membranes, J Biol Chem. 259 (1979) 9933-9937.

[167] C. Deboux, S. Ladraa, S. Cazaubon, S. Ghribi-Mallah, N. Weiss, N. Chaverot, et al., Overexpression of CD44 in Neural Precursor Cells Improves Trans-Endothelial Migration and Facilitates Their Invasion of Perivascular Tissues In Vivo, PLoS ONE. 8 (2013) e57430.

[168] M. Cohen, Z. Kam, L. Addadi, B. Geiger, Dynamic study of the transition from hyaluronan- to integrin-mediated adhesion in chondrocytes, Embo J. 25 (2006) 302–311.

[169] J.L. Lee, M.J. Wang, P.R. Sudhir, J.Y. Chen, CD44 Engagement Promotes Matrix-Derived Survival through the CD44-SRC-Integrin Axis in Lipid Rafts, Mol Cell Biol. 28 (2008) 5710–5723.

[170] G. Martino, S. Pluchino, The therapeutic potential of neural stem cells, Nature Rev Neurosci. 7 (2006) 395–406.

[171] E.A. Turley, P.W. Noble, L.Y.W. Bourguignon, Signaling Properties of Hyaluronan Receptors, J Biol Chem. 277 (2002) 4589–4592.

[172] M.A. Wozniak, K. Modzelewska, L. Kwong, P.J. Keely, Focal adhesion regulation of cell behavior, BBA-Mol Cell Res. 1692 (2004) 103–119.

[173] Y.-S. Huang, C.-Y. Cheng, S.-H. Chueh, D.-Y. Hueng, Y.-F. Huang, C.-M. Chu, et al., Involvement of SHP2 in focal adhesion, migration and differentiation of neural stem cells, Brain Devel. 34 (2012) 674–684.

[174] M.-S. Kim, M.-J. Park, E.-J. Moon, S.-J. Kim, C.-H. Lee, H. Yoo, et al., Hyaluronic acid induces osteopontin via the phosphatidylinositol 3-kinase/Akt pathway to enhance the motility of human glioma cells, Cancer Res. 65 (2005) 686–691.

[175] P. Rooney, M. Wang, P. Kumar, S. Kumar, Angiogenic oligosaccharides of hyaluronan enhance the production of collagens by endothelial cells, J Cell Sci. 105 (1993) 213–218.

[176] J. Price, R.O. Hynes, Astrocytes in culture synthesize and secrete a variant form of fibronectin, J Neurosci. 5 (1985) 2205–2211.

[177] J.B. Jensen, M. Parmar, Strengths and limitations of the neurosphere culture system, Mol Neurobiol. 34 (2006) 153–161.

[178] O.N. Suslov, V.G. Kukekov, T.N. Ignatova, D.A. Steindler, Neural stem cell heterogeneity demonstrated by molecular phenotyping of clonal neurospheres, P Natl Acad Sci-USA. 99 (2002) 14506–14511.

[179] P.H. Wu, A. Giri, S.X. Sun, D. Wirtz, Three-dimensional cell migration does not follow a random walk, P Natl Acad Sci-USA. 111 (2014) 3949–3954.

[180] P. Friedl, K. Wolf, Plasticity of cell migration: a multiscale tuning model, The J Cell Biol. 188 (2010) 11–19.

[181] S.I. Fraley, Y. Feng, R. Krishnamurthy, D.-H. Kim, A. Celedon, G.D. Longmore, et al., A distinctive role for focal adhesion proteins in three- dimensional cell motility, Nature Cell Biol. 12 (2010) 598–604.

[182] P. Friedl, E.-B. Bröcker, The biology of cell locomotion within three-dimensional extracellular matrix, Cell Mol Life Sci. 57 (2000) 41–64.

[183] F.C. Barone, K.S. Kilgore, Role of inflammation and cellular stress in brain injury and central nervous system diseases, Clin Neurosci Res. 6 (2006) 329–356.

[184] T. Itoh, T. Satou, S. Nishida, M. Tsubaki, S. Hashimoto, H. Ito, The Novel Free Radical Scavenger, Edaravone, Increases Neural Stem Cell Number Around the Area of Damage Following Rat Traumatic Brain Injury, Neurotox Res. 16 (2009) 378–389.

[185] B. Saha, S. Peron, K. Murray, M. Jaber, A. Gaillard, Cortical lesion stimulates adult subventricular zone neural progenitor cell proliferation and migration to the site of injury, Stem Cell Res. 11 (2013) 965–977.

[186] J.H. Shin, Y.M. Park, D.H. Kim, G.J. Moon, O.Y. Bang, T. Ohn, et al., Ischemic brain extract increases SDF-1 expression in astrocytes through the CXCR2/miR-223/miR-27b pathway, BBA-Gene Regul Mech. 1839 (2014) 826–836.

[187] D. Woodbury, E.J. Schwarz, D.J. Prockop, I.B. Black, Adult rat and human bone marrow stromal cells differentiate into neurons, J Neurosci Res 61 (2000) 364–370.

[188] R.O.C. Oreffo, C. Cooper, C. Mason, M. Clements, Mesenchymal stem cells: lineage, plasticity, and skeletal therapeutic potential, Stem Cell Rev. 1 (2005) 169–178.

[189] C.E. Dixon, G.L. Clifton, J.W. Lighthall, A.A. Yaghmai, R.L. Hayes, A Controlled Cortical Impact Model of Traumatic Brain Injury in the Rat, J Neurosci Meth. 39 (1991) 253–262.

[190] A.G. Dayer, B. Jenny, M.-O. Sauvain, G. Potter, P. Salmon, E. Zgraggen, et al., Expression of FGF-2 in neural progenitor cells enhances their potential for cellular brain repair in the rodent cortex, Brain. 130 (2007) 2962–2976.

[191] H. Kim, M.J. Cooke, M.S. Shoichet, Creating permissive microenvironments for stem cell transplantation into the central nervous system, Trends Biotechnol. (2011) 1–9.

[192] A. Helmy, M.-G. De Simoni, M.R. Guilfoyle, K.L.H. Carpenter, P.J. Hutchinson, Cytokines and innate inflammation in the pathogenesis of human traumatic brain injury, Prog Neurobiol. 95 (2011) 352–372.

[193] P. Moshayedi, S.T. Carmichael, Hyaluronan, neural stem cells and tissue reconstruction after acute ischemic stroke, Biomatter. 3 (2014) e23863–9.

[194] S. Hou, Q. Xu, W. Tian, F. Cui, Q. Cai, J. Ma, et al., The repair of brain lesion by implantation of hyaluronic acid hydrogels modified with laminin, Journal of Neuroscience Methods. 148 (2005) 60–70.

[195] M. Bacigaluppi, S. Pluchino, L.P. Jametti, E. Kilic, U. Kilic, G. Salani, et al., Delayed post-ischaemic neuroprotection following systemic neural stem cell transplantation involves multiple mechanisms, Brain. 132 (2009) 2239–2251.

[196] M. Hagan, Neuroprotection by human neural progenitor cells after experimental contusion in rats, Neurosci Lett. (2003) 1–4.

[197] E. Sbaa-Ketata, M.-N. Courel, B. Delpech, J.-P. Vannier, Hyaluronan-derived oligosaccharides enhance SDF-1-dependent chemotactic effect on peripheral blood hematopoietic CD34(+) cells, Stem Cells. 20 (2002) 585–587.

[198] A. Zernecke, I. Bot, Y. Djalali-Talab, E. Shagdarsuren, K. Bidzhekov, S. Meiler, et al., Protective role of CXC receptor 4/CXC ligand 12 unveils the importance of neutrophils in atherosclerosis, Circ Res. 102 (2008) 209-217.

[199] V. Braunersreuther, F. Mach, S. Steffens, The specific role of chemokines in atherosclerosis, Thromb Haemost. 97 (2007) 714-721.

[200] E.A. Liehn, N. Tuchscheerer, I. Kanzler, M. Drechsler, L. Fraemohs, A. Schuh, et al., Double-edged role of the CXCL12/CXCR4 axis in experimental myocardial infarction, J Am Coll Cardiol. 58 (2011) 2415-2423.

[201] A. Orimo, P.B. Gupta, D.C. Sgroi, F. Arenzana-Seisdedos, T. Delaunay, R. Naeem, et al., Stromal fibroblasts present in invasive human breast carcinomas promote tumor growth and angiogenesis through elevated SDF-1/CXCL12 secretion, Cell 121 (2005) 335-348.

[202] A. Müller, B. Homey, H. Soto, N. Ge, D. Catron, M.E. Buchanan, et al., Involvement of chemokine receptors in breast cancer metastasis, Nature. 410 (2001) 50-56.

[203] F. Balkwill, Cancer and the chemokine network, Nat Rev Cancer. 4 (2004) 540-550.

[204] A. Fox, J. Smythe, N. Fisher, M.P.H. Tyler, D.A. McGrouther, S.M. Watt, et al., Mobilization of endothelial progenitor cells into the circulation in burned patients, Br J Surg. 95 (2007) 244-251.

[205] T. Kitaori, H. Ito, E.M. Schwarz, R. Tsutsumi, H. Yoshitomi, S. Oishi, et al., Stromal cell-derived factor 1/CXCR4 signaling is critical for the recruitment of mesenchymal stem cells to the fracture site during skeletal repair in a mouse model, Arthritis Rheum. 60 (2009) 813-823.

[206] P. Fiorina, G. Pietramaggiori, S.S. Scherer, M. Jurewicz, J.C. Matthews, A. Vergani, et al., The mobilization and effect of endogenous bone marrow progenitor cells in diabetic wound healing, Cell Transplant. 19 (2010) 1369-1381.

[207] M. Kucia, J. Ratajczak, R. Reca, A. Janowska-Wieczorek, M.Z. Ratajczak, Tissue-specific muscle, neural and liver stem/progenitor cells reside in the bone marrow, respond to an SDF-1 gradient and are mobilized into peripheral blood during stress and tissue injury, Blood Cells, Molecules, and Disease. 32 (2004) 52-57.

[208] S.K. Ghadge, S. Mühlstedt, C. Özcelik, M. Bader, SDF-1α as a therapeutic stem cell homing factor in myocardial infarction, Pharmacol and Thera. 129 (2011) 97-108.

[209] J.D. Abbot, Y. Huang, D. Liu, R. Hickey, D.S. Krause, F.J. Giordano, Stromal cell-derived factor-1α plays a critical role in stem cell recruitment to the heart after myocardial infarction but is not sufficient to induce homing in the absence of injury, Circulation. 110 (2004) 3300-3305.

[210] A.T. Askari, S. Unzek, Z.B. Popovic, C.K. Goldman, F. Forudi, M. Kiedrowski, et al., Effect of stromal-cell-derived factor 1 on stem-cell homing and tissue regeneration in ischaemic cardiomyopathy, The Lancet. 362 (2003) 697-703.

[211] M. Uematsu, T. Yoshizaki, T. Shimizu, J. Obata, T. Nakamura, D. Fujioka, et al., Sustained myocardial production of stromal cell-derived factor-1α was associated with left ventricular adverse remodeling in patients with myocardial infarction, Am J Physiol Heart Circ Physiol. 309 (2015) H1764-1771.

[212] C. Bearzi, M. Rota, T. Hosoda, J. Tillmanns, A. Nascimbene, A. De Angelis, et al., Human cardiac stem cells, P Natl Acad Sci USA. 104 (2007) 14068-14073.

[213] K. Urbanek, D. Cesselli, M. Rota, A. Nascimbene, A. De Angelis, T. Hosoda, et al., Stem cell niches in the adult mouse heart, P Natl Acad Sci USA. 103 (2006) 9226-9231.

[214] T. Sugiyama, H. Kohara, M. Noda, T. Nagasawa, Matinenance of the hematopoietic stem cell pool by CXCL12-CXCR4 chemokine signaling in bone marrow stromal cell niches, Immunity. 25 (2006) 977-988.

[215] B.J. Bhattacharyya, G. Banisadr, H. Jung, D. Ren, D.G. Cronshaw, Y. Zou, et al., The chemokine stromal cell-derived factor-1 regulates GABAergic inputs to neural progenitors in the postnatal dentate gyrus, J Neurosci. 28 (2008) 6720-6730.

[216] A.R. Goazigo, J. Van Steenwinckel, W. Rostène, S.M. Parsadaniantz, Current status of chemokines in the adult CNS, Prog Neurobiol. 104 (2013) 67-92.

[217] I. Decimo, F. Bifari, M. Drampera, G. Fumagalli, Neural stem cell niches in health and diseases, Curr Pharm Des. 18 (2012) 1755-1783.

[218] A. Corcione, F. Benvenuto, E. Ferretti, D. Giunti, V. Cappiello, F. Cazzanti, et al., Human mesenchymal stem cells modulate B-cell functions, Blood. 107 (2006) 367-372.

[219] D.C. Hargreaves, P.L. Hyman, T.T. Lu, V.N. Ngo, A. Bidgol, G. Suzuki, et al., A coordinated change in chemokine responsiveness guides plasma cell movements, J Exp Med. 194 (2001) 45-56.

[220] Q. Ma, D. Jones, P.R. Borghesani, R.A. Segal, T. Nagasawa, T. Kishimoto, Impaired B-lymphopoiesis, myelopoiesis, and derailed cerebellar neuron migration in CXCR4-and SDF-1-deficient mice, P Natl Acad Sci USA. 95 (1998) 9448-9453.

APPENDIX A

DETAILED PROTOCOLS

A.1 Western Blotting and Sample Preparation from Neural Stem Cells Seeded on Hyaluronic Acid-Laminin

A2.1.1. Required Materials

80 μL HA-Lm gel per sample (see Chapter 3: Section 3.2.2. for material list, manufacturer information, monomer and crosslinker preparation, and method for gel preparation)

Sterile 6-well plate

Accutase*

Millipore centrifugal filter units† (0.5 mL)

Cold RIPA buffer (see Chapter 3: Section 3.2 for manufacturer)

Protease inhibitor cocktail (see Chapter 3: Section 3.2 for manufacturer and working concentration)

8 or 12% Bis-acrylamide gel (depedent on protein of interest)

Note: western blotting reagents should be optimized based on target protein. Listed below are those used commonly by me and may be used as a starting point for optimization.

PVDF transfer membranes

Blocking buffer (5 w/v% non-fat dry milk in 0.1% Tween-20, 1X Tris-buffered saline(TBST))

Wash solution (1X TBST)

Antibody diluent (1 w/v% non-fat dry milk in 1X TBST)

*Accutase was not used in the original experiments, however its use is recommended (see *Notes*)

†Will need if Accutase is not used

A2.1.2. Methods

Notes:

1. When forming HA-Lm gels on the bottom of the 6-well plate, make sure not to extend gel entirely to edge of well as this will create a meniscus around the well perimeter and may alter plating surface.

2. Accutase may be used according to manufacturer instructions to lift cells off of HA-Lm gel prior to lysing with cold RIPA buffer. Trypsin-EDTA is not recommended as it is too harsh for the NPSCs and may have adverse effects. To use Accutase, incubate according to manufacturer protocol and ensure cells have detached from HA-Lm gel prior to collecting into a centrifuge tube and spinning down at 170 rcf for 3 min. Gently remove supernatant and add cold RIPA buffer, indicated in step 5. If Accutase is not used, cell lysate will most likely need to be concentrated using Millipore centrifugal filter units as described in the protocol.

Protocol

1. Form 80 μL HA-Lm gel films on the bottom of a 6-well plate, making sure not to extend the gel to the perimenter of the well.

2. Allow gel to form in cell incubator for 15 hours prior to seeding.

    a. HA-Lm gel is fully formed at 6 hours and plating at this point would be fine as long as consistent across samples. Typically 15 hours of gelation can allow for overnight incubation.

3. Seed 5×10^5 NPSCs in 200 μL directly on top of the HA-Lm gel and allow to adhere within the cell incubator for 1-2 hours (as long as consistent across all samples in studies) before adding remaining media (most likely mitogenic growth-factor free, but dependent on study design) on top of NPSCs.

4. At study time point, remove excess media from well. If using Accutase, incubate with Accutase at this point.

5. Add 300 μL cold RIPA buffer supplemented with protease cocktail inhibitor (100 μL if using Accutase method) and rock on ice for 30 minutes.

a. If using Accutase method, vortex at 0 and 15 minutes into incubation.

b. If not using Accutase method, gently encourage cell removal from gel by pipetting RIPA buffer across the gel without disrupting gel too severely at same time points. If gel becomes too disrupted, it will become very difficult to spin down and separate gel from cell lysate.

6. Transfer lysate to cold, autoclaved 0.65 mL microcentrifuge tube and spin down at 13000 rpm for 5 min at 4°C.

7. If using Accutase method, aliquot supernatant and store at -80°C. If not using Accutase method, you will most likely need to concentrate your supernatant using the Millipore centrifugal filter units according to manufacturer's protocol. Be sure to keep the filter tubes/units cold throughout. Following concentration, aliquot and store at -80°C.

a. Supernatant will not be easy to visibly discern. It is useful to keep track of the direction in which you place your tube into the centrifuge so that you will know where the insoluble protein pellet will form. I will typically pull off ~80% of the total volume to store as supernatant, being sure to avoid the tube area where I anticipate the pellet to have formed.

8. Quantify protein concentration using the bicinchoninic acid (BCA) assay, prepare bis-acrylamide gels of appropriate percentage, and prepare lysate samples with sample buffer.

9. The gel electrophoresis parameters can be optimized (i.e. when targeting smaller proteins, the gel may need longer), but gels were typically run at 120 V for 70 min.

10. Gel transfer time may also require optimization, however gels were typically

transferred for 9 minutes using the standard voltage and amperage. Protein transfer was ensured by Simply Blue stain.

11. Wash membranes with 1X TBST to remove any remaining SDS prior to blocking for 1 hour rocking at room temperature in a solution of 5w/v% non-fat dry milk in 1X TBST.

12. Rinse once between blocking and primary antibody staining. Primary antibodies were added at optimized dilutions to a solution of 1 w/v% non-fat dry milk in 1X TBST and rocked overnight at 4°C. Antibodies and their concentrations used for publications were as follows:

a. anti-CXCR4 @ 1:500 (abcam, cat no: ab2074)

b. anti-nestin @1:250 (abcam, cat no: ab27952)

c. anti-β III tubulin @1:1000 (EMD Millipore, cat no: MAB1637)

d. anti-GFAP@1:1000 (EMD Millipore, cat no: MAB3402)

e. anti-Olig2@1:500 (EMD Millipore, cat no: AB9610)

13. Wash membranes 3x for 5 minutes each prior to incubating with secondary antibody. Secondary antibodies were added at optimized dilutions to a solution of 1 w/v% non-fat dry milk in 1X TBST and rocked in the dark at room temperature for 2 hours, followed by a final rinse before imaging with LI-COR Odyssey scanner. Antibodies and their concentrations used for publications were as follows:

a. IRDye 800 anti-rabbit@1:50k (LICOR, cat no: NC0217916)

b. IRDye 680 anti-mouse@1:50k (LICOR, cat no: 926-32220)

A.2 Preparation and Transplantation of Neural Stem Cells Within Hyaluronic Acid-Laminin Hydrogels

A2.2.1. Required Materials

A2.2.1.1. Materials needed during transplantation

Stereotaxic frame

Stereotaxic needle holder

Surgical tools and consumables

25 µL Hamilton syringe

Blunt (point style 3) 22G Hamilton needle

Tapered (point style 2) 26G Hamilton needle*

Tapered (point style 2) 22G Hamilton needle†

Micropipette tips (to fit P20 and P2)

Micropipette (P20 and P2)

*Must use 26G if transplanting into intact brain

†Okay (and easier) to use 22G if transplanting into injured brain if needed, although 26G is recommended

1M NaOH

A2.2.1.2. Materials needed during preparation

Sterile microcentrifuge tubes (2 mL and 0.2 mL)

Sterile centrifuge tubes (15 mL)

Sterile serological pipettes (10 mL)

Micropipettes (P1000, P20, and P2)

Sterile micropipette tips (to fit P1000, P20 and P2)

Sterile Pasteur pipettes

Sterile filters (0.22 µm pore)

Fine tip forceps

Sterile thiolated hyaluronic acid (HA-S)

Poly(ethylene glycol)-divinyl sulfone (PEGDVS)

Growth-factor free NSC media (see section 2.2.1.)

Growth-factor free NSC media titrated to pH 2 - 4 (yellow in color)

A2.2.2. Methods

Notes:

1. HA-S and PEGDVS must be dissolved immediately prior to transplantation. Rheological tests run 1 hour after dissolution indicated that the stiffness of the formed gel was significantly lower.

2. If using QTracker kit to label and track cells, cells must be labeled the day of use *exactly* as per manufacturer protocol. Labeling cells and then maintaining in growth media for prolonged periods of time will result in lost signal due to proliferation.

3. Counting and calculating amount of cell suspension to pull from incubator per animal is useful to perform at the beginning of the day. Either aliquoting cells per animal or keeping volume per animal written nearby during preparation is useful.

4. Weighing out HA-S per animal into 2 mL centrifuge tubes at the beginning of the day is useful. Avoid stock HA-S freeze/thaw by aliquotting all at once and storing in freezer until needed per animal.

5. While PEGDVS freeze/thaw is not as detrimental as HA-S, aliquotting likewise is useful to minimize work between animals and to conserve reagent. Prepare 300 μL of PEGDVS solution, sterile filter through 0.22 μm syringe filter and aliquot into sterile 0.65 mL microcentrifuge tubes.

5. Determine the exact volume of 1M NaOH needed to titrate pH 2-4 media (volume calculated by HA-Lm hydrogel template for NPSC encapsulation) until media turns orange/pink. Subtract this NaOH volume from the calculated volume of HA-S solution to determine the volume of pH 2-4 media in which to dissolve HA-S.

Protocol

1. All materials listed for preparation will be used in the biosafety cabinet/tissue culture hood.

2. HA-S and PEGDVS concentrations should be calculated using HA-Lm hydrogel for NPSC encapsulation.

3. Add pH 2-4 media to HA-S (volume calculated in *Notes*) and vortex for at least 1 min.

4. Remove appropriate volume/aliquot of labeled cells and spin down at 170 rcf for 3 min.

    a. During centrifugation, mix PEGDVS and laminin in sterile 0.2 mL microcentrifuge tube and pipette up and down several times with micropipette.

    b. During centrifugation, mix HA-S solution by pipetting up and down with micropipette several times and vortexing where appropriate.

5. Aspirate old media, resuspend NPSCs in less than 200 μL of growth factor-free NPSC media with micropipette, and transfer to sterile 0.2 mL microcentrifuge tube.

6. Spin down NPSCs at 170 rcf for 3 min.

    a. Continue to vortex HA-S during centrifugation.

7. Gently aspirate off almost all of old media with micropipette, leaving 15 μL or less in tube.

8. Resuspend NPSCs in remaining media, being sure to get NSPCs off the side of the tube. Determine volume of NSPC suspension and bring up to 15 μL (or alternative volume as determined by HA-Lm hydrogel template for NPSC encapsulation).

9. Add NPSCs to PEGDVS-Lm solution at appropriate volume and pipette up and down several times with micropipette.

10. Take NPSC-PEGDVS-Lm solution and HA-S solution to surgical table in separate tubes.

11. Prior to craniotomy, clean Hamilton syringe and needles with 70% EtOH. Leave to dry during craniotomy.

12. Following craniotomy, add 1M NaOH as calculated in *Notes* and mix thoroughly with micropipette.

a. Puncturing dura is easier if dura is not allowed to dry out. Add warm saline to brain surface immediately following craniotomy while the gel is prepared.

13. Add appropriate volume of titrated HA-S to NPSC-EPGDVS-Lm solution and mix thoroughly with micropipette.

14. Immediately following mixing, use blunt needle to pull NPSC-HA-Lm gel solution into syringe.

a. Ensure that needle tip avoids touching the bottom of the microcentrifuge tube to minimize bending the needle.

b. Ensure that no bubbles are pulled into syringe.

15. Change needles to tapered needle and depress plunger until NPSC-HA-Lm gel solution fills needle.

16. Place Hamilton syringe into needle holder with the eye of the needle facing towards the microscope such that it is clearly visible through the scope.

17. Stereotactically place needle and lower into cortical tissue until dura is punctured and eye of needle is fully hidden by cortical tissue, monitoring needle eye through microscope.

a. Puncturing dura is similar to puncturing a balloon in that the cortical surface will depress significantly (~0.5 mm) prior to puncture. During this time, it is easiest to continue lowering slowly but steadily rather than pausing. Immediately after dura is punctured, stop lowering and allow dura to relax for ~30 s before continuing if needed until the eye of the needle is completely covered by cortical tissue (as seen under microscope). This is considered “zero”; the dorsal/ventral

coordinates should be reset at this point and the time of injection should be recorded.

18. Lower into cortical tissue at a rate of 0.15 mm every 30 s. Upon reaching appropriate depth, hold for 1 min prior to injecting.

19. Inject at a rate of 0.25 μL every 30 s. After entire volume is injected, hold for 1 min prior to retracting needle.

20. Retract needle at a rate of 0.15 mm every 30 s, watching for eye of needle under the microscope.

21. Clean Hamilton syringe both tapered and blunt needles immediately after injection with 70% EtOH to avoid clogging due to gelation.

a. Clogging will still occur after several transplants and it is recommended to use the wire needle cleaners as needed to minimize clogging.